

AD-A158 010

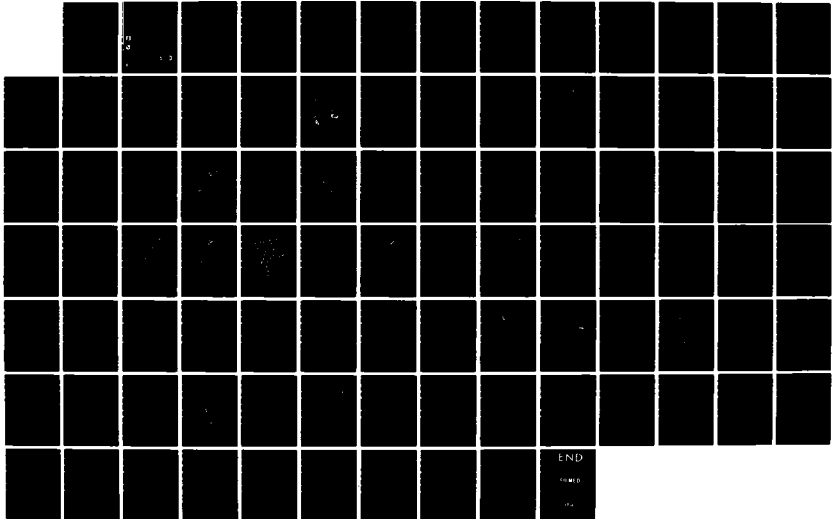
A CONCEPTUAL MODEL OF THE SEVERE-STORM ENVIRONMENT FOR
INCLUSION INTO AIR (U) AIR FORCE GEOPHYSICS LAB
HANSCOM AFB MA J M LANICCI 16 NOV 84 AFGL-TR-84-0311

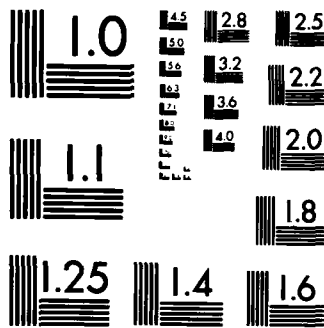
1/1

UNCLASSIFIED

F/G 4/2

NL





MICROCOPY RESOLUTION TEST CHART
NATIONAL BUREAU OF STANDARDS-1963-A

AD-A158 010

AFGL-TR-84-0311
ENVIRONMENTAL RESEARCH PAPERS, NO. 898

A Conceptual Model of the Severe-Storm Environment for Inclusion Into Air Weather Service Severe-Storm Analysis and Forecast Procedures

JOHN M. LANICCI, Capt, USAF



16 November 1984



Approved for public release; distribution unlimited.



DTIC FILE COPY



DTIC
ELECTE
JUL 29 1985
S D
G

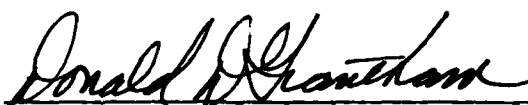
ATMOSPHERIC SCIENCES DIVISION PROJECT 6670
AIR FORCE GEOPHYSICS LABORATORY
HANSCOM AFB, MA 01731

85 7 10 009

This report has been reviewed by the ESD Public Affairs Office (PA) and is releasable to the National Technical Information Service (NTIS).

"This technical report has been reviewed and is approved for publication"

FOR THE COMMANDER


DONALD D. GRANTHAM
Chief, Tropospheric Structure Branch


ROBERT A. McCLATCHEY
Director, Atmospheric Sciences Division

Qualified requestors may obtain additional copies from the Defense Technical Information Center. All others should apply to the National Technical Information Service.

If your address has changed, or if you wish to be removed from the mailing list, or if the addressee is no longer employed by your organization, please notify AFGL/DAA, Hanscom AFB, MA 01731. This will assist us in maintaining a current mailing list.

Accession For	
NTIS GRA&I	<input checked="" type="checkbox"/>
DTIC TAB	<input type="checkbox"/>
Unannounced	<input type="checkbox"/>
Justification	
By	
Distribution/	
Availability Codes	
Dist	Avail and/or Special
AI	



Do not return copies of this report unless contractual obligations or notices on a specific document requires that it be returned.

Unclassified

SECURITY CLASSIFICATION OF THIS PAGE

REPORT DOCUMENTATION PAGE

1a. REPORT SECURITY CLASSIFICATION Unclassified		1b. RESTRICTIVE MARKINGS	
2a. SECURITY CLASSIFICATION AUTHORITY		3. DISTRIBUTION/AVAILABILITY OF REPORT Approved for public release; distribution unlimited	
2b. DECLASSIFICATION/DOWNGRADING SCHEDULE			
4. PERFORMING ORGANIZATION REPORT NUMBER(S) AFGL-TR-84-0311 ERP No. 898		5. MONITORING ORGANIZATION REPORT NUMBER(S)	
6a. NAME OF PERFORMING ORGANIZATION Air Force Geophysics Laboratory	6b. OFFICE SYMBOL (If applicable) LYT	7a. NAME OF MONITORING ORGANIZATION	
6c. ADDRESS (City, State and ZIP Code) Hanscom AFB Massachusetts 01731		7b. ADDRESS (City, State and ZIP Code)	
8a. NAME OF FUNDING/SPONSORING ORGANIZATION	8b. OFFICE SYMBOL (If applicable)	9. PROCUREMENT INSTRUMENT IDENTIFICATION NUMBER	
8c. ADDRESS (City, State and ZIP Code)		10. SOURCE OF FUNDING NOS.	
		PROGRAM ELEMENT NO. 62101F	PROJECT NO. 6670
		TASK NO. 10	WORK UNIT NO. 14
11. TITLE (Include Security Classification) A Conceptual Model of the Severe-Storm Environment (Contd)			
12. PERSONAL AUTHOR(S) Lanicci, John M., Capt. USAF			
13a. TYPE OF REPORT Scientific. Interim	13b. TIME COVERED FROM Jan 84 TO Sept 84	14. DATE OF REPORT (Yr., Mo., Day) 1984 November 16	15. PAGE COUNT 92
16. SUPPLEMENTARY NOTATION			
17. COSATI CODES		18. SUBJECT TERMS (Continue on reverse if necessary and identify by block number)	
FIELD	GROUP	SUB. GR.	
0401			
		Severe-storm conceptual model Elevated mixed-layer Fawbush-Miller theory - inversion (lid) Carlson-Ludlam theory (Contd)	
19. ABSTRACT (Continue on reverse if necessary and identify by block number) A severe-storm conceptual model first proposed by Carlson and Ludlam is described, and its relevance to identifying potential areas for severe thunderstorms is discussed. The theory complements that of Fawbush and Miller, but revises some ideas concerning large-scale atmospheric structure preceding the outbreak of severe storms, particularly the presence of a capping inversion (or lid) in the pre-storm environment. The processes that produce the lid are then discussed along with methods for identifying the lid on both conventional pressure charts and Skew T-Log P diagrams. The diagrams are used to define a new stability index that considers the strength of the restraining inversion. Two detailed case studies are presented that illustrate the role of the lid in determining the location of severe weather and the analysis techniques used to identify the lid, and that incorporate the lid concept into the operational severe-storm analysis and forecast procedures used by the Air Weather Service.			
20. DISTRIBUTION/AVAILABILITY OF ABSTRACT UNCLASSIFIED/UNLIMITED <input type="checkbox"/> SAME AS RPT. <input checked="" type="checkbox"/> DTIC USERS <input type="checkbox"/>		21. ABSTRACT SECURITY CLASSIFICATION Unclassified	
22a. NAME OF RESPONSIBLE INDIVIDUAL Capt. John M. Lanicci		22b. TELEPHONE NUMBER (Include Area Code) (617) 861-2971	22c. OFFICE SYMBOL LYT

Unclassified

SECURITY CLASSIFICATION OF THIS PAGE

Block 11 (Contd)
for Inclusion Into Air Weather Service Severe-Storm Analysis and Forecast Procedures

Block 18 (Contd)
Lid strength index
Severe-storm forecasting

Unclassified

SECURITY CLASSIFICATION OF THIS PAGE

Preface

Many of the results presented in this report were drawn from the author's M.S. thesis at Pennsylvania State University, funded by the Air Force Institute of Technology and the Air Force Office of Scientific Research (Grant Nos. AFOSR-79-0125 and AFOSR-83-0064). I extend my sincere gratitude to Professors Toby N. Carlson and Thomas T. Warner for their assistance and guidance during my thesis research. Professor Gregory S. Forbes also provided useful ideas and suggestions, particularly with regard to the information in Table 2 and Appendixes B and C.

Much of the research presented in this report was also done at the Air Force Geophysics Laboratory. Dr. H. Stuart Muench provided many suggestions for improving the techniques developed for this report. Maj. Ed Jenkins, HQ Air Weather Service, offered many useful suggestions during its preparation. Don Chisholm, Capt. Dan Ridge, USAF, Don Grantham, and Bruce Kunkel reviewed the manuscript. Mrs. Helen Connell skillfully typed this report.

Contents

1. INTRODUCTION	1
1.1 Historical Review	2
1.2 The Severe-Storm Model	7
2. THE CARLSON-LUDLAM CONCEPTUAL MODEL OF SEVERE STORMS	8
2.1 The Carlson-Ludlam Theory	8
2.2 Applications to Fawbush-Miller Theory	14
3. THE FORMATION OF THE ELEVATED MIXED LAYER	18
3.1 The Mexican Plateau	18
3.2 The Desert Southwest and the High Plains	19
4. IDENTIFICATION OF A LID	19
4.1 Conventional Charts	20
4.2 Skew T-Log P Charts	22
4.2.1 The Lid Strength Index (LSI)	26
4.2.2 Single Sounding Techniques	27
4.3 The Lid Composite Chart	27
5. SEVERE-STORM FORECASTING IN A LID SITUATION	31
5.1 The Outbreak of 3-4 April 1981	31
5.1.1 Synoptic Situation	31
5.1.2 Composite Analyses	31
5.1.3 Review of Lid Parameters	33
5.1.4 Forecast and Verification	43
5.2 The Outbreak of 13 May 1981	48
5.2.1 Synoptic Situation	48
5.2.2 Composite Analyses	50
5.2.3 Review of Lid Parameters	52
5.2.4 Forecast and Verification	59

6. CONCLUSIONS	70
REFERENCES	71
APPENDIX A: CHART SYMBOLOGY	75
APPENDIX B: ALTERNATE METHOD OF CONSTRUCTING THE LID COMPOSITE CHART	79
APPENDIX C: SINGLE-STATION LID FORECAST TECHNIQUES	81

Illustrations

1. Topographic Map of the Central United States, Showing the Important Geographic Features Contributing to the Severe-Storm Environment of the Great Plains	9
2. Median of 230 Soundings Representing Type I Air Structure Where Tornadoes Have Formed	10
3a. Skew T-Log P Sounding Taken at 1200 GMT 8 May 1979 for the Mexican Plateau	11
3b. Skew T-Log P Sounding Taken at 1200 GMT 8 May 1979 for Del Rio, Texas	11
3c. Skew T-Log P Sounding Taken at 1200 GMT 8 May 1979 for Brownsville, Texas	12
4. Schematic Flow Diagram Representing in Three Dimensions the Moist Airstream (M), the Left Edge of the Mexican Airstream (CD), and the Airstream of Subsiding Polar Air (SP) Shown in Perspective Against Topography of the Southern Great Plains of the United States and Mexico	13
5. Total Number of Tornadoes per 50-Mile Square Reported From 1920 to 1949, by Months	16
6. Mean Sounding of Type IV Tornado Air Mass	20
7. Major Lid Features at 700 mb	21
8. Relevant Lid Features at 850 mb	23
9. Surface Chart Showing Relevant Features	24
10. Illustration of Lid Parameters Calculation for a Typical Lid Sounding	25
11. Composite Chart of Lid Parameters	28
12a. Schematic Diagram Illustrating 850- and 700-mb Winds With Associated Shear Vectors and Their Relation to the Lid	29
12b. Schematic Diagram Illustrating 850- and 700-mb Winds With Plotted Vectors as the Components of the 850-700-mb Shear Perpendicular to the Lid Strength Isotherms	30
13. Surface Composite Chart for 1200 GMT 3 April 1981	32
14a. Upper-Air Composite Analyses for 1200 GMT 3 April 1981 With 850-mb Chart	34

Illustrations

14b. Upper-Air Composite Analyses for 1200 GMT 3 April 1981 With 700-mb Chart	35
14c. Upper-Air Composite Analyses for 1200 GMT 3 April 1981 With 500-mb Chart	36
14d. Total Totals Analysis for 1200 GMT 3 April 1981	37
15. 700-mb Lid Parameter Chart for 1200 GMT 3 April 1981	38
16. 850-mb Lid Parameter Chart for 1200 GMT 3 April 1981	40
17a. Lid Strength Analysis (in °C) for 1200 GMT 3 April 1981	41
17b. Buoyancy Term Analysis (in °C) for 1200 GMT 3 April 1981	42
17c. Skew T-Log P Sounding for Topeka, Kansas, at 1200 GMT 3 April 1981	43
18. Composite Lid Chart Using Lid Strength Analysis, 850-mb Features, and 850-700-mb Shear Vectors, for 1200 GMT 3 April 1981	44
19. LFM Analyses for 1200 GMT 3 April 1981	45
20. 12-Hour LFM Forecasts for 0000 GMT 4 April 1981	46-47
21a. Severe Weather Reports for 1200 GMT 3 April to 0000 GMT 4 April 1981	49
21b. Lid Strength Analysis for 0000 GMT 4 April 1981	50
22. Surface Composite Chart for 0000 GMT 13 May 1981	51
23a. Upper-Air Composite Analyses for 0000 GMT 13 May 1981 With 850-mb Chart	53
23b. Upper-Air Composite Analyses for 0000 GMT 13 May 1981 With 700-mb Chart	54
23c. Upper-Air Composite Analyses for 0000 GMT 13 May 1981 With 500-mb Chart	55
23d. Total Totals Analysis for 0000 GMT 13 May 1981	56
24. 700-mb Lid Parameter Chart for 0000 GMT 13 May 1981	57
25. 850-mb Lid Parameter Chart for 0000 GMT 13 May 1981	58
26a. Lid Strength Analysis (in °C) for 0000 GMT 13 May 1981	60
26b. Buoyancy Term Analysis (in °C) for 0000 GMT 13 May 1981	61
26c. Skew T-Log P Sounding for Oklahoma City, Oklahoma, at 0000 GMT 13 May 1981	62
27. Composite Lid Chart Using Lid Strength Analysis, 850-mb Features, and 850-700-mb Shear Vectors for 0000 GMT 13 May 1981	63
28. LFM Analyses for 0000 GMT 13 May 1981	64-65
29. 12-Hour LFM Forecast for 1200 GMT 13 May 1981	66-67
30a. Severe Weather Reports for 0000-1200 GMT 13 May 1981	68
30b. Lid Strength Analysis for 1200 GMT 13 May 1981	69
A1. Chart Symbology Used in This Report	76-77
B1. Composite Chart of Lid Parameters Using 700-mb Isotherms	80

Illustrations

- | | |
|---|----|
| C1. Skew T-Log P Sounding for Topeka, Kansas, at 1200 GMT
3 April 1981 | 82 |
| C2. Skew T-Log P Sounding for Topeka, Kansas, at 1200 GMT
3 April 1981 Showing CCL and Tc Analyses | 83 |

Tables

- | | |
|--|----|
| 1. Relationship of Severe Weather Intensities to Magnitude of
Total Totals Index | 5 |
| 2. Additions to Miller Synoptic Patterns A, B, C, D, and E
Based on Carlson-Ludlam Theory | 17 |

A Conceptual Model of the Severe-Storm Environment for Inclusion Into Air Weather Service Severe-Storm Analysis and Forecast Procedures

1. INTRODUCTION

Severe-thunderstorm forecasting is one of the most challenging areas of modern meteorology. Our knowledge of the large-scale environment preceding severe-storm outbreaks has increased greatly over the last 40 years, but much more work must be done. The purpose of this report is to revise some of the ideas concerning the large-scale structure preceding the outbreak of severe storms, with special emphasis on the role of the temperature inversion present over a large area in the pre-storm environment. Since many of the severe-storm analysis and forecast procedures currently used by the Air Weather Service (AWS) were based on research by Fawbush and Miller during the 1950s, it is appropriate to review the advances made in severe-storm forecasting during the years leading up to the publication of AWSTR-200¹ that are relevant to this report.

(Received for publication 19 November 1984)

1. Miller, R.C. (1972) Notes on Analysis and Severe-Storm Forecasting Procedures of the Air Force Global Weather Central, AWSTR-200 (Rev.), Air Weather Service (MAC), Scott AFB, Ill.

1.1 Historical Review

The scientific literature on severe thunderstorms and tornadoes in the United States throughout most of the 19th century consisted mainly of statistics and descriptions of storm damage. Two important papers by Ferrel² and Finley³ pointed out some atmospheric features commonly observed in tornado occurrences. One of the most significant features was unstable equilibrium (warm, moist air lying below cold, dry air) described as a necessary condition for tornado development. It was also known that the "southeastern quadrant" of a low-pressure area (the warm sector as described using frontal theory) was a preferred zone for tornadic storms.

In the early part of the 20th century, a trend developed towards describing the thermodynamic structure of the severe-storm environment. Varney⁴ was the first investigator to document the presence of a capping inversion and vertical wind shear in the sounding preceding a severe thunderstorm. Humphreys^{5,6} attempted to explain the inversion as a result of subsidence (section 2 deals with this explanation). He also offered the hypothesis that geographically favored areas for tornadic storms were linked to topography (namely, the Gulf of Mexico, the colder areas of Canada, and the great plateau to the west).

The concepts of fronts and air masses, along with the introduction of radio-sonde observations in the 1930s, helped to advance the study of severe weather. An important paper by Lloyd⁷ referred to the air above the inversion as a "dry superior air mass" that originates as marine polar air to the west and subsides as it travels eastward, eventually overrunning the moist tropical air from the Gulf of Mexico. At this time, the idea of frontal lifting of the unstable air as a thunderstorm-triggering mechanism was introduced. In fact, Lloyd goes on to state that tornadoes appear to form only in connection with "upper" cold fronts (the upper fronts shown in his paper were based on data taken at 4000 ft above the ground). The two types of upper cold fronts he described were the maritime polar-maritime tropical boundary and the prefrontal squall line. The prefrontal squall line was also analyzed by Harrison and Orendorf.⁸

2. Ferrel, W. (1885) Recent Advances in Meteorology, Report of the Chief Signal Officer for 1885, Appendix 71, 324-325, 327.
3. Finley, J. P. (1890) Tornadoes, Am. Meteorol. J. 7:165-179.
4. Varney, B. M. (1926) Aerological evidence as to the causes of tornadoes, Mon. Wea. Rev. 54:163-165.
5. Humphreys, W. J. (1926) The tornado, Mon. Wea. Rev. 54:501-503.
6. Humphreys, W. J. (1940) Physics of the Air, 3rd ed., McGraw-Hill, New York.
7. Lloyd, J. R. (1942) The development and trajectories of tornadoes, Mon. Wea. Rev. 70:65-75.
8. Harrison, H. T., and Orendorf, W. K. (1941) Pre-Coldfrontal Squall Lines, United Air Lines Meteorology Department Circular No. 16.

In the 1930s and 1940s, research began to link severe thunderstorms and tornadoes with individual features in the atmosphere, but a comprehensive method of prediction had yet to be developed. In March 1948, a very damaging tornado struck Tinker AFB, Oklahoma, without prior warning. Two Air Force officers, Lt. Col. E. J. Fawbush and Capt. R. C. Miller, were asked to find a way to forecast such occurrences. The resulting work of Fawbush and Miller contributed a great deal to our knowledge concerning the large-scale environment preceding severe-storm outbreaks and signaled the birth of severe-storm forecasting in the AWS.

The first paper by Fawbush et al⁹ dealt mainly with synoptic relations to severe thunderstorm occurrences. It was based on investigations of forecasting criteria presented since 1940 and tested since 1949. The six original "rules" developed by Fawbush et al have since been modified, but these rules were the beginning of the development of a comprehensive method for severe-thunderstorm prediction. A year later, Fawbush and Miller published a paper¹⁰ utilizing a compilation of 72 proximity soundings taken within 6 hours and 200 miles of tornado occurrence from 1948 to 1952. From these soundings, a "mean" sounding of the tornado air mass was presented.

This approach was not unique, however. Showalter and Fulks¹¹ had previously presented a mean sounding of the tornado environment similar to that of Fawbush and Miller. In fact, both soundings indicated the presence of a capping inversion with a layer above that is conditionally unstable and, in many cases, nearly dry-adiabatic. In 1953, Fawbush and Miller¹² presented a method of hail-size prediction again based on the concept of proximity soundings and the famous "wet-bulb zero" parameter. In 1954, they further expanded the use of proximity soundings by defining three types of tornado air masses in the United States.¹³ This was one of the first attempts to develop a severe-storm forecast procedure to be used outside the midwestern United States.

-
9. Fawbush, E. J., Miller, R. C., and Starrett, L. G. (1951) An empirical method of forecasting tornado development, Bull. Am. Meteorol. Soc. 32:1-9.
 10. Fawbush, E. J., and Miller, R. C. (1952) A mean sounding representative of the tornado air mass, Bull. Am. Meteorol. Soc. 33:303-307.
 11. Showalter, A. K., and Fulks, J. R. (1943) A Preliminary Report on Tornadoes, U.S. Weather Bureau, Washington, D. C.
 12. Fawbush, E. J., and Miller, R. C. (1953) A method of forecasting hailstone size at the earth's surface, Bull. Am. Meteorol. Soc. 34:235-244.
 13. Fawbush, E. J., and Miller, R. C. (1954) The types of airmasses in which American tornadoes form, Bull. Am. Meteorol. Soc. 35:154-165.

A comprehensive, synoptic-scale severe-weather forecast scheme was finally introduced by Miller¹⁴ in 1959. This scheme classified tornadic thunderstorms according to five synoptic patterns that permitted predictions of favorable areas of severe thunderstorm development 12 to 24 hours in advance. This paper appeared three years after publication of AWS Manual 105-37,¹⁵ which contained many of the Fawbush-Miller results from the early and mid-1950s. To incorporate the results of the late 1950s and early 1960s, the AWS published the first edition of AWSTR 200 in 1967.¹⁶ This new manual included chapters on squall-line development, summertime thunderstorm forecasting, and a new stability index (total totals index) based on temperatures and dewpoints at 850 mb, and temperatures at 500 mb. The total totals index is described in Table 1.

Before the publication of AWSTR-200, several other important papers were written on severe-storm prediction. The first of these was by Means,¹⁷ who was among the first researchers to discuss the concept of differential advection (a topic dealt with in sections 2.2 and 4.3) and to notice the relationship between the low-level jet and nocturnal thunderstorms. The use of temperature-dewpoint soundings to develop a static stability index was introduced by Showalter¹⁸ and later expanded by Galway.¹⁹ The Showalter stability index and the Lifted Index (LI) are still used today by operational forecasters.

During this period, several papers dealt with destabilization of the severe-storm environment through dynamic processes. Work done by Sugg and Foster,²⁰ Beebe and Bates,²¹ and Whitney and Miller²² dealt with the roles of the low-level

14. Miller, R.C. (1959) Tornado producing synoptic patterns, Bull. Am. Meteorol. Soc. 40:465-472.
15. Air Weather Service (1956) Severe Weather Forecasting, AWSM 105-37, 2nd ed., Air Weather Service (MATS), Scott AFB, Ill.
16. Miller, R.C. (1967) Notes on Analysis and Severe-Storm Forecasting Procedures of the Military Weather Warning Center, Air Weather Service (MAC), Scott AFB, Ill.
17. Means, L.L. (1952) On thunderstorm forecasting in the central United States, Mon. Wea. Rev. 80:165-189.
18. Showalter, A.K. (1953) A stability index for thunderstorm forecasting, Bull. Am. Meteorol. Soc. 34:250-252.
19. Galway, J.G. (1956) The lifted index as a prediction of latent instability, Bull. Am. Meteorol. Soc. 37:528-529.
20. Sugg, A.L., and Foster, D.S. (1954) Oklahoma tornadoes, May 1, 1954, Mon. Wea. Rev. 82:131-140.
21. Beebe, R.G., and Bates, F.C. (1955) A mechanism for assisting in the release of convective instability, Mon. Wea. Rev. 83:1-10.
22. Whitney, L.F., and Miller, J.E. (1956) Destabilization by differential advection in the tornado situation of 8 June 1953, Bull. Am. Meteorol. Soc. 37:224-229.

Table 1. Relationship of Severe Weather Intensities to Magnitude of Total Totals Index*

Total Totals = $(T_{850} - T_{500}) + (T_{d850} - T_{500})$ where T = temperature, T_d = dew-point, and 850, 500 refer to pressure levels.	
<u>Forecast</u>	<u>Total Totals</u>
Isolated to few thunderstorms, orange	44
Scattered thunderstorms orange with few green	46
Scattered thunderstorms orange, few green thunderstorms, isolated blue	48
Scattered thunderstorms green, few blue, isolated red	50
Scattered to numerous green, few to scattered blue, few red	52
Numerous green, scattered blue and red	56
Definition of Severe Weather Intensities by Color	
Color	Severe Weather
Red	Tornadoes or tornado waterspouts
Blue	Severe Thunderstorms (those with maximum wind gust of 50 knots or greater, or hail greater than or equal to three-fourths of an inch in diameter, or locally damaging windstorms)
Green	Moderate Thunderstorms (those with maximum wind gusts greater than or equal to 35 knots but less than 50 knots, and hail, if any, one-half inch or greater but less than three-fourths of an inch in diameter)
Orange	Thunderstorms (those with maximum wind gusts less than 35 knots and hail, if any, less than one-half inch in diameter)
*After AWSTR-200	

and upper-level jets in the destabilization process. Finally, several works began to address various individual phenomena present in the severe-storm environment over the central United States. Research on the "instability," or squall line, had

been done by Fulks,²³ Beebe,²⁴ and House.²⁵ The dryline, a small-scale "frontal" feature appearing over the southern plains in the spring, was documented by Fawbush et al⁹ and further investigated by Fujita,²⁶ Miller,¹⁴ McGuire,²⁷ the NSSP staff,²⁸ and Rhea.²⁹ The low-level jet was further investigated by Blackadar,³⁰ Pitchford and London,³¹ and Bonner.^{32, 33, 34} It was also during this time that interest in mesoanalysis of the severe-storm environment began. Papers by Fujita,^{35, 36} Fujita et al,³⁷ and Magor³⁸ presented mesoanalyses of severe-storm

23. Fulks, J.R. (1951) The instability line, in Compendium of Meteorology, T. P. Malone, Ed., Am. Meteorol. Soc., pp. 647-652.
24. Beebe, R.G. (1958) An instability line development as observed by the tornado research airplane, J. Meteorol. 15:278-282.
25. House, D.C. (1959) The mechanics of instability line formation, J. Meteorol. 16:108-120.
26. Fujita, T.T. (1958) Structure and movement of a dry front, Bull. Am. Meteorol. Soc. 39:574-582.
27. McGuire, E.L. (1962) The Vertical Structure of Three Drylines as Revealed by Aircraft Traverses, National Severe Storms Project Report No. 7, U.S. Weather Bureau, Washington, D.C.
28. National Severe Storms Project Staff (1963) Environmental and thunderstorm structures as shown by National Severe Storms Project observations in spring 1960-61, Mon. Wea. Rev. 91:271-292.
29. Rhea, J.O. (1966) A study of thunderstorm formation along drylines, J. Appl. Meteorol. 5:58-63.
30. Blackadar, A.K. (1957) Boundary-layer wind maxima and their significance for the growth of nocturnal inversions, Bull. Am. Meteorol. Soc. 38:283-290.
31. Pitchford, K.L., and London, J. (1962) The low-level jet as related to nocturnal thunderstorms over the midwest United States, J. Appl. Meteorol. 1:43-47.
32. Bonner, W.D. (1963) An Experiment in the Determination of Geostrophic and Isalobaric Winds from NSSP Pressure Data, Research Paper 26, Mesometeorology Project, U. of Chicago.
33. Bonner, W.D. (1966) Case study of thunderstorm activity in relation to the low-level jet, Mon. Wea. Rev. 94:167-178.
34. Bonner, W.D. (1968) Climatology of the low-level jet, Mon. Wea. Rev. 96:833-850.
35. Fujita, T.T. (1955) Results of detailed synoptic studies of squall lines, Tellus 7:405-436.
36. Fujita, T.T. (1958) Mesoanalysis of the Illinois tornadoes of 9 April 1953, J. Meteorol. 15:288-296.
37. Fujita, T.T., Newstein, H., and Tepper, M. (1956) Mesoanalysis, An Important Scale in the Analysis of Weather Data, Research Paper No. 39, U.S. Weather Bureau, Washington, D.C.
38. Magor, B.W. (1959) Mesoanalysis: Some operational analysis techniques utilized in tornado forecasting, Bull. Am. Meteorol. Soc. 40:499-511.

cases that sought to identify small-scale features known to be associated with tornadoes, such as meso-highs and lows, and thunderstorm outflow boundaries.

The advent of the computer as a tool in operational meteorology was an important development in the 1960s, and helped lead to the creation of another stability index, the Severe Weather Threat (SWEAT) index, by Miller et al.³⁹ This index included the effects of vertical wind shear between 850 mb and 500 mb in diagnosing stability as well as the traditional thermodynamic parameters used in earlier indices. In fact, this index was used in other procedures besides analysis. Forecast fields of SWEAT index were produced from output of the Air Force Global Weather Central (AFGWC) numerical prediction models. By the time the revised AWSTR-200* was published in 1972, automated products were being routinely used by AWS and NWS personnel at AFGWC and the National Severe Storms Forecast Center.

The use of meteorological satellite data by operational forecasters became routine during the 1970s. A manual describing severe-storm synoptic patterns through combined use of AWSTR-200 rules and satellite data was published by Miller and McGinley.⁴⁰ Satellite data has also been extensively used for identification of mesoscale features, and is an integral part of operational mesoanalysis performed by the severe-storm forecaster.

1.2 The Severe-Storm Model

The historical review presented in section 1.1 illustrates the fact that many of the severe-storm analysis and forecast procedures currently used by AWS forecasters date back to the Fawbush-Miller results of the 1950s. Except for automated products derived from numerical model output and satellite identification techniques for both large-scale and mesoscale forecasting, the original ideas of Fawbush and Miller have remained intact for nearly 30 years. It is not the intent of this report to replace the methods that have served operational forecasters so well. Rather, we intend to introduce a conceptual model of the severe-storm environment that can easily be integrated into operational procedures both at the base weather level and at AFGWC.

*All further references to AWSTR-200 are to the revised version.¹

39. Miller, R.C., Bidner, A., and Maddox, R.A. (1971) The use of computer products in severe weather forecasting, Preprints of the Seventh Conference on Severe Local Storms, Am. Meteorol. Soc., Boston, Mass., 1-6.
40. Miller, R.C., and McGinley, J.A. (1978) Using Satellite Imagery to Detect and Track Comma Clouds and the Application of the Zone Technique in Forecasting Severe Storms, Environmental Sciences Group, GE/Management and Technical Services Company, Beltsville, Md.

2. THE CARLSON-LUDLAM CONCEPTUAL MODEL OF SEVERE STORMS

The conceptual model that forms the basis for the results presented in this report was first presented by Carlson and Ludlam.⁴¹ The aspects of the model discussed here are primarily extracted from the results of Carlson et al.⁴² This chapter is divided into two sections, the first dealing with the conceptual model itself and the second addressing how the conceptual model complements the ideas of Fawbush and Miller concerning large-scale structure of the severe-storm environment.

2.1 The Carlson-Ludlam Theory

The basic thrust of the Carlson-Ludlam theory differs from that of other researchers. In contrast with schemes that attempt to identify the most favorable convective areas, the Carlson-Ludlam approach first seeks to eliminate areas unfavorable for severe-storm outbreaks before identifying those areas that are likely to experience severe thunderstorms. This is a very subtle distinction. In order to fully clarify its meaning, we present the following scenario:

Consider a region such as the southern Great Plains of the United States (Figure 1). Because of the unique combination of geographic influences such as the Rocky Mountains to the west, the Gulf of Mexico to the south, and the Canadian Plains to the north, this region has the greatest frequency of severe weather events in the world.⁴³ However, one of the most important geographical influences on severe-thunderstorm outbreaks over the southern Great Plains has been neglected in previous theories, namely, that of the arid, elevated Mexican plateau to the south. During the springtime, a combination of strong insolation, dry soil conditions, and terrain elevations as high as 1500 m above sea level lead to the formation of deep, hot, mixed layers with surface potential temperatures frequently in excess of 40°C. With the approach of an upper-level trough in the westerlies, the winds over the plateau shift to a southwesterly direction, advecting this hot, dry air mass northeastward, where it loses contact with the surface and becomes elevated over the southern plains of the United States. In the prestorm environment over the southern plains, a situation occurs where moist tropical air from the

41. Carlson, T.N., and Ludlam, F.H. (1968) Conditions for the occurrence of severe local storms, *Tellus* 20:203-226.

42. Carlson, T.N., Benjamin, S.G., Forbes, G.S., and Li, Y.-F. (1983) Elevated mixed layers in the regional severe storm environment - Conceptual model and case studies, *Mon. Wea. Rev.* 111:1453-1473.

43. Palmen, E., and Newton, C.W. (1969) *Atmospheric Circulation Systems*, Academic Press, New York.



Figure 1. Topographic Map of the Central United States, Showing the Important Geographic Features Contributing to the Severe-Storm Environment of the Great Plains

Gulf of Mexico is advected in at low levels, while the hot, dry Mexican air is advected in aloft and effectively forms a lid over the moist low-level air. This lid prevents convection by limiting the depth to which the moist air can vertically mix with the air above. This restriction to vertical mixing also causes an increase in low-level potential instability by allowing low-level moisture to increase through advection and surface evaporation. It should be noted that, in this scenario, the presence of moist low-level air and cold air at upper levels lead to very unstable values of the Lifted Index (LI) and the Severe Weather Threat (SWEAT) index. However, over a large portion of this region, convection is effectively inhibited by the presence of this inversion. The presence of a capping inversion is not considered in the formulation of these severe-weather indices.

Another unique aspect of the Carlson-Ludlam model is its assertion that the inversion frequently present over regions such as the Great Plains in the classical Miller synoptic patterns is caused by an upstream arid source region rather than by subsidence. A look at Miller's Type I sounding (Figure 2) reveals a drying out at the level of the inversion and a conditionally unstable lapse rate above with a steady increase in relative humidity. These characteristics of the air above the inversion indicate dry mixed layers like those present over regions such as the Mexican plateau during the springtime. An illustration of this similarity is presented in Figures 3a, 3b, and 3c, which illustrate temperature-dewpoint soundings taken over the Mexican plateau and two other stations downstream (Del Rio and

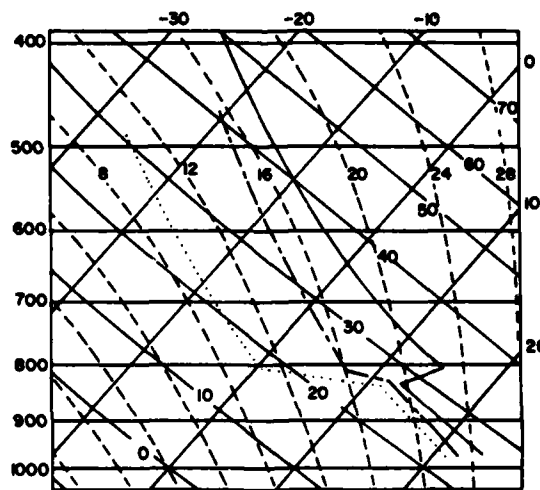


Figure 2. Median of 230 Soundings Representing Type I Air Structure Where Tornadoes Have Formed. Plotted on Skew T, Log P diagram: solid curves = temperature, dashed curve = wet-bulb temperature, dotted curve = dewpoint¹³

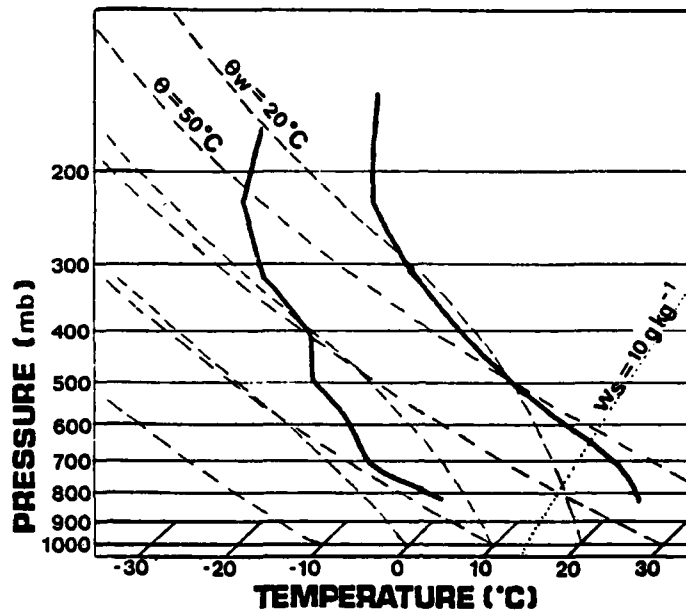


Figure 3a. Skew T-Log P Sounding Taken at 1200 GMT 8 May 1979 for the Mexican Plateau

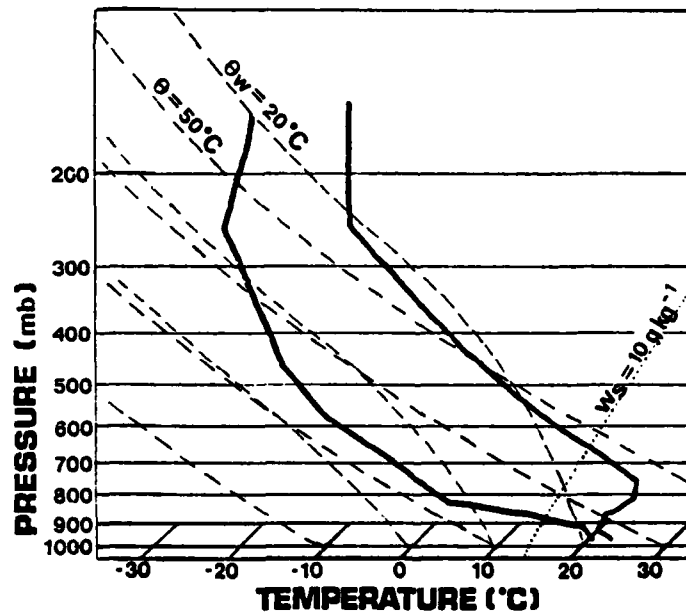


Figure 3b. Skew T-Log P Sounding Taken at 1200 GMT 8 May 1979 for Del Rio, Texas

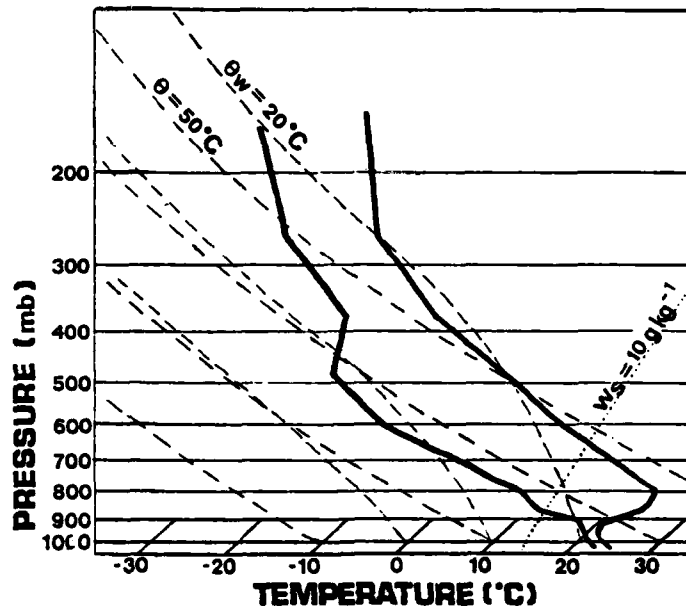


Figure 3c. Skew T-Log P Sounding Taken at 1200 GMT 8 May 1979 for Brownsville, Texas⁴⁷

Brownsville, Texas). A comparison of the well-mixed layers present in these soundings indicates a similar average potential temperature of about 47 C. Notice that the elevation of the inversion tops in the Del Rio and Brownsville soundings (Figures 3b and 3c) are similar to the elevation of the Mexican plateau (Figure 3a). Also notice the similarity between the soundings in Figures 3b and 3c and the Miller Type I sounding shown in Figure 2.

A schematic three-dimensional picture of the lid scenario is presented in Figure 4. Notice that the airstreams marked SP in the diagram represent subsided polar air that originates to the west of the upper-level trough and forms a line of confluence with the moist airstream (M) at low levels over west Texas. This line of confluence between the SP and M airstreams denotes the position of the dryline. From Figure 4, then, it can be seen that an additional consideration in the lid scenario is the role of low-level convergence associated with the dryline zone.

Notice from Figure 4 that there are basically two ways that severe storms can occur in a lid situation. One way is through "underrunning," low-level outflow of the moist air from beneath the lid edge into an area where the temperature inversion no longer exists (see location E in Figure 4). In areas of upward motion along the lid edge, severe storms can occur through the underrunning process. Another way severe storms can occur is through the removal of the lid by strong surface

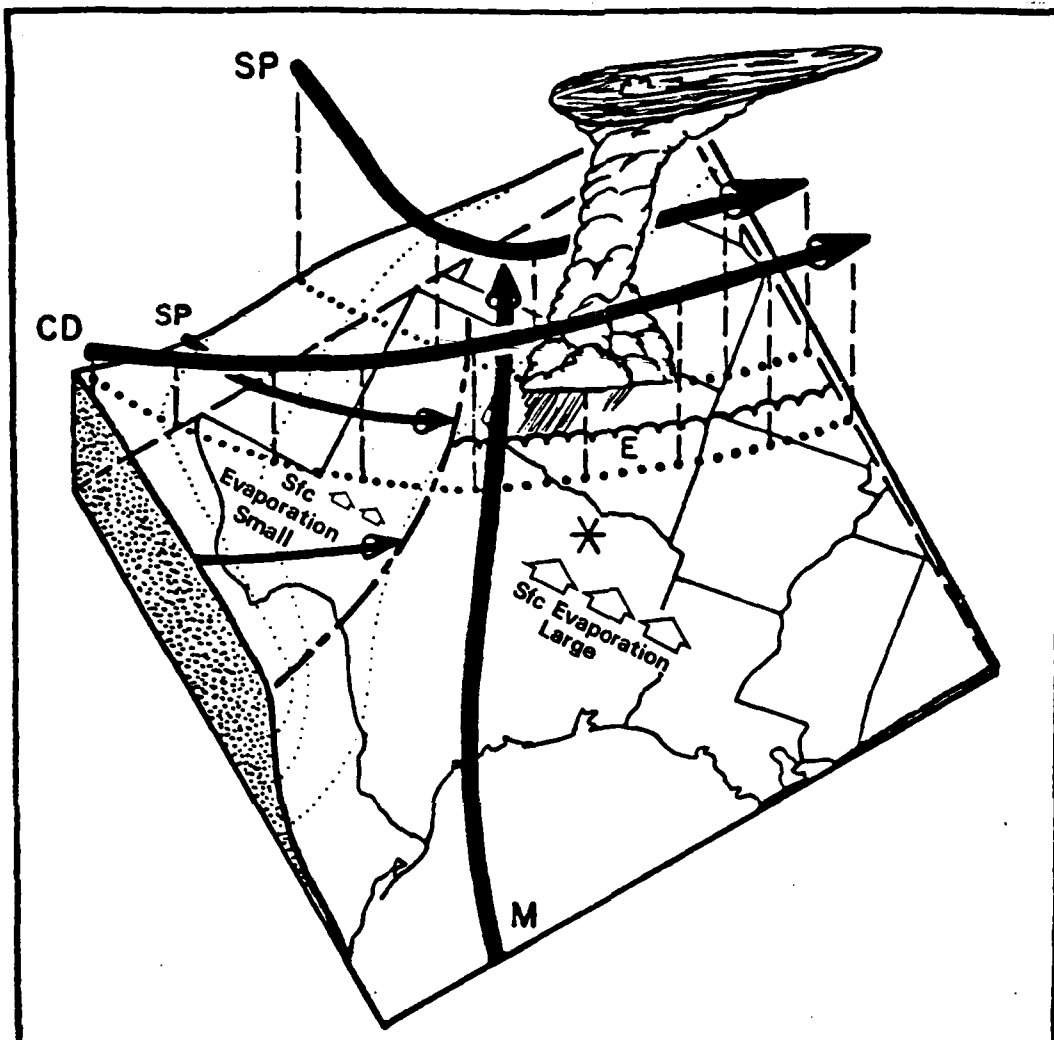


Figure 4. Schematic Flow Diagram, Representing the Airstreams M, CD, and SP in Three Dimensions, Is Shown in Perspective Against Topography of the Southern Great Plains of the United States and Mexico. The dotted lines denote surface terrain elevation contours and illustrate the gradient of surface elevation north and east of the high plateau of Mexico (shown in a cut-away section). The left edge of the moist airstream (M) is shown bounded by the dryline (dot-dash line); the left edge of the Mexican airstream (CD), which is forming a lid over the moist air, is denoted by the scalloped border. The latent instability of the air beneath the lid is increased both through advection of moist air from the Gulf of Mexico and through surface evaporation over eastern Texas. Little surface evaporation occurs over the arid region west of the dryline, as indicated by the schematic arrows. Under-running (see section 2.1) is shown to be occurring at the location of the thunderstorm near E, the area most favored for the violent release of the latent instability in the under-running process. Thunderstorms can also occur underneath the lid at the location of the asterisk where large-scale ascent coupled with surface heating may be removing the lid. The third airstream (SP) is subsiding polar air that originates west of the trough⁴⁷

heating and vertical mixing, or through strong upward motion associated with an approaching short-wave trough (see location of asterisk in Figure 4). In this scenario, disappearance of the lid restriction over a region allows the potential instability of the low-level air to be released in violent convection.

It should be noted that the presence of a capping inversion over an area before the outbreak of severe thunderstorms is not restricted to the southern Great Plains in the springtime. In fact, Carlson and Ludlam's original theory was presented for severe thunderstorms over southern England, where the lid-source regions were the Spanish plateau and the North African desert. Various researchers have observed lids before severe-storm outbreaks in other parts of the world. For instance, over northeastern India and Bangladesh, moist, potentially unstable air at low levels can be capped by a well mixed layer aloft originating in the dry westerly-to-northwesterly flow from the Arabian and Iranian plateaus.⁴⁴ Carlson et al.⁴² have listed other studies that document lid occurrences associated with severe-storm outbreaks over Australia, South Africa, Brazil, Uruguay, and Argentina. In addition, the presence of warm air layers in the middle troposphere before summertime severe-storm outbreaks over the central and northern Great Plains has been noted by Miller,¹ Miller and McGinley,⁴⁰ and Crisp.⁴⁵ The origin of this summertime warm air layer is usually over the southwestern U.S. deserts or the western high plains, as will be mentioned in section 3. The appearance of lids as far east as the Ohio River Valley and the Appalachian region has been documented by Goldman.⁴⁶

2.2 Applications to Fawbush-Miller Theory

The most important impact of the Carlson-Ludlam model on the Fawbush-Miller theory is the cause assigned to the temperature inversion present in the pre-storm environment. Fawbush and Miller, and indeed many other researchers, attribute this inversion entirely to subsidence. Carlson and Ludlam assert that this inversion is caused by the advection of a well mixed layer from an upwind, arid plateau over cool, moist air below.

A question one may ask at this point is: What difference does it make what type of inversion is present? The answer to this question concerns the different

-
44. Ramaswamy, C. (1956) On the sub-tropical jet stream and its role in the development of large-scale convection, *Tellus* 8:26-60.
 45. Crisp, C.A. (1979) Training Guide for Severe Weather Forecasters, AFGWC Technical Note 79/002, Air Force Global Weather Central, Offutt AFB, Neb.
 46. Goldman, J.D. (1981) A Conceptual Model and Its Application in the Analysis of Severe Convective Storm Situations, M.S. thesis, The Pennsylvania State U., University Park, Pa.

processes that create subsidence and elevated mixed-layer inversions. The subsidence inversion is created by downward vertical motion. This process is not geographically restricted. However, an examination of springtime-tornado frequency charts such as those presented in Figure 5 reveals a geographical preference that cannot be explained entirely by vertical motion patterns. Second, a subsidence inversion is usually associated with patterns of low-level divergence and anticyclogenesis, which are not favorable for the outbreak of severe thunderstorms.

The elevated mixed-layer inversion is created by the processes of strong surface-heating upwind and differential advection downwind, which are geographically related and can be traced through time by a forecaster. In fact, a typical Great Plains severe-storm situation has veering winds with height as a vital ingredient. This veering environment favors low-level moist advection from the Gulf of Mexico and mid-level dry advection from the Mexican plateau (or desert southwest). The dry air aloft has been documented as a critical factor in the potential instability of the tornado environmental sounding. Additionally, the veering wind environment is associated with warm air advection in the layer and upward vertical motion, two more factors present in severe-storm cases. The upward motion is particularly important because it can remove the lid, leading to severe convection. Thus, the destabilization over an area caused by differential advection may be predicted by examining horizontal advection patterns, giving the forecaster an additional tool to use in severe-storm prediction. Another point is that the lid, by virtue of its origin, is actually an air mass aloft as it traverses the Great Plains. Thus, the lid edge can be considered a mid-level frontal zone. This important result means that identification of the lid edge can allow a forecaster to locate potential areas for mesoscale convective development.

A third consideration is that, when a lid is present over a large area, the 700-mb dry front is likely to appear far downstream of a favorable severe-weather area. The two cases presented in section 5 illustrate this fact in detail. This is important because the 700-mb dry front is given as being an important ingredient in severe-storm outbreaks. Also, the rapid rise in dewpoint that occurs several hours before the onset of convection is probably the result of the combined processes of advection and surface evaporation which, under the restriction of the lid, confine the moisture to a shallow layer under the inversion, thus increasing the low-level instability.

Table 2 summarizes the additions to the Miller synoptic patterns based on the theory of Carlson and Ludlam.

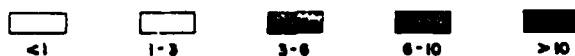
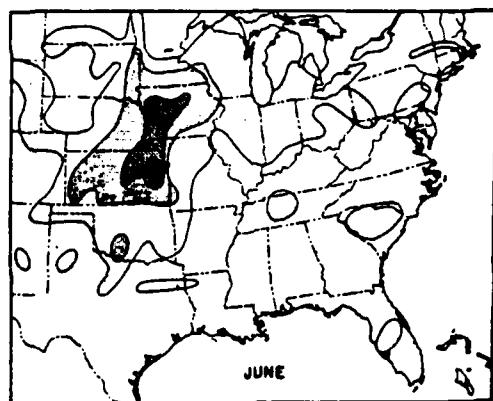
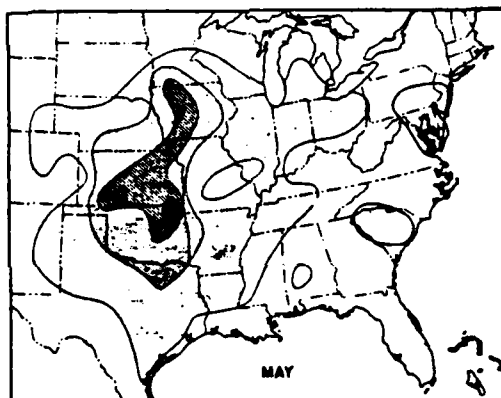
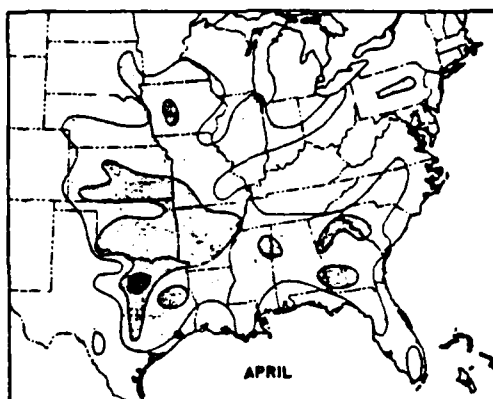


Figure 5. Total Number of Tornadoes per 50-Mile Square Reported From 1920 to 1949, by months⁹

Table 2. Additions to Miller Synoptic Patterns A, B, C, D, E Based on Carlson-Ludlam Theory

<p>Synoptic Type A (AWSTR-200, Figure 12)</p>	<p>Synoptic pattern A is nearly identical to the three-airstream model shown in Figure 4. The exception is that, in the example shown in AWSTR-200, the dry front at 700 mb is located over the western plains, whereas in Figure 4, the 700-mb dry front would be further north. If the dry front shows up on the 700-mb chart, the forecaster should be alerted to the presence of a lid, characterized by 700-mb temperatures in excess of 8 C. If such an area exists, the zones for severe weather occurrence should be modified to reflect the presence of the lid, as severe storms will form either along the lid edge in areas of upward motion, or in areas where the lid is being removed by surface heating or upward motion. Note that the occurrence of thunderstorms at time of maximum surface heating or within six hours thereafter reflects the importance of lid removal through surface heating and vertical mixing in the boundary layer.</p>
<p>Synoptic Type B (AWSTR-200, Figure 13)</p>	<p>The presence of a major upper-level trough to the west of the outbreak region and the presence of dry air at mid levels over the threat region mean that synoptic pattern B will also support the occurrence of a lid.</p>
<p>Synoptic Type C (AWSTR-200, Figure 14)</p>	<p>Synoptic pattern C could also support a lid presence (possibly originating over the desert southwest or high western plains). This pattern could be a severe-storm producer if the moist air undercuts the lid just to the south of the stationary front. Frontal lifting along the stationary front can also act as a lid-removal mechanism in this case. The lid in this example would typically travel from the southern plains states into the Gulf Coast states and lower Mississippi valley, closely paralleling the upper flow direction.</p>
<p>Synoptic Type D (AWSTR-200, Figure 15)</p>	<p>Synoptic pattern D will probably not support a lid because the large positive vorticity advection (PVA) everywhere ahead of the upper cold core can remove the lid rather quickly in this case. Notice the strong low-level flow crossing beneath the upper jet in this example, which is characteristic of the flow pattern under the left exit region of an upper-level jet streak.</p>
<p>Synoptic Type E (AWSTR-200, Figure 16)</p>	<p>Synoptic pattern E represents a situation where the lid has been cut off from its source region by the advancing cold front and west-southwesterly upper jet. The lid at this point will weaken; severe storms can occur north of the lid edge along the warm-frontal boundary in this example.</p>

3. THE FORMATION OF THE ELEVATED MIXED LAYER

In general, any arid region can be a source region for an elevated mixed layer. The reason is that these areas normally receive abundant sunshine during the warmer months and can use the available solar radiation for heating the ground, since the dry soil provides little, if any, moisture for evaporation. This strong surface-heating promotes convective overturning of the air, and deep adiabatic layers result. Since the low-level potential temperatures over these arid regions are warmer than those over more temperate, vegetated areas, the overrunning of such a warm, dry air mass over cooler, moister air will create an elevated mixed-layer inversion. Thus, a source region for a lid is not restricted to an elevated area such as northern Mexico, as long as the warm, dry air mass maintains its well mixed character after it overruns the moist air, and it restricts vertical mixing in the cooler, moister air below it.

3.1 The Mexican Plateau

Carlson et al⁴² described the environment where this type of lid is produced as follows:

"The extreme dryness of this region through the winter months, the strong spring insolation, and the high elevation (an area of 250,000 square km above 1500 m elevation) results in a mean daily maximum surface potential temperature of 42-46° C for the month of April."

Lanicci⁴⁷ used precipitation records for over 500 stations in northern and central Mexico to reveal that precipitation during the months January through April averages between 10 and 20 mm per month. He also found that over many stations, this precipitation greatly increases between May and June with the onset of the Mexican wet season. Thus, he hypothesized that one reason why Mexican lids do not normally appear over the southern plains states after early June is the onset of the wet season over the plateau. This suggests that lids observed during the summer months have source regions over the desert southwest (in areas not dominated by the monsoon), the high plains, the intermountain region, or the central plains (during drier than normal periods). A typical sounding over the Mexican plateau is illustrated in Figure 3a. Mexican lids can generally have potential temperatures between 38° C and 48° C.⁴²

47. Lanicci, J. M. (1984) The Influence of Soil Moisture Distribution on Severe-Storm Environment of the Southern Great Plains: A Numerical Study of the SESAME IV Case, M.S. thesis, The Pennsylvania State U., University Park, Pa.

3.2 The Desert Southwest and the High Plains

Goldman⁴⁶ has documented the appearance of a "secondary" elevated mixed-layer inversion over west Texas in the SESAME IV case (9-10 May 1979). In this case, the secondary lid originated over the desert southwest and the high plains of Texas as strong surface-heating produced a deep, hot, mixed layer that was advected over west Texas during the day. Carlson et al⁴² proposed that the source region of the lid in the SESAME III case (25-26 April 1979) was the desert southwest. Carlson and Farrell⁴⁸ used isentropic analyses to locate a lid whose source region was over the desert southwest in a case of severe storms over Oklahoma on 13 May 1981 (see section 5.2 for a further discussion of this case).

In general, lids originating over the southwest United States or the western plains do not have potential temperatures as high as the Mexican lids do. One reason is that lids originating over the desert southwest are part of the subsiding polar airstream (SP) (see Figure 4), originally descended from the west side of the upper trough and originally cooler than the Mexican air, whereas the Mexican air mass can experience several days of intense surface-heating before it is advected northward by the mid-tropospheric flow.⁴⁹ Another reason why the southwestern lids tend to be cooler than the Mexican lids is that the elevation of the desert southwest is not as high as that of the Mexican plateau. This difference in elevation causes the surface potential temperatures over the desert southwest to be somewhat lower than those over the Mexican plateau. An illustration of the Type IV tornado sounding¹ shown in Figure 6 indicates that the dry mixed layers present over the desert southwest and western high plains have a mean potential temperature between 36° C and 42° C.

4. IDENTIFICATION OF A LID

A combination of different types of analyses identify a lid. This section will explain how to use conventional analyses and soundings. The determination of the lid strength is then introduced by a new stability index that considers the low-level moisture and the strength of the inversion.

48. Carlson, R.N., and Farrell, R.J. (1983) The lid strength index as an aid in predicting severe local storms, Nat. Wea. Digest 8:27-39.

49. Benjamin, S.G. (1983) Some Effects of Heating and Topography on the Regional Severe Storm Environment, Ph.D. thesis, The Pennsylvania State U., University Park, Pa.

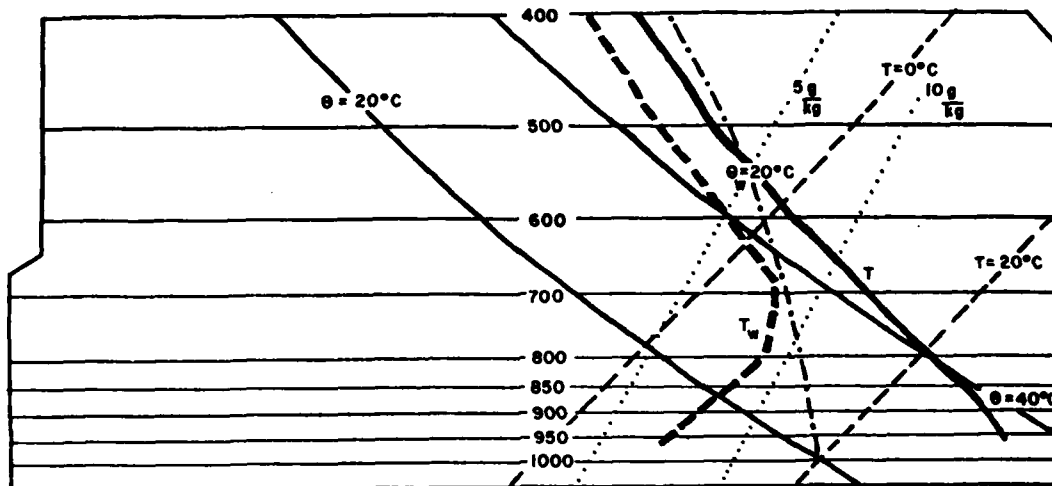


Figure 6. Mean Sounding of Type IV Tornado Air Mass. Solid lines are temperature, and dashed lines are wet-bulb temperature

4.1 Conventional Charts

Perhaps the two most easily utilized charts available to the forecaster to identify a lid occurrence are the 850- and 700-mb analyses. Because the 700-mb analysis is the most important conventional chart for identifying a lid occurrence, it will be discussed first.

Several features on the 700-mb chart indicate the presence of an elevated mixed layer (see Figure 7). The first of these is the presence of a thermal ridge associated with 700-mb temperatures in excess of 8°C (a 700-mb temperature of 8°C corresponds to a potential temperature of about 38°C). The isotherms equal to or greater than 8°C help to identify the lid region at 700 mb, although a lid can be present with 700-mb temperatures less than 8°C (see section 5).

The next feature to look for is the crossing angle between the 700-mb winds and the lid isotherms. The purpose of studying this crossing angle is to evaluate the advection of the air mass in order to predict its trajectory. Note that the air mass is usually lifted along this trajectory since it is east of the upper-trough axis (in an area of large-scale vertical ascent) so that the lid weakens through adiabatic cooling along its ascent. A second purpose of studying the wind direction at 700 mb is to identify the lid source region. Generally, lids originating over the southwest United States, the high plains, and the Mexican plateau are advected over cooler, moister air from the Gulf of Mexico if the 700-mb winds are between about 180° and 270° in direction.

The last feature to identify on the 700-mb chart is dewpoint depression greater

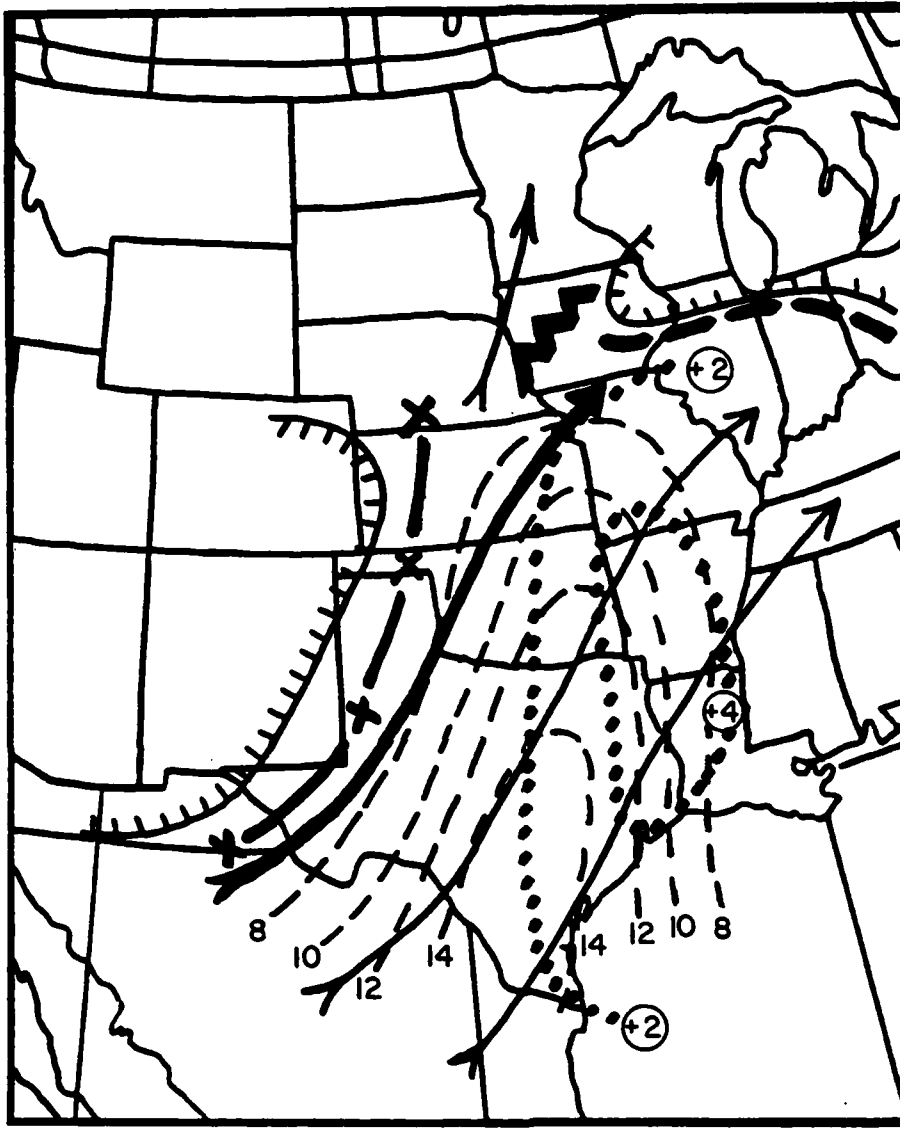


Figure 7. Major Lid Features at 700 mb. The ribbed border denotes dewpoint depressions of 6°C or less. The dotted lines represent 12-hour temperature changes of 2°C and 4°C . The middle troposphere has become more stable during the last 12 hours over the areas enclosed by the dotted lines. The locations of temperature-change lines (including the no-change line) and the cross-isotherm flow angles help determine the movement of the lid by advection. Other symbols are defined in Figure A1

than 6°C . Although an elevated mixed-layer has dewpoint depressions much greater than 20°C , this is done in order to delineate moist areas at 700 mb, and a

dewpoint depression of 6° C or less certainly does not correspond to an elevated mixed-layer air mass. Ideally, a temporal continuity of 700-mb lid charts should be kept so that the formation and trajectory of the lid can be determined.

On the 850-mb chart (Figure 8), several features indicate the presence of a lid source-region. First, the location of a warm pocket of air, usually with temperatures in excess of 20° C, indicates a lid source-region, especially if the 700-mb wind direction over the lid area is from this region. Second, the air must be dry, and dewpoint depressions less than 6° C are used to delineate moist areas on the analysis, since the dewpoint depressions over a lid source-region exceed 20° C. Other features on the 850-mb analysis identify various aspects of the Carlson-Ludlam model. For instance, the confluence over west Texas of warm, dry air from the southwest with moist air from the Gulf of Mexico is usually an indication of the confluence between the SP and M airstreams in Figure 4, which constitutes the dryline zone. Note that this boundary is important since it can act as a triggering zone for severe thunderstorms if the proper stratification and dynamics are present.²⁹ A temporal continuity of 850-mb charts can be used to trace the evolution of the lid source-region and the low-level airstreams in the Carlson-Ludlam model.

Finally, the surface analysis (Figure 9) can be used to identify a lid occurrence. This chart is just as important in a lid situation as it is during other types of severe weather occurrences. Pressure falls and rises, significant cross-isobar flow angles, and the presence of moisture axes are all important in the identification of potential underrunning or lid-removal situations. Both the pressure falls and cross-isobar flow indicate the surface response to an upper-level feature such as a jet streak. The moisture axes are important since the potential instability of the air is released in strong convection when it underruns the lid edge.

4.2 Skew T-Log P Charts

The Skew T-Log P chart is an invaluable tool for detecting the presence of a lid. Four basic criteria, all easily identifiable, must be met on a sounding to classify it as a lid-type sounding. These criteria are:

- (1) A relative humidity break in the sounding must exist above the lowest 50 mb and below 600 mb, and it should be at least 1%/mb over a 40-mb layer (40%/40mb).
- (2) Either an isothermal layer or a layer in which temperature increases with height must exist within 100 mb of the level of the relative humidity break in the sounding and below 500 mb.
- (3) The buoyancy, computed as the difference between the saturation wet-bulb potential temperature at 500 mb, θ_{sw5} , and the highest wet-bulb potential temperature in the lowest 50 mb, $\bar{\theta}_w$, must be less than 1 C.
- (4) The lid strength, computed as the difference between the maximum saturation wet-bulb potential temperature between the level of the relative humidity break

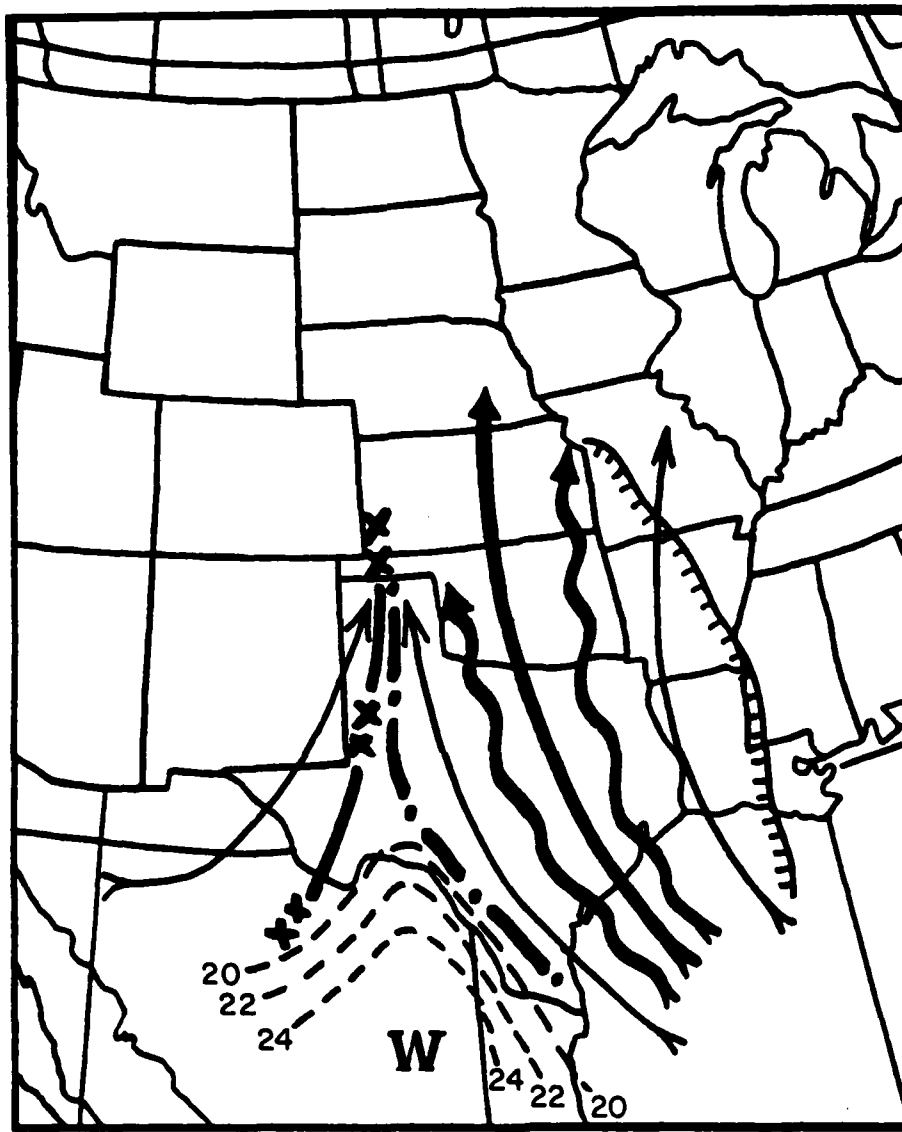


Figure 8. Relevant Lid Features at 850 mb. Symbols are defined in Figure A1. Notice that the dryline at 850 mb (dot-dashed line) can extend as far south as the Rio Grande valley. This occurs because air to the south of the dryline originates over the Mexican plateau, implying that the base of the dry-air layer is below 850 mb. To the north of the 850-mb dryline, the air is moist (originating over the Gulf of Mexico), implying that the base of the dry Mexican air is above 850 mb. This suggests that the base of the Mexican air mass rises as one proceeds north from the Mexican border

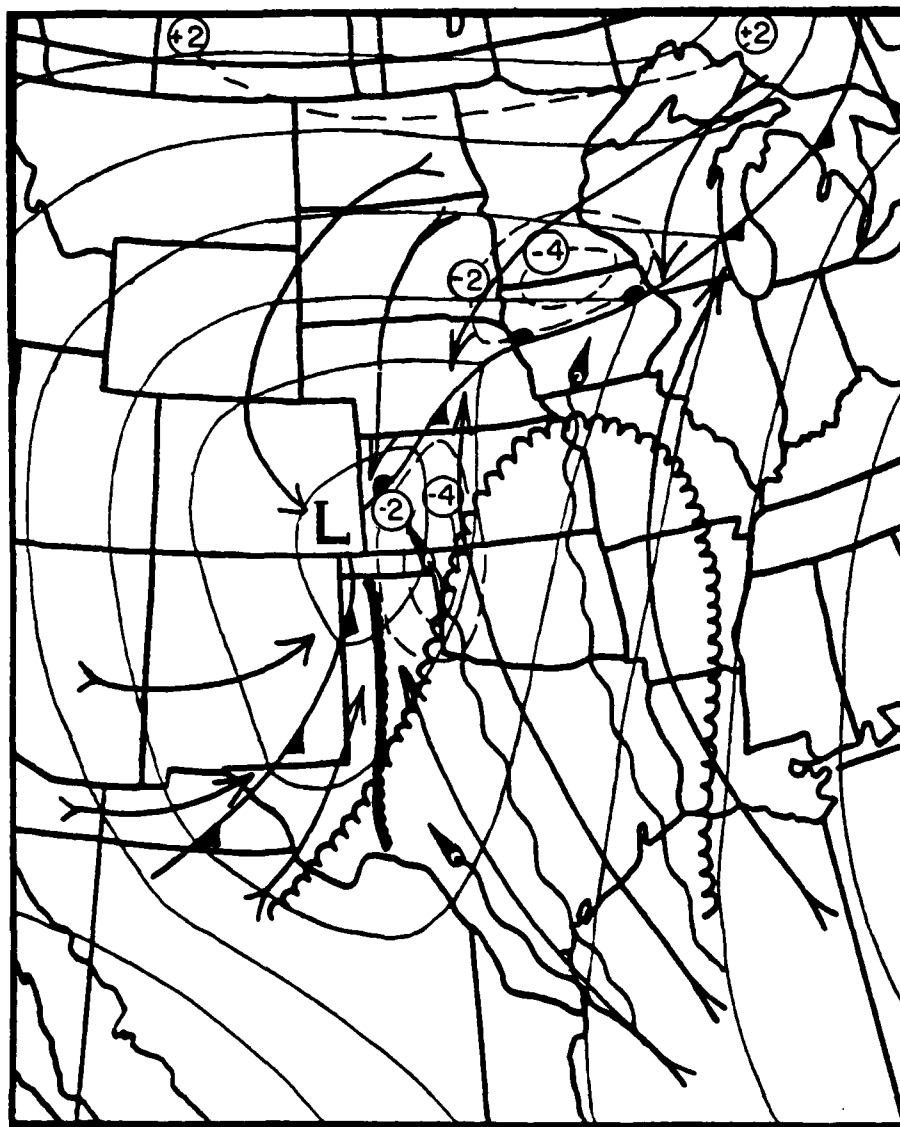


Figure 9. Surface Chart Showing Relevant Features. Streamlines (straight lines with arrows) denote surface windflow, while moist axes are denoted using standard AWSTR-200 notation (see Appendix A, Figure A1). Three-hourly pressure changes of 2 mb or greater are shown by dashed lines. The dryline is denoted by the closed scalloped line. The open scalloped line indicates the lid edge as determined by lid-strength analysis (see section 4.2), outlining the approximate region covered by a lid. Underrunning exists where the surface flow crosses the lid edge at an angle (the 850-mb flow should be considered as well), especially when a moisture axis crosses the lid edge

and 500 mb, θ_{swMAX} , and the highest wet-bulb potential temperature in the lowest 50 mb, $\bar{\theta}_w$, must be greater than or equal to 1° C.

A description of how to locate these parameters on a typical lid sounding appears in Figure 10. The θ_{sw5} term is the value of the moist adiabat that intersects the temperature sounding at 500 mb. The θ_{swMAX} term is found by locating the value of the moist adiabat that intersects the warmest point of the temperature sounding within 100 mb of the relative humidity break and below 500 mb. This warmest point is usually the top of the inversion layer (the "nose" of the inversion). The $\bar{\theta}_w$ term is determined the same way for both the buoyancy and lid strength terms, and is the maximum value of θ_w over the lowest 50 mb of the sounding, computed by methods described in AWSM 105-124,⁵⁰ section 4.10. Once determi-

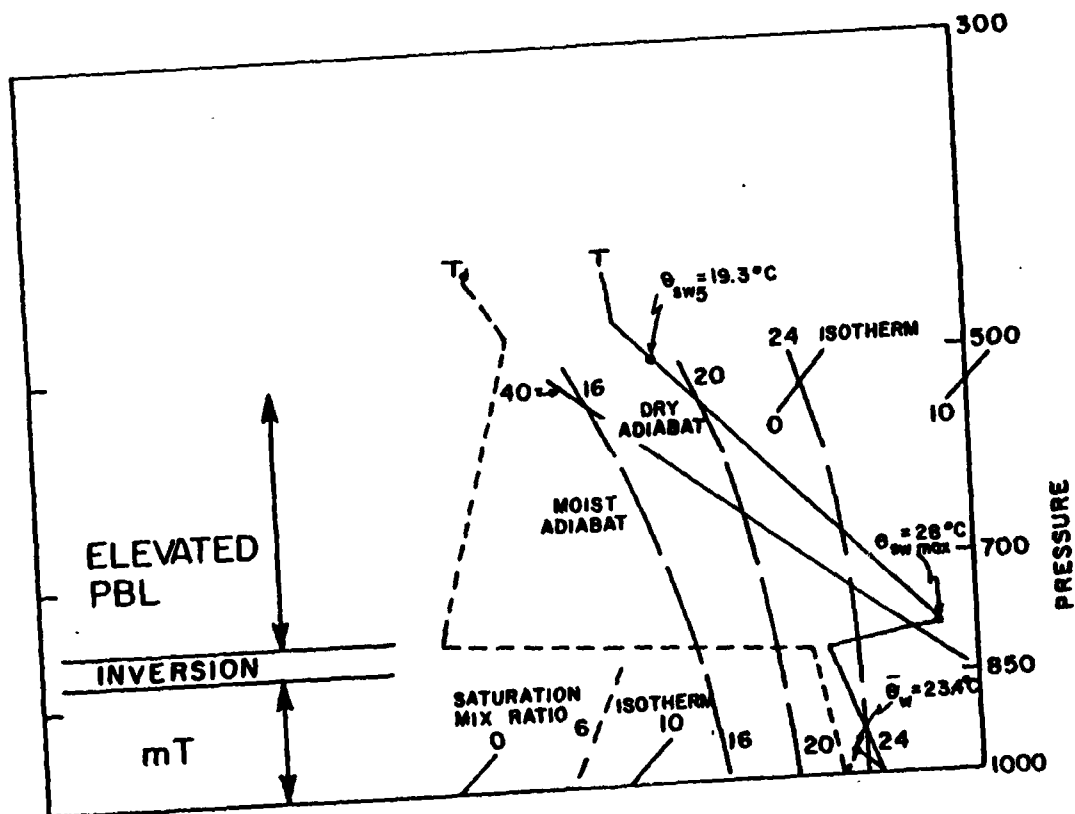


Figure 10. Illustration of Lid Parameters Calculation for a Typical Lid Sounding

50. Air Weather Service (1969) Use of the Skew T, Log P Diagram in Analysis and Forecasting, AWSM 105-124, Air Weather Service (MAC), Scott AFB, Ill.

nation is made whether a lid is present or not, the Skew T-Log P diagram can be used to compute a new stability index, introduced in the following section (4.2.1).

4.2.1 THE LID STRENGTH INDEX (LSI)

The purpose of the lid strength index (LSI) is twofold: (1) It determines the strength of the restraining inversion present over the lower troposphere; and (2) it determines the instability of air below the lid by computing a buoyancy term. The key to the LSI is its accounting for the presence of restraining inversion, something which no stability index currently in use by either the NWS* or AWS takes into account.

The LSI consists of the following two terms: (1) Buoyancy, defined as $(\theta_{sw5} - \bar{\theta}_w)$, and (2) lid strength, defined as $(\theta_{swMAX} - \bar{\theta}_w)$.

The buoyancy term is analogous to the Lifted Index (LI) and possesses about half of the numerical value of the LI under most circumstances. In fact, in an operational setting, the LI can be used in place of the buoyancy term. The lid strength term is a measure of the stabilizing effect of the inversion and is positive for cases where a lid exists. Recent work by Graziano⁵¹ suggests that the lid strength term and the buoyancy term (or LI) should be used separately (instead of being added together) to diagnose favorable conditions for severe thunderstorms. The results of Benjamin,⁴⁹ Lanicci,⁴⁷ and Graziano⁵¹ suggest that a critical value of lid strength appears to be around 2-3° C. Above this value, the lid effectively suppresses convection, and, below it, conditions for convection can be considered more favorable. This value corresponds to a lid strength appearing along the lid-edge region, and is based on both conventional analyses and numerical modeling results. A buoyancy term below about 1° C indicates potentially unstable conditions. The determination of both terms of the LSI on a typical lid sounding appears in Figure 10.

Another factor to be considered in the LSI is its sensitivity to diurnal changes in $\bar{\theta}_w$. Diurnal tendencies in surface heating, evaporation, and advection can alter $\bar{\theta}_w$, giving it a maximum during the late afternoon and a minimum during the nighttime hours.⁴⁷ This diurnal change in $\bar{\theta}_w$ influences both the lid strength and buoyancy terms by giving them smaller values during the afternoon than at night.

*NOAA Eastern Region Computer Programs and Problems Report No. 9 describes an automated procedure for computing stability for a parcel using the idea of energy areas. This procedure does take negative areas created by lid inversions into account.

51. Graziano, T. (1984) M.S. thesis, research in progress, The Pennsylvania State U., University Park, Pa.

This effect is real; it should be considered by the forecaster in regions where it may lead to important changes in the stability of the air mass.

4.2.2 SINGLE SOUNDING TECHNIQUES

In a base weather station setting, only one sounding can be plotted and analyzed because of time constraints. Appendix C contains two single-station forecast techniques that can be used to predict local changes in the lid resulting from advection, vertical mixing, and surface heating. These techniques can be used in conjunction with those methods outlined in this section.

4.3 The Lid Composite Chart

A lid composite chart is presented in Figure 11. The chart consists of the lid strength isotherms, 6° C dewpoint isopleth at 850 mb, plus the 850-mb convergence zones, moist axes, and drylines. The chart also contains two other parameters, the 850-700-mb shear vectors and the zone of maximum anticyclonic curvature of the shear vectors. These two parameters need some further explanation.

The 850-700-mb shear vectors represent the degree of stabilization or destabilization over the analysis region caused by differential advection. Differential advection is a process by which air at one level may be advected into an area at a speed and direction different from air at another level. In the case of the lid, if moist low-level air is being advected northward while the warm, dry air aloft is being advected northeasterly, a situation will soon occur where the moist air is advected into a region where the warm air aloft has been advected away. That region experiences a destabilization resulting from increasing low-level moisture combined with cold advection aloft. This situation most commonly occurs either just along the western lid edge or to the west of the edge, and the 850-700-mb shear vectors over this area are southwesterly (see Figure 12a). Conversely, the other areas will have low-level moist advection from the south, but warm air aloft is being advected in from the southwest. This situation results in the stability either staying the same or increasing because of the warm advection aloft.

Warm advection aloft usually occurs over the area that extends eastward from under the strongest portion of the lid. These 850-700-mb shear vectors are north or northwesterly, as indicated in Figure 12a. The zone of maximum anticyclonic curvature, then, denotes the area where the destabilization caused by low-level moist advection and cold advection aloft is just beginning to take place. If one were to examine only the components of the shear perpendicular to the lid isotherms, the zone of anticyclonic curvature would correspond to the area where these perpendicular components appear to "convergence" (see Figure 12b). Note that the anticyclonic curvature zone usually appears either along the lid edge or just slightly to the west or east of the edge. Thus, the area where this curvature

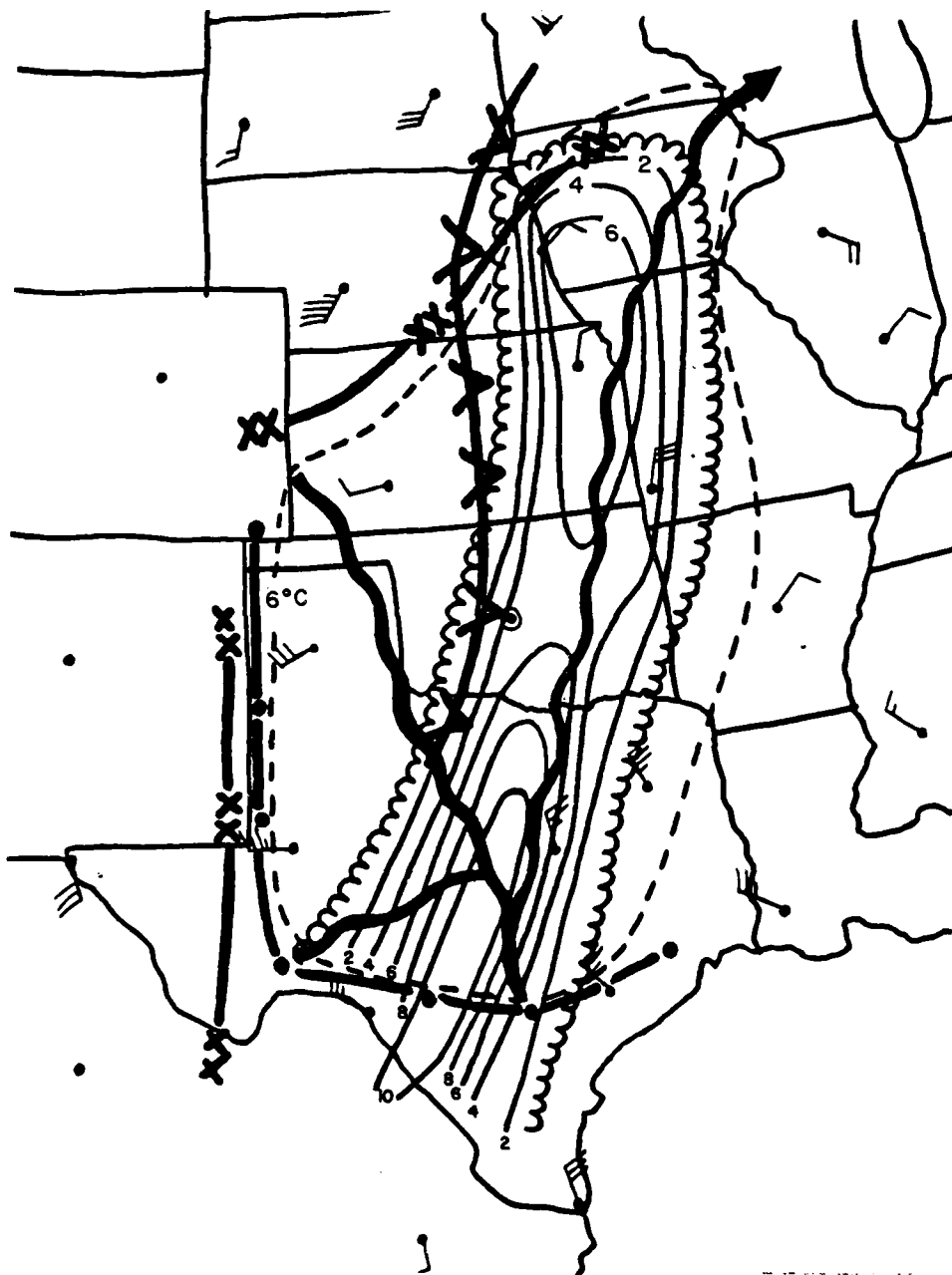


Figure 11. Composite Chart of Lid Parameters. The thin solid lines denote lid strength (in °C), with the scalloped border outlining the lid edge. The dashed line is the 6° C dewpoint isopleth at 850 mb. The plotted vectors denote 850-700-mb wind shear, and the thick solid line with V's denotes the axis of maximum anticyclonic curvature. Other symbols are shown in Figure A1

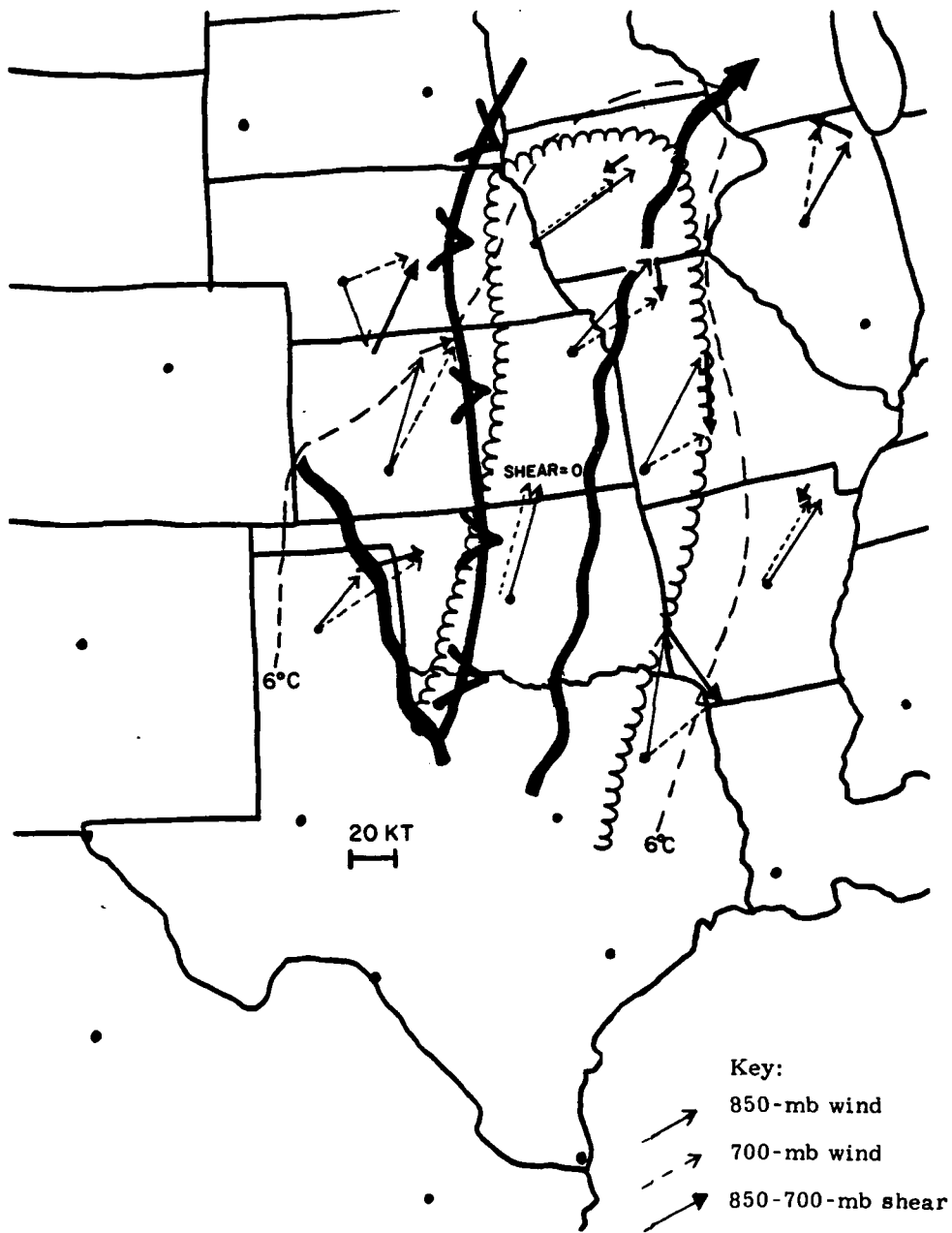


Figure 12a. Schematic Diagram Illustrating 850- and 700-mb Winds With Associated Shear Vectors and Their Relation to the Lid. Notice the sharp anticyclonic curvature zone appearing just west of and long the lid edge. This axis represents destabilization of the air mass through differential advection between 850 mb and 700 mb

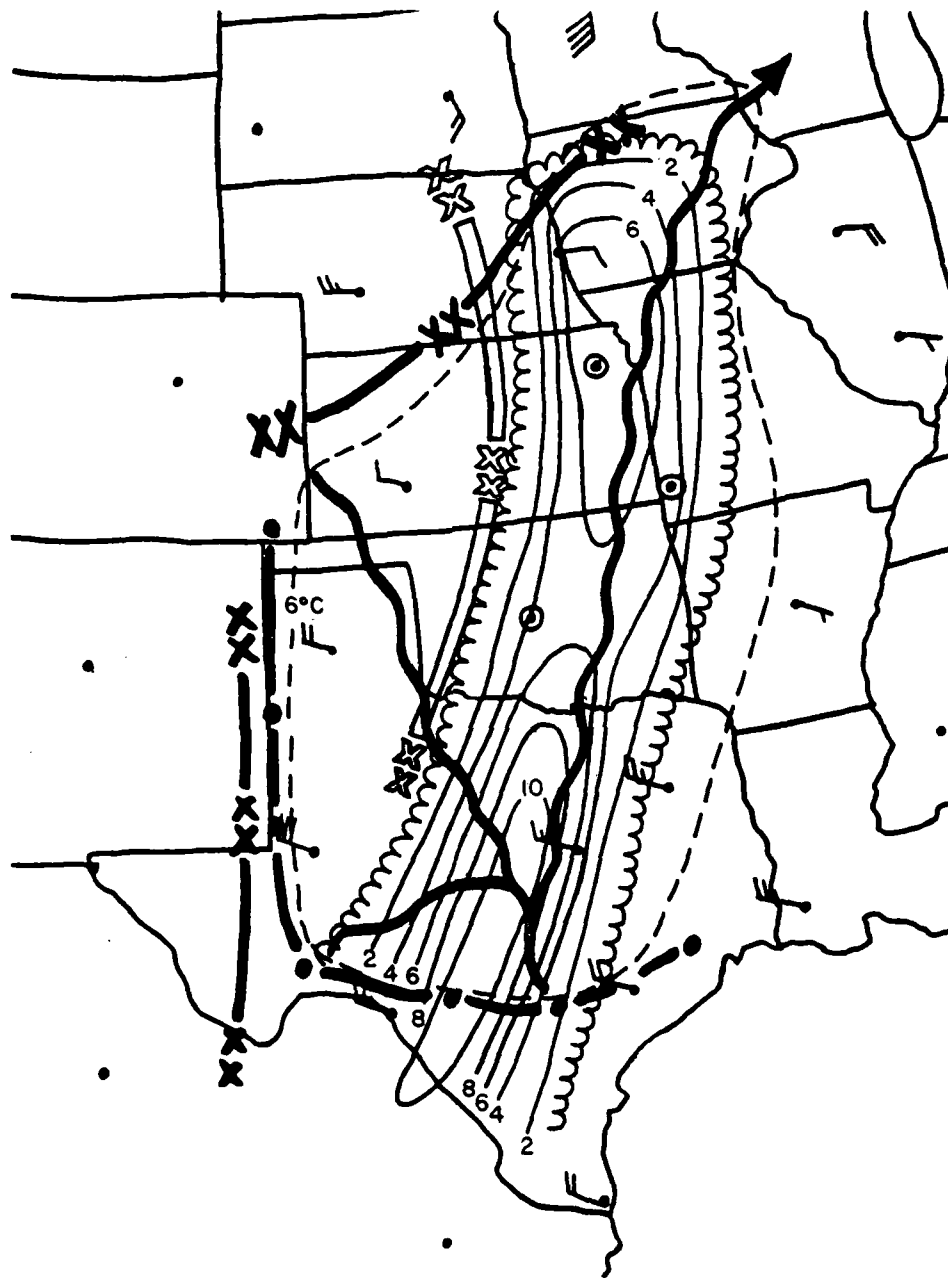


Figure 12b. Composite Chart of Lid Parameters. The thin solid lines denote lid strength (in °C), with the scalloped border outlining the lid edge. The dashed line is the 6°C dewpoint isopleth at 850 mb. The plotted vectors are the components of the 850-700-mb shear perpendicular to the lid strength isotherms. The line with open x's denotes the "convergence" of the component shear vectors, indicating lid removal through advection and coincident with the anticyclonic curvature zone shown in Figures 11 and 12a

axis appears, in combination with 850-mb moist advection, convergence, and other favorable low- and upper-level dynamic features, will be the location of the first thunderstorm cells.

Several reasons exist for choosing 850 mb and 700 mb. First, 850 mb represents the level of the moist air in most cases, while 700 mb represents the level of the warm, dry air above the inversion. Second, both 850- and 700-mb data are operationally available. In Appendix B, an alternate method for constructing the lid composite chart is presented in which 700-mb isotherms are used instead of lid strength. This method may be desirable in areas where an automated LSI program is not available.

5. SEVERE-STORM FORECASTING IN A LID SITUATION

In this section, two detailed case studies are presented where the presence of a lid played a major role in determining the extent and severity of the outbreak. In the first case, 3-4 April 1981, the lid clearly originated over the Mexican plateau. In the second case, 13 May 1981, the lid source-regions were the Mexican plateau and the desert southwest.

5.1 The Outbreak of 3-4 April 1981

5.1.1 SYNOPTIC SITUATION

On the morning of 3 April 1981, a vigorous frontal system was beginning to enter the Great Plains from the southern Rocky Mountains. A deep upper trough existed at this time over the western United States, and several embedded short waves moved through this trough into the southern and central plains states during the next 24 hours. This case falls into the Miller Synoptic Type B category (see Table 2). Precipitation associated with this storm was varied, ranging from very heavy snows over most of Wyoming to rainshowers and isolated thunderstorms over South Dakota, Minnesota, and northern Iowa. Isolated rain and rainshowers were occurring over northern Kansas and central Oklahoma at this time as well.

5.1.2 COMPOSITE ANALYSES

The composite surface analysis for 1200 GMT on 3 April 1981 is shown in Figure 13. Notice the low-level convergence taking place along the warm-frontal boundary over Kansas, Nebraska, and Minnesota. Also notice the axes of moisture advection over the eastern halves of Texas, Oklahoma, Kansas, and Nebraska. Strong surface-pressure falls appear over western Oklahoma, northeastern Kansas, most of Iowa, and north of the warm front over Minnesota and South Dakota. A short dryline is present over southwest Texas at this time.

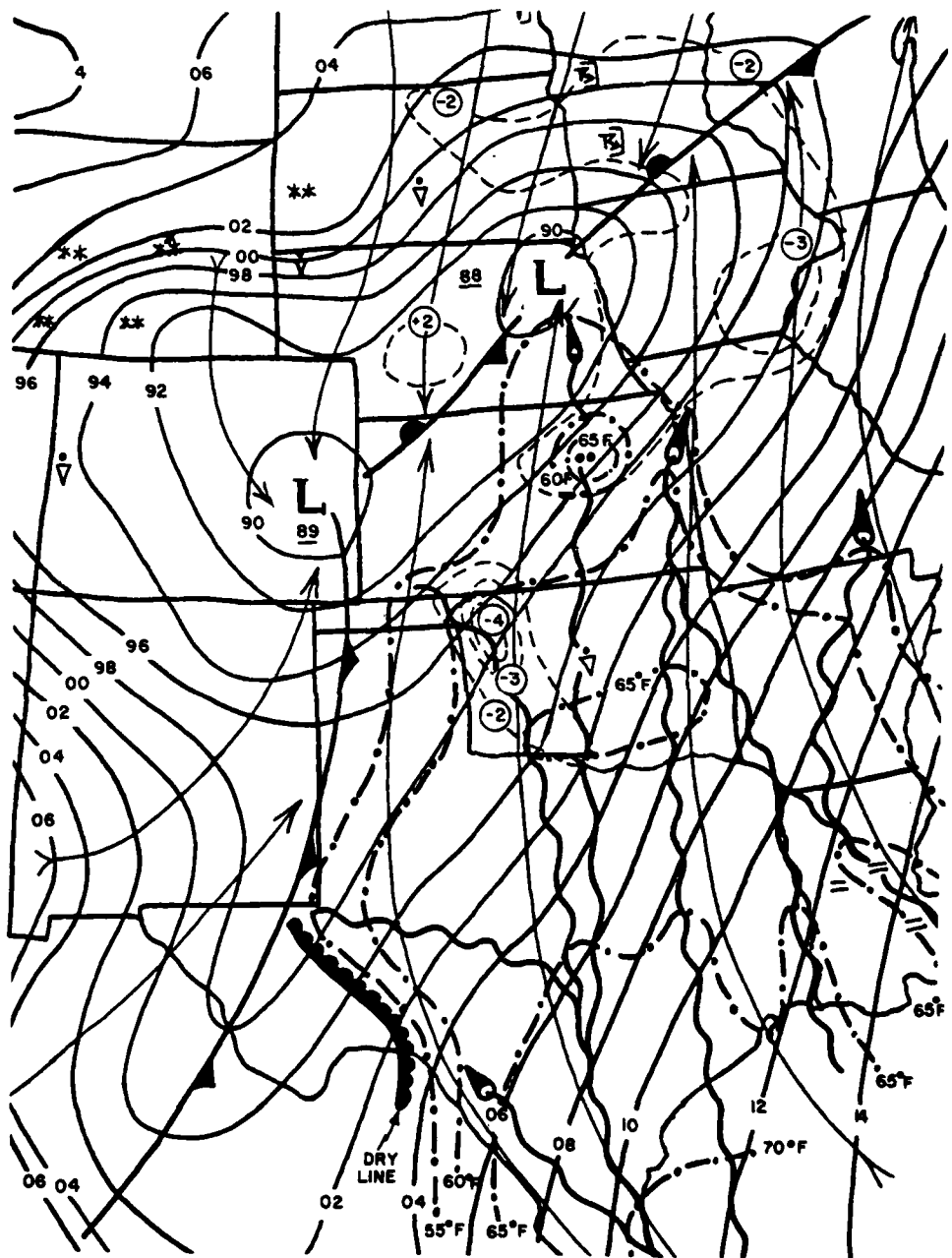


Figure 13. Surface Composite Chart for 1200 GMT 3 April 1981. Streamlines are denoted by thin arrows, while moisture axes are shown by thick curvy lines. Isallobars are dashed lines, and isodrosotherms are dot-dashed lines. Other symbols are conventional

The upper air composite analyses shown in Figures 14a, 14b, and 14c reveal several important features. Over Kansas, eastern Nebraska, and western Iowa, favorable 850-mb parameters (Figure 14a) include convergence, a favorable thermal ridge/moisture axis configuration, and a 55-knot jet. At 700 mb (Figure 14b), the beginnings of cold advection can be seen across Kansas and Nebraska (see the 700-mb temperature no-change line). At 500 mb (Figure 14c), 12-hour height falls in excess of 100 m exist over most of Nebraska, and a jet is present over Kansas, Nebraska, and Iowa with an embedded 90-knot jet streak over the Texas Panhandle. Total totals indices greater than 56 extend from western Oklahoma across Kansas into southeastern Nebraska, southwestern Iowa, and northwest Missouri (see Figure 14d). Total totals indices greater than 56 are favorable for the formation of tornadic thunderstorms (see Table 1). Another key area is western and central Oklahoma and northern Texas. Two 850-mb moisture axes exist over this area, one over the central portion and the other over the panhandles of Oklahoma and Texas. The low-level thermal ridge is west of the moist axis over Oklahoma and central Texas. Low-level convergence and a dryline are present over the Texas-New Mexico border and are associated with the advancing surface front. Two low-level jets appear over Oklahoma and central Texas. The 700-mb temperature no-change line is located over the eastern portion of the Texas Panhandle, but the crossing angle with the winds is small. There are two jets at 500 mb, one over the panhandle (with the 90-knot jet streak) and one over northern Texas and southeastern Oklahoma. A 500-mb diffluence zone exists from extreme eastern Oklahoma into Arkansas, and 12-hour height falls are in excess of 50 m over western Texas and Oklahoma. Total totals in excess of 56 cover western Oklahoma and the eastern Texas Panhandle.

An overall inspection of the surface and upper-air analyses for 1200 GMT on 3 April 1981 indicates that the regions of eastern Kansas, eastern Nebraska, and western Iowa are favorable for the development of tornadic thunderstorms during the next 12 hours. The regions of western and central Oklahoma and northern Texas also appear favorable for severe-thunderstorm development during the next 12 hours. Notice from the 700-mb analysis (Figure 14b) that a dry front does not appear over any of these Kansas, Nebraska, and Iowa regions. The absence of this feature (as explained in section 5.1.3) is the result of the presence of a lid over most of the southern plains states at this time.

5.1.3 REVIEW OF LID PARAMETERS

A Mexican lid was present over a good portion of the southern Great Plains on the morning of 3 April 1981. A 700-mb lid-parameter chart is shown in Figure 15. It shows that the thermal ridge associated with temperatures greater than 8° C extends from northern Mexico into southeastern Kansas and western Missouri. The

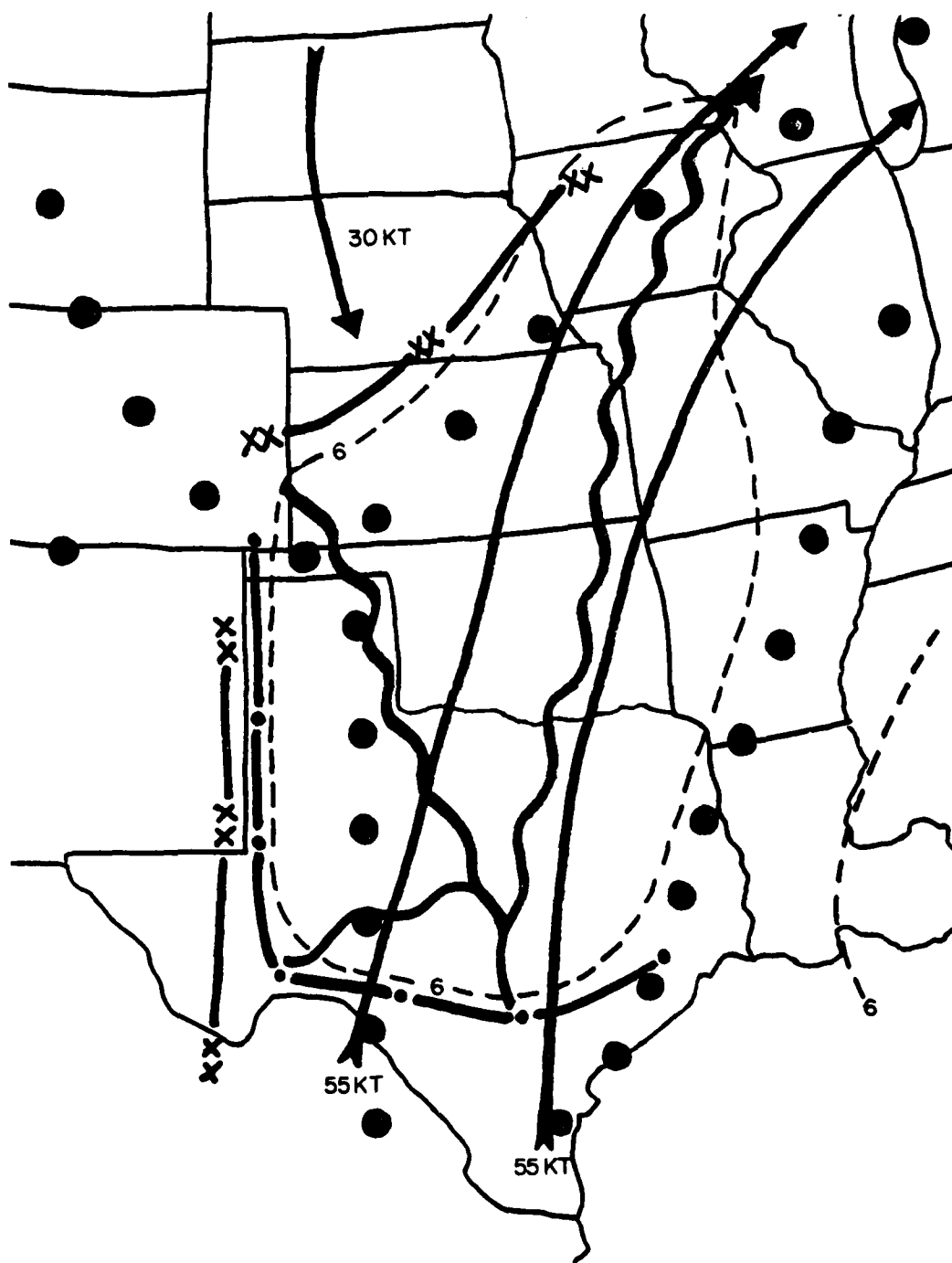


Figure 14a. Upper-Air Composite Analysis for 1200 GMT 3 April 1981. Chart shown is 850 mb. Symbols are defined in Figure A1

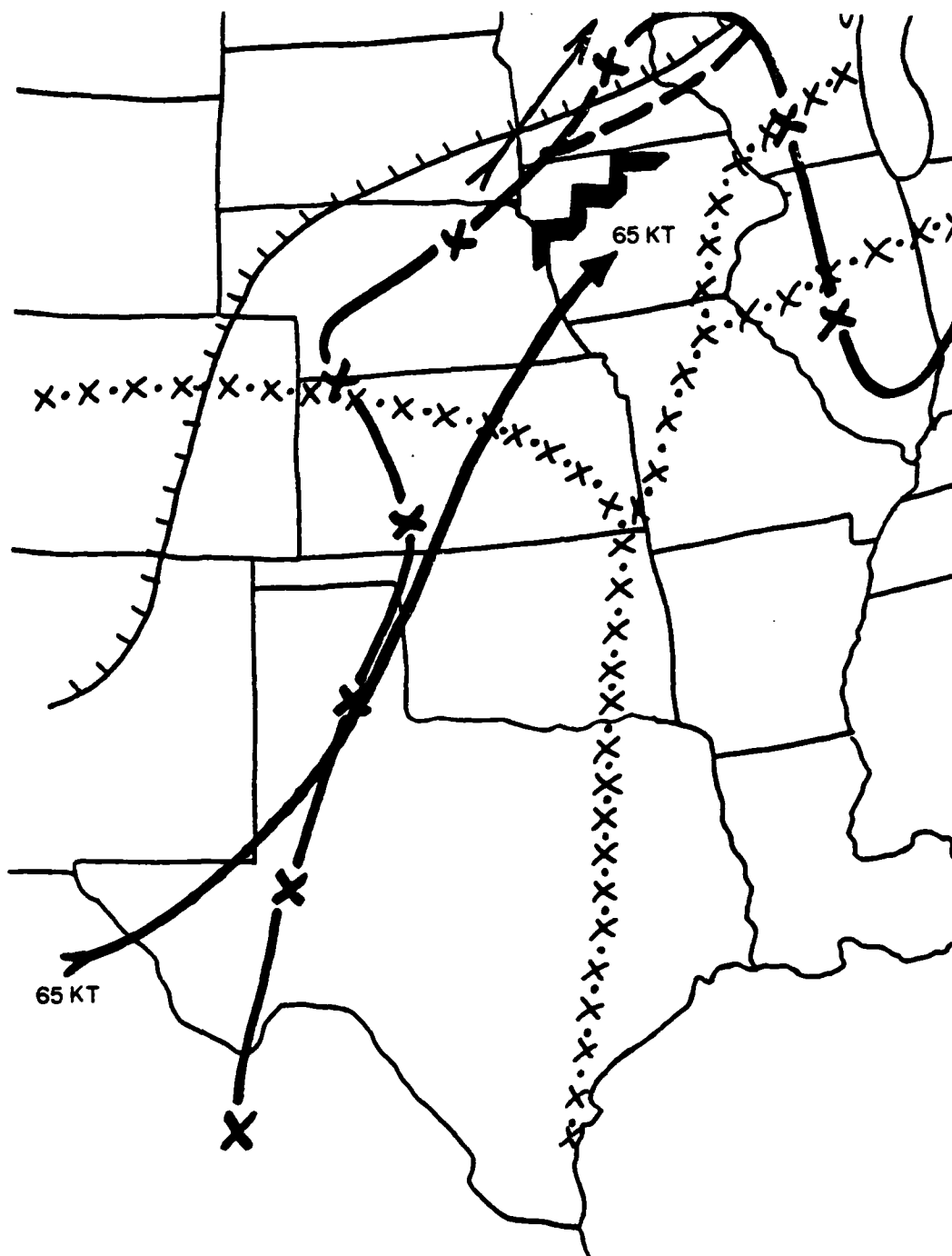


Figure 14b. Upper-Air Composite Analysis for 1200 GMT 3 April 1981. Chart shown is 700 mb. Symbols are defined in Figure A1

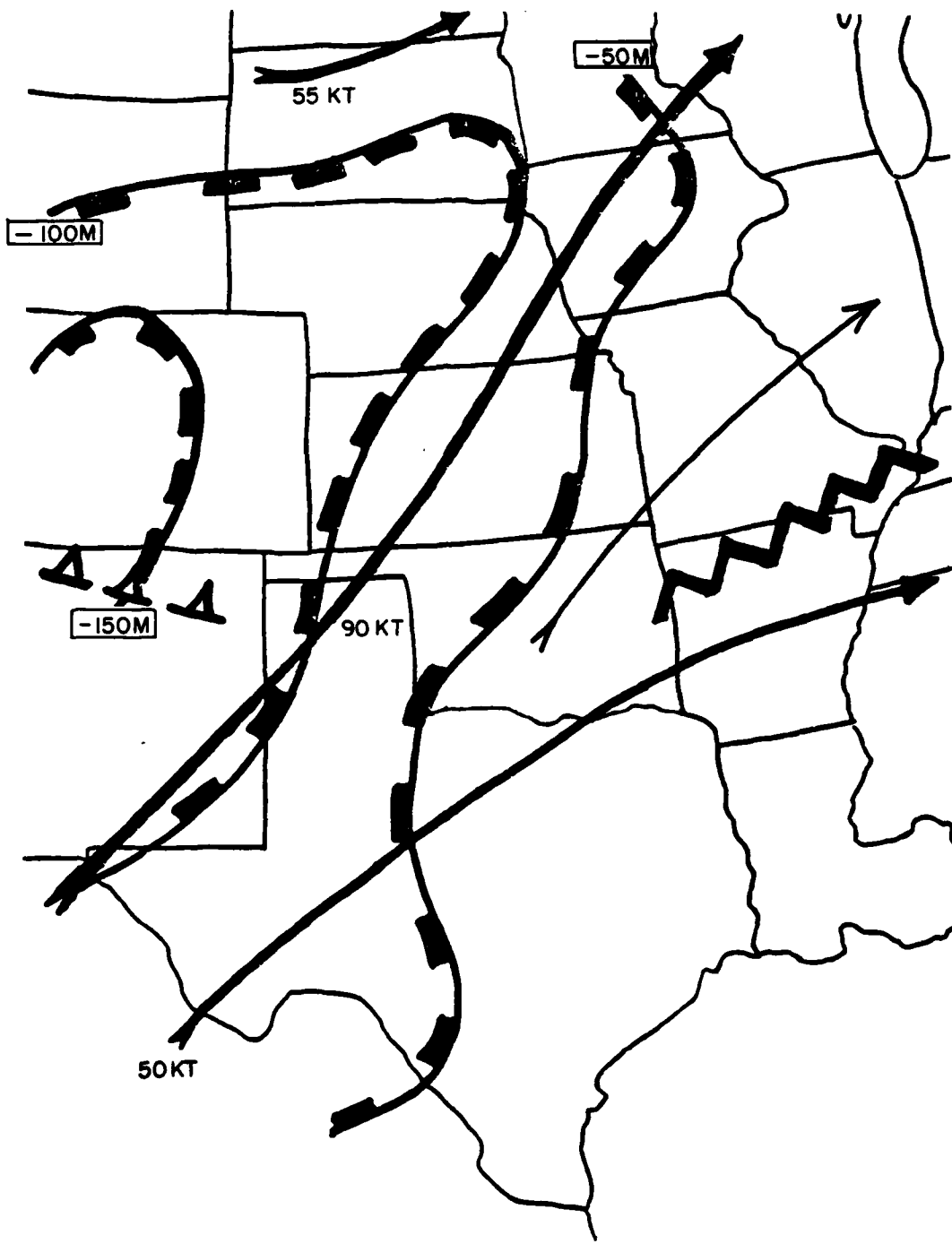


Figure 14c. Upper-Air Composite Analysis for 1200 GMT 3 April 1981. Chart shown is 500 mb. Symbols are defined in Figure A1

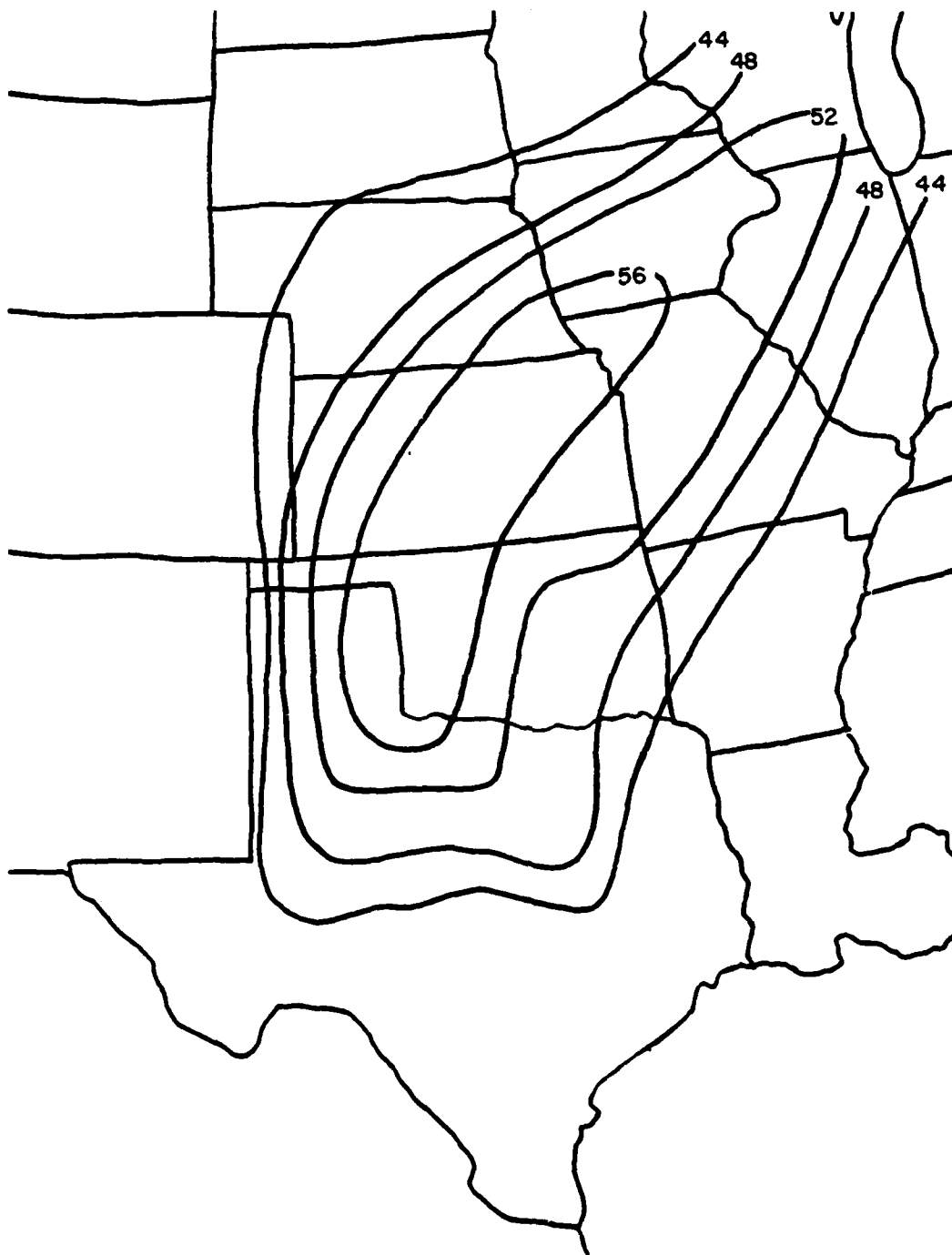


Figure 14d. Total Totals Analysis for 1200 GMT 3 April 1981

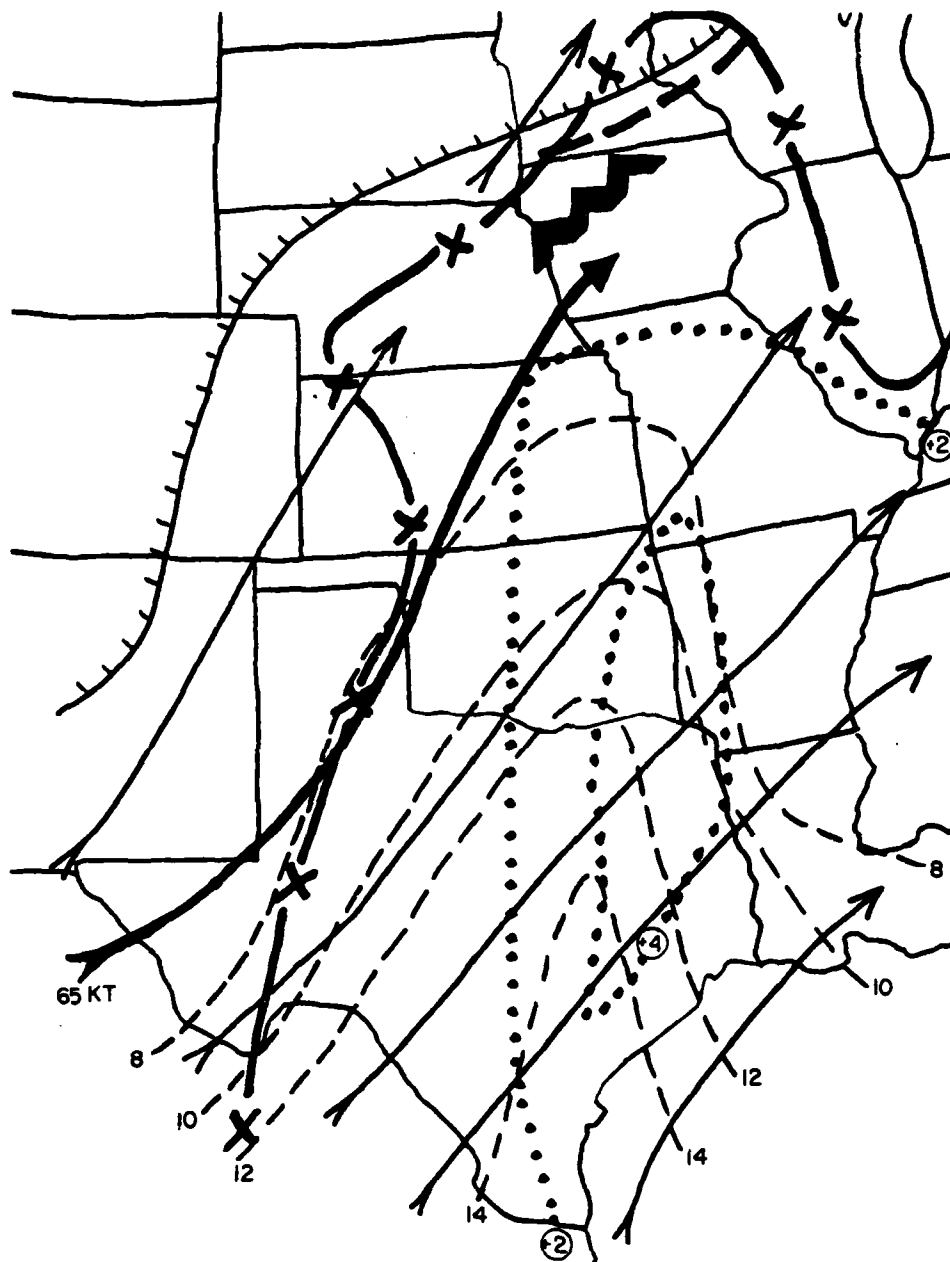


Figure 15. 700-mb Lid-Parameter Chart for 1200 GMT 3 April 1981. The ribbed border denotes dewpoint depressions of 6°C or less. The dotted lines represent 12-hour temperature changes of 2°C and 4°C . The middle troposphere has become more stable during the last 12 hours over the areas enclosed by the dotted lines. The locations of temperature-change lines (including the no-change line) and the cross-isotherm flow angles help determine the movement of the lid by advection. Other symbols are defined in Figure A1

flow at 700 mb suggests that the lid source-region is over northern Mexico and that the lid is being advected towards the northeast. The temperature no-change line indicates areas where convection is likely to begin because of cold advection, and the 2° C and 4° C 12-hour temperature-change lines indicate areas where warming has taken place over the last 12 hours at 700 mb and where the onset of convection will be delayed. The 700-mb lid-parameter chart shows that the eastern halves of Texas and Oklahoma are effectively capped by the lid, as indicated by the thermal ridge, temperatures $\geq 8^{\circ}$ C, the cross-isotherm flow angle (warm advection), and the 2-4° C 12-hour temperature-change lines. However, most of Kansas and the western halves of Texas and Oklahoma are likely to see the lid weaken or completely disappear during the next 12 hours because the cross-isotherm flow angle indicates cold advection, the thermal ridge is located east of this region, and the 12-hour temperature changes are weakly positive or zero.

A look at the 850-mb lid-parameter chart (Figure 16) indicates that the lid source-region is indeed over northern Mexico, and the presence of the 850-mb dryline in an east-west orientation across southern Texas suggests that the lid base is below 850 mb over southern Texas (that is, the air at 850 mb over southern Texas is dry Mexican air), while over the areas to the north, the air at 850 mb is moist Gulf air (implying a lid base above 850 mb, suggesting that the lid base is rising towards the north).

Next, the lid analyses for 1200 GMT 3 April 1981 are presented (Figures 17a and 17b). The lid-strength analysis presented in Figure 17a indicates that the strongest lid ($>10^{\circ}$ C) is present over south central Texas, and lid strengths greater than 6° C exist over eastern Kansas, southeastern Nebraska, southwestern Iowa, and northwestern Missouri. Compare the location of the strongest lid contours with the 700-mb lid chart in Figure 15. Note that the strongest lid corresponds to the 700-mb thermal ridge from northern Texas to eastern Kansas. However, also notice that the lid is present as far north as northern Iowa, while this area is cooler than 8° C at 700 mb. This occurs because the potential temperature of the adiabatic layer above the inversion is less than 38° C over this area. Keep in mind that the lid strength is a temperature difference between two levels, while the 700-mb chart considers temperatures at only one level. Thus, examination of both upper-air soundings and conventional charts is essential in identifying the lid region. The western lid edge, according to Figure 17a, extends from southwestern Texas into western Oklahoma, central Kansas, and eastern Nebraska. Notice the break in the 6° C lid-strength contour over central Oklahoma. This suggests that the lid is weaker over central Oklahoma than over areas to the north and south. The buoyancy analysis in Figure 17b shows that the most potentially unstable air is from central Oklahoma to eastern Kansas. A typical lid sounding from this case is shown for Topeka, Kansas (Figure 17c). Notice the dramatic relative humidity

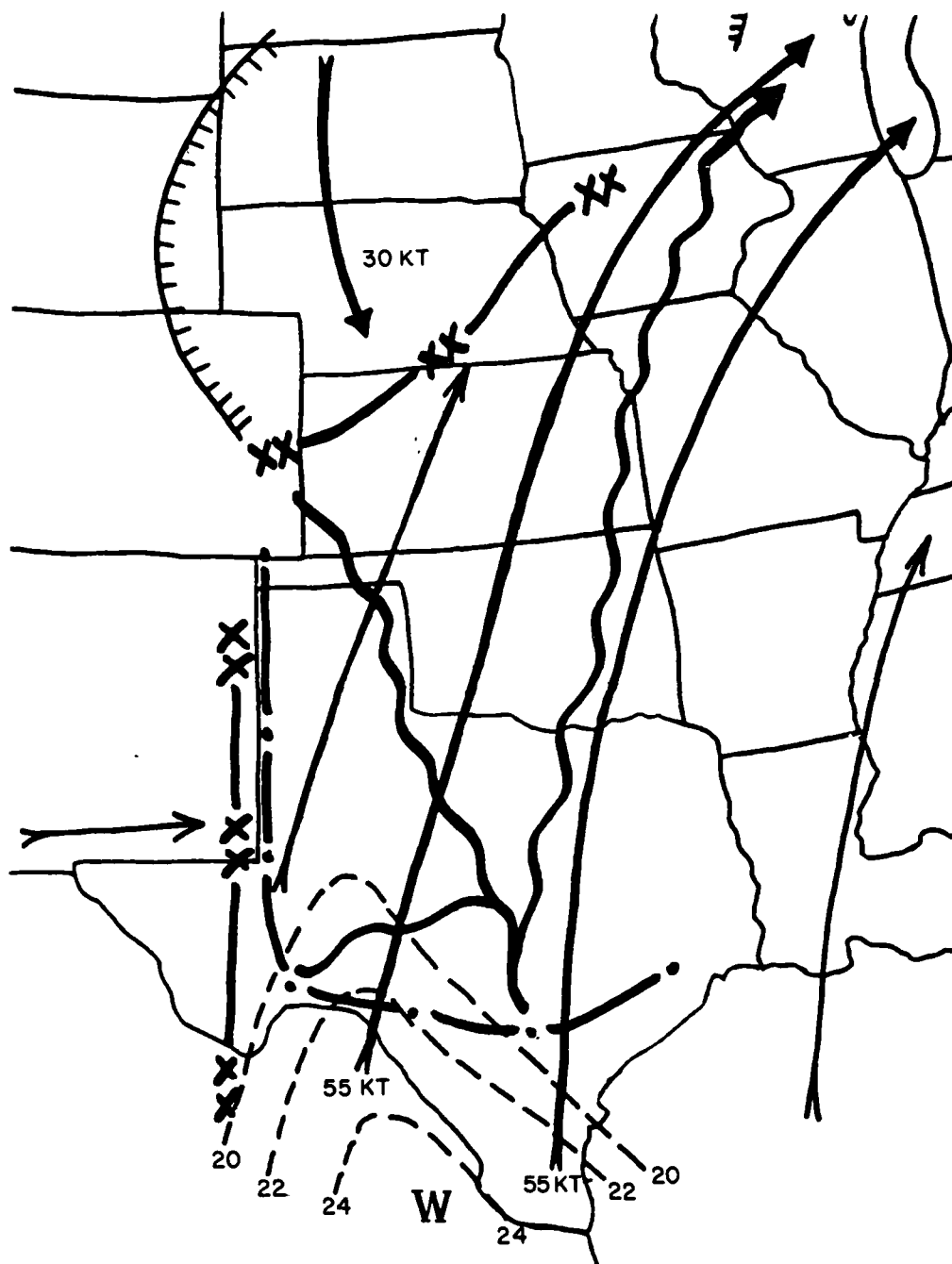


Figure 16. 850-mb Lid-Parameter Chart for 1200 GMT 3 April 1981. Symbols are defined in Figure A1

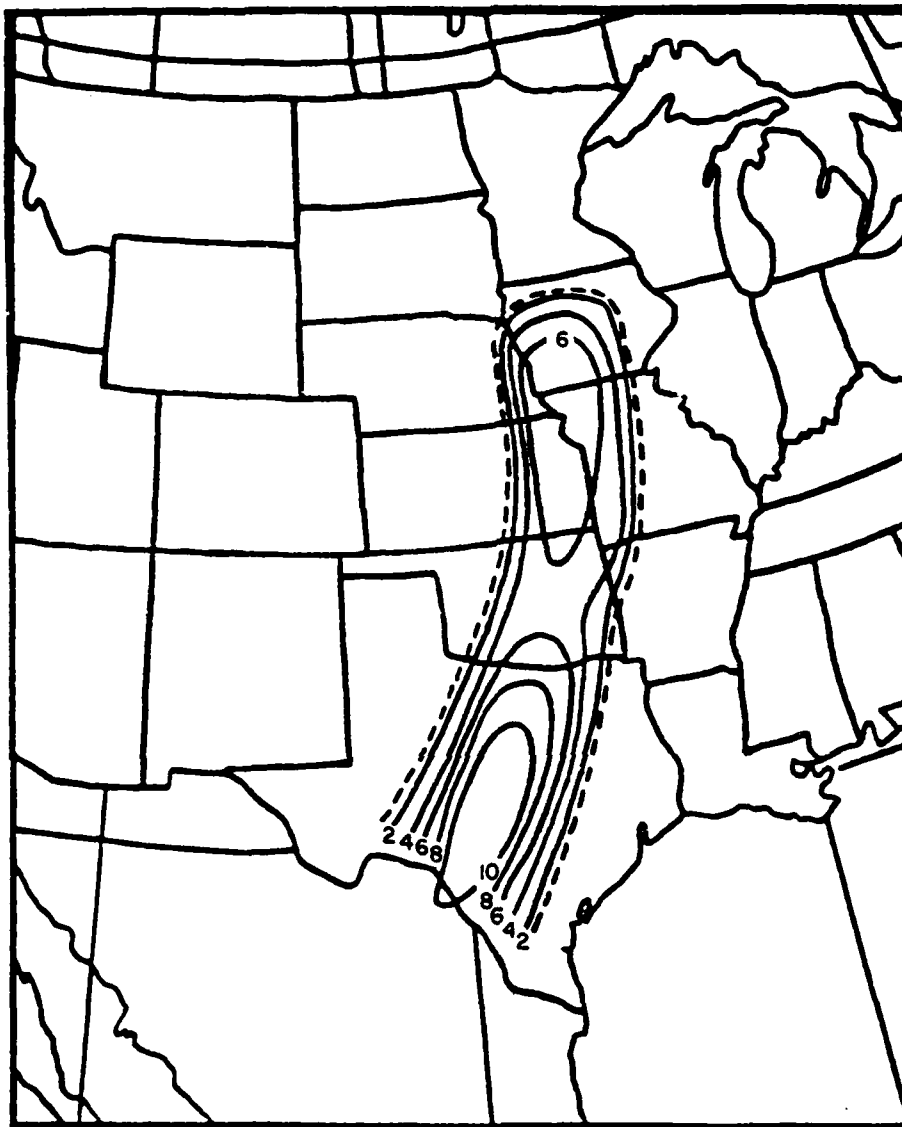


Figure 17a. Lid-Strength Analysis (in °C) for 1200 GMT 3 April 1981. Dashed contour (1° C lid strength) denotes lid edge

break at 850 mb, the inversion from 836 mb to 815 mb, and the nearly dry-adiabatic layer between 815 mb and 550 mb. Using the methods outlined in section 4.2, the buoyancy term is -1.7°C , and the lid strength is 7.4°C .

Finally, a composite lid chart is shown in Figure 18. Note the location of the anticyclonic curvature zone from South Dakota through east-central Nebraska, cen-

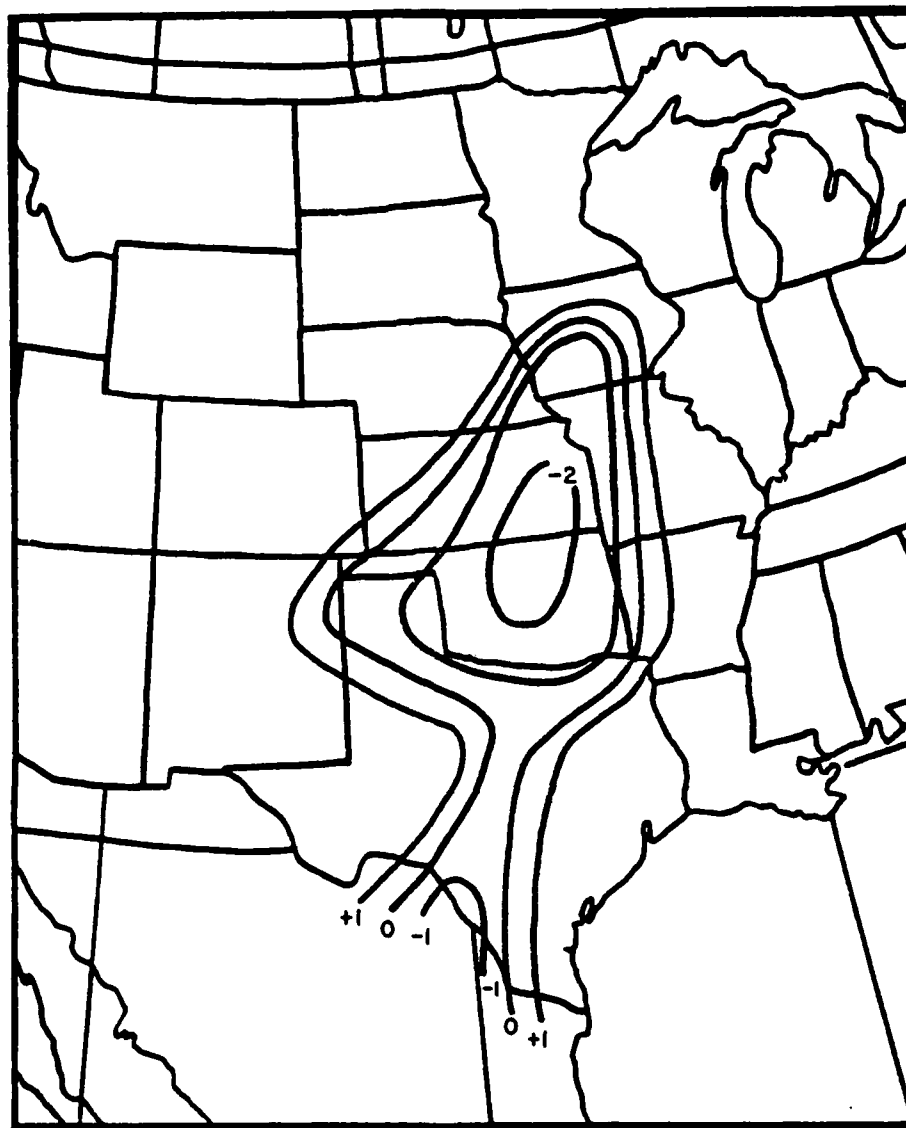


Figure 17b. Buoyancy Term Analysis (in °C) for 1200 GMT 3 April 1981. Analysis is performed over areas both inside and outside of lid to reveal regions of potential instability

tral Kansas and Oklahoma, and into northern Texas. Notice the proximity of the curvature zone to the lid edge and low-level convergence zone over east central-Nebraska. The combination of convergence and differential advection will remove the lid rapidly over this region, allowing thunderstorms to begin developing in the moist air. If the relatively weak lid is removed over central Oklahoma, this area

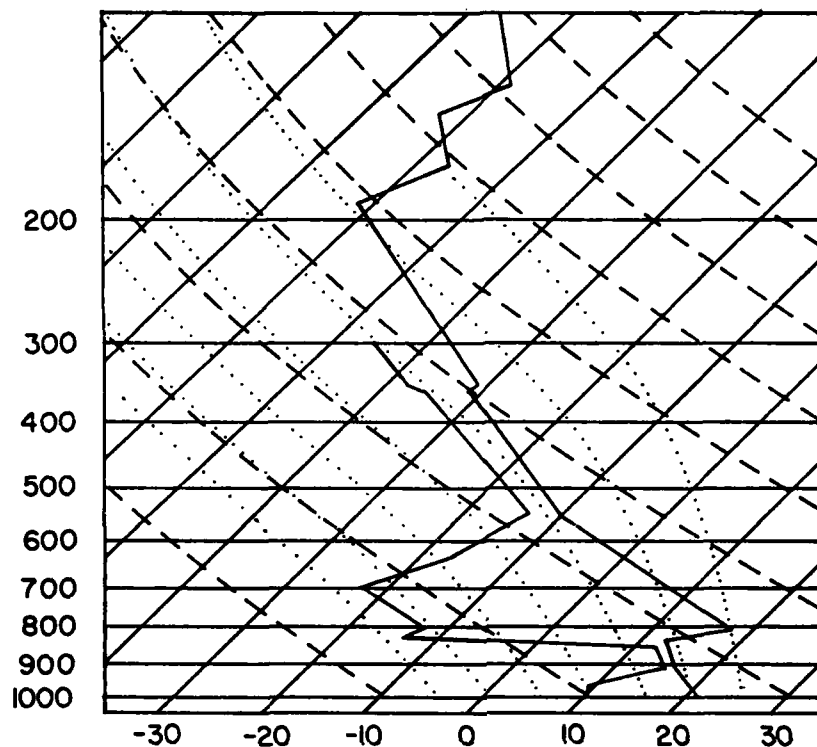


Figure 17c. Skew T-Log P Sounding for Topeka, Kansas, at 1200 GMT 3 April 1981. Notice the strong inversion and relative humidity break near the base of the Mexican air mass (around 830 mb)

will also be a favorable one for severe-storm development. Thunderstorms are unlikely from central and southern Texas eastward, because of the strong lid present and relative stabilization of the air mass occurring as the lid moves eastward into this region. Severe convection over eastern Kansas, eastern Nebraska, and western Iowa will be delayed until the lid is eroded in this area. The same is true for northern Texas. Since the lid is being advected towards the northeast, a combination of advection and convective erosion can allow thunderstorms to spread into regions with initially high lid-strength values.

5.1.4 FORECAST AND VERIFICATION

Figures 19 and 20 show the analysis and 12-hour forecast panels, respectively, of the LFM model for this case. Figure 19 shows that positive vorticity advection (PVA) is taking place over northern Oklahoma and southern Kansas. The 12-hour forecast in Figure 20 suggests that PVA will exist from the Texas Panhandle through Oklahoma, Kansas, and western Iowa by 0000 GMT on 4 April. The surface low is predicted to move from southeastern Colorado into northeastern Kansas

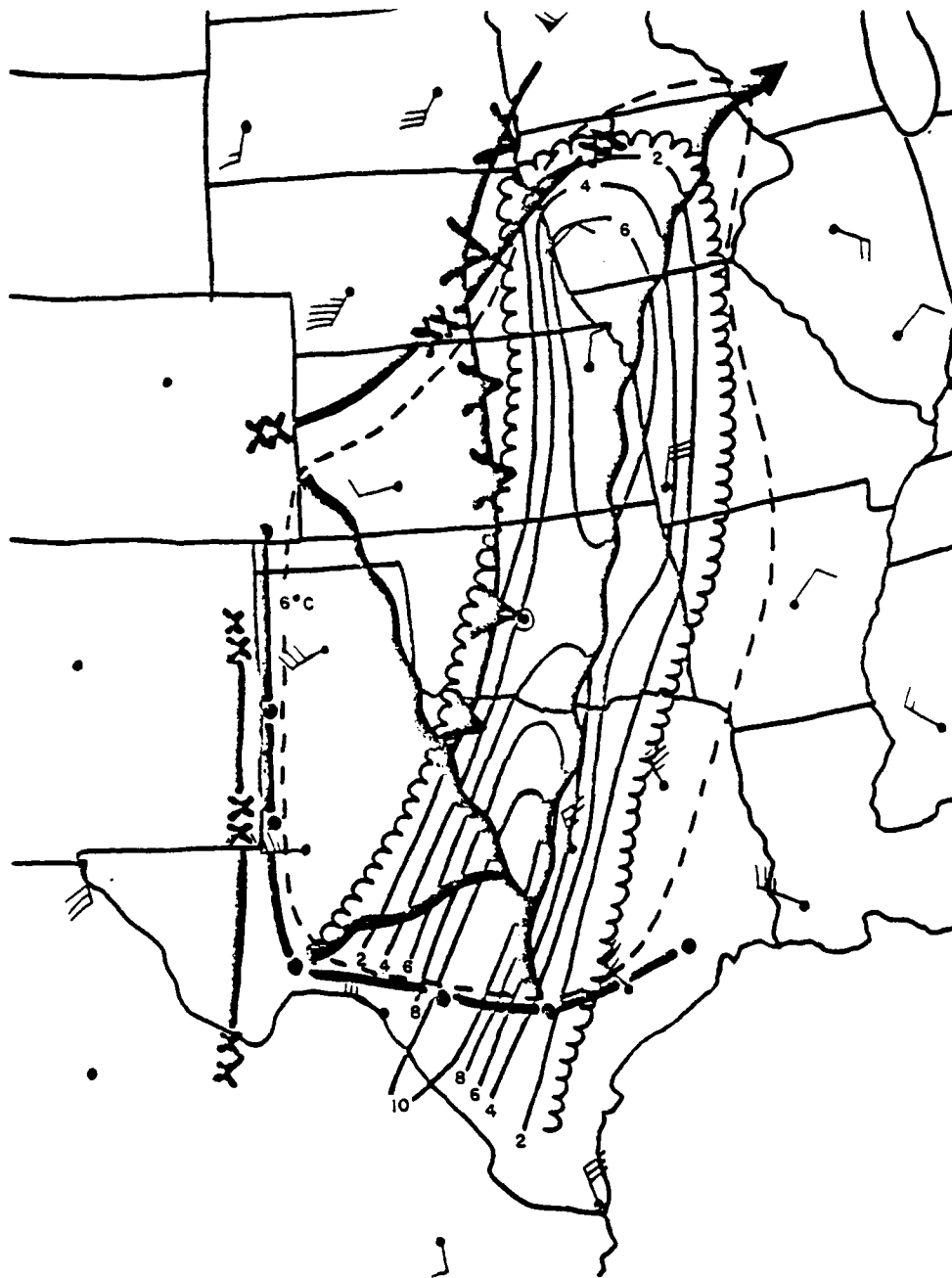


Figure 18. Composite Lid Chart Using Lid-Strength Analysis, 850-mb Features, and 850-700 mb Shear Vectors, for 1200 GMT 3 April 1981. The thin solid lines denote lid strength (in ° C), with the scalloped border outlining the lid edge. The dashed line is the 6° C dewpoint isopleth at 850 mb. The plotted vectors denote 850-700 mb wind shear, and the thick solid line with V's denotes the axis of maximum anticyclonic curvature. Other symbols are as in Figure A1

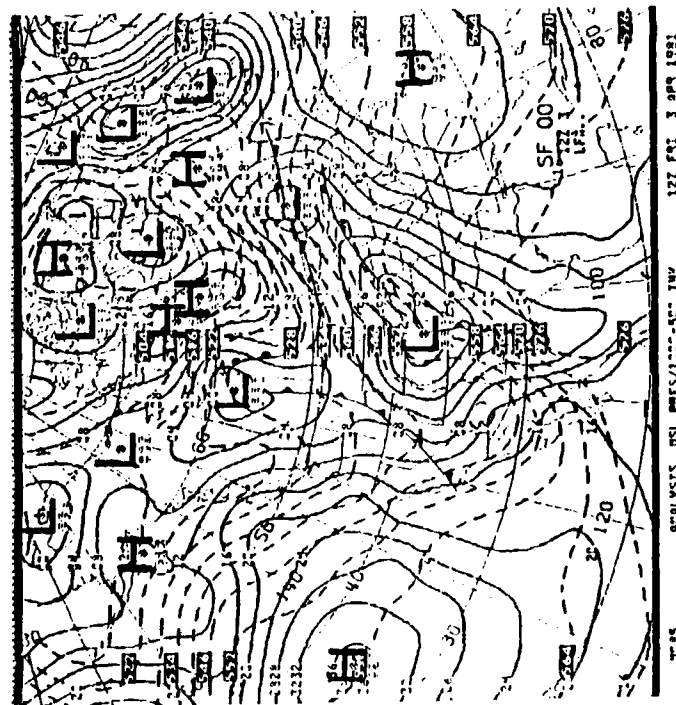
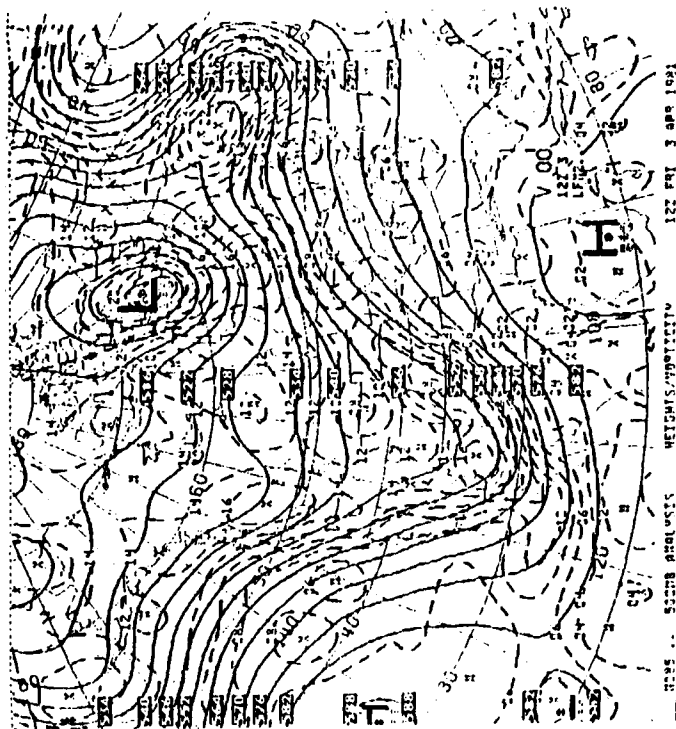


Figure 19. LFM Analyses for 1200 GMT 3 April 1981. Left panel is sea level pressure and 1000-500 mb thickness (with analyzed surface fronts superimposed). Right panel is the 500 mb height and absolute vorticity analysis

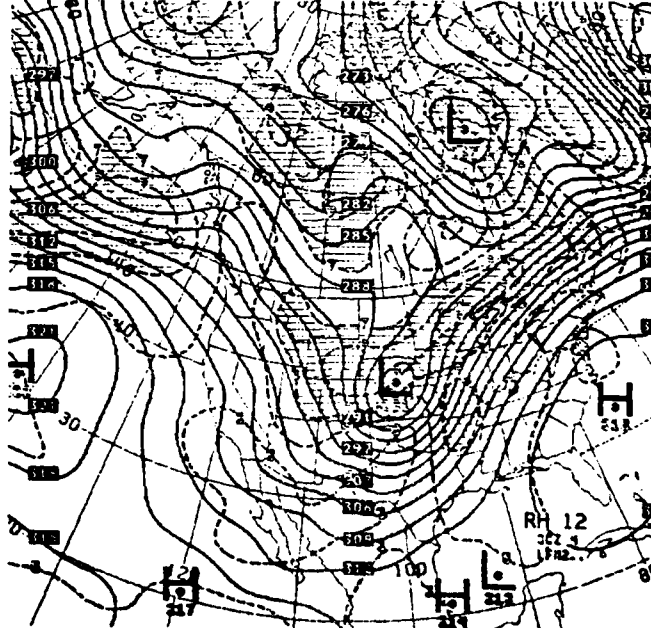
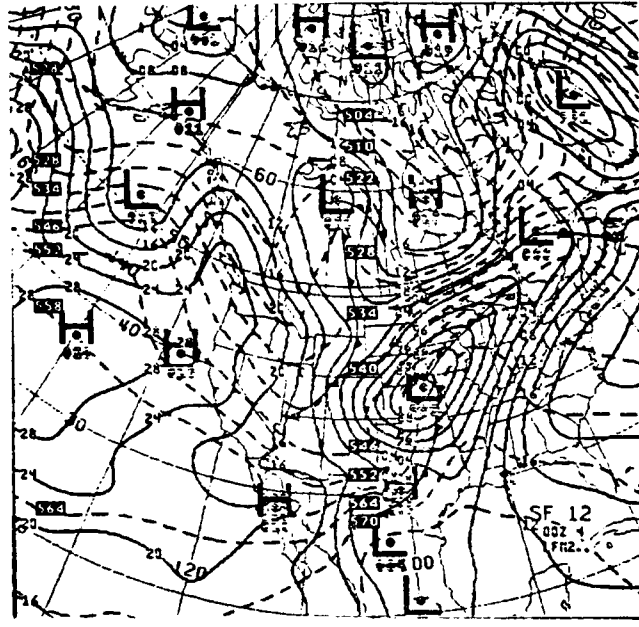


Figure 20. 12-Hour LFM Forecasts for 0000 GMT 4 April 1981. Top panel is sea level pressure and 1000-500 mb thickness (with frontal positions superimposed). Bottom panel is 700 mb height and mean relative humidity between 1000 mb and 500 mb

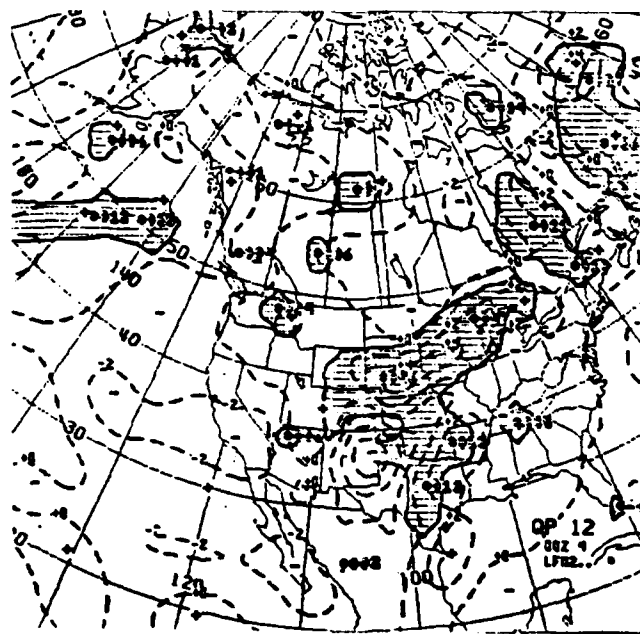
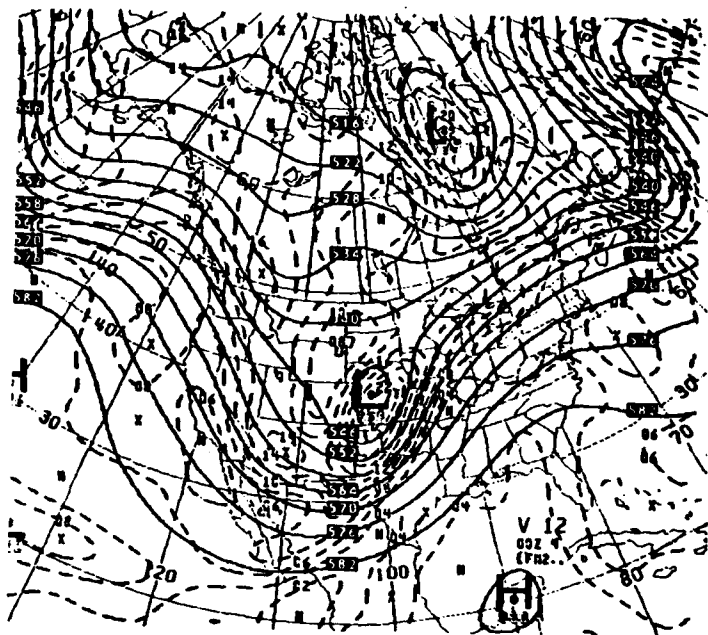


Figure 20 (Contd). 12-Hour LFM Forecasts for 0000 GMT 4 April 1981. Top panel is 500 mb height and absolute vorticity. Bottom panel is 6-hour precipitation (in inches) and 700 mb vertical velocities (in cm s^{-1})

by 0000 GMT, while the surface cold front moves from the Texas-New Mexico border, across central Texas and Oklahoma, and into eastern Kansas. Significant vertical velocities ($w \geq 4 \text{ cm s}^{-1}$) are predicted by 0000 GMT over Nebraska, Iowa, and southern Minnesota, and areas of $w \geq 2 \text{ cm s}^{-1}$ exist from southern Missouri through Arkansas, eastern Oklahoma, and southward into eastern Texas.

A complete severe-weather forecast based on the composite and LFM analyses, lid parameter charts, and 12-hour LFM forecast panels can now be presented for the period 1200 GMT 3 April to 0000 GMT 4 April 1981. Tornadoic thunderstorms appear likely from eastern Kansas into eastern Nebraska and western Iowa. These storms will likely develop along the lid edge over Kansas and Nebraska and spread eastward. Central Oklahoma is also likely to experience severe thunderstorms associated with the approaching surface front and removal of the weaker lid there, and these storms may spread into northern Texas through erosion of the lid.

The verification for this case is presented in Figure 21a. Early on the morning of 3 April, several isolated severe thunderstorms, associated with warm-frontal convergence and the approaching surface low from Nebraska, occurred over southern Minnesota and northwestern Illinois before the lid was advected into that area. An intense outbreak of severe thunderstorms and tornadoes began over east-central Nebraska (along the lid edge) around 1900 GMT (1300 LST) and spread into northeastern Kansas and the western half of Iowa by 2300 GMT (1700 LST). A second outbreak associated with lid removal caused by the approaching surface cold front occurred over central Oklahoma beginning around 2000 GMT (1400 LST) and spread into northern Texas during the next four hours. It should be noted that during this 12-hour period, no severe storms were reported over the area from southern and central Texas eastward, where the lid was strongest and warm advection aloft took place. The lid strength analysis for 0000 GMT 4 April 1981 (Figure 21b) indicates this movement of the Mexican airmass. It should also be noted that this outbreak continued into the night and did not dissipate over the central and southern plains states until the early morning hours of 4 April.

5.2 The Outbreak of 13 May 1981

5.2.1 SYNOPTIC SITUATION

At 0000 GMT 13 May 1981, a quasi-stationary frontal system extended from southern Nevada through the southern Rockies to a low along the Texas New-Mexico border. A warm front was beginning to form across the Texas Panhandle and northern Texas. High pressure from western Canada was moving into the intermountain region. This case most closely resembles the Miller synoptic Type C (see Table 2). Precipitation associated with the frontal system consisted of light

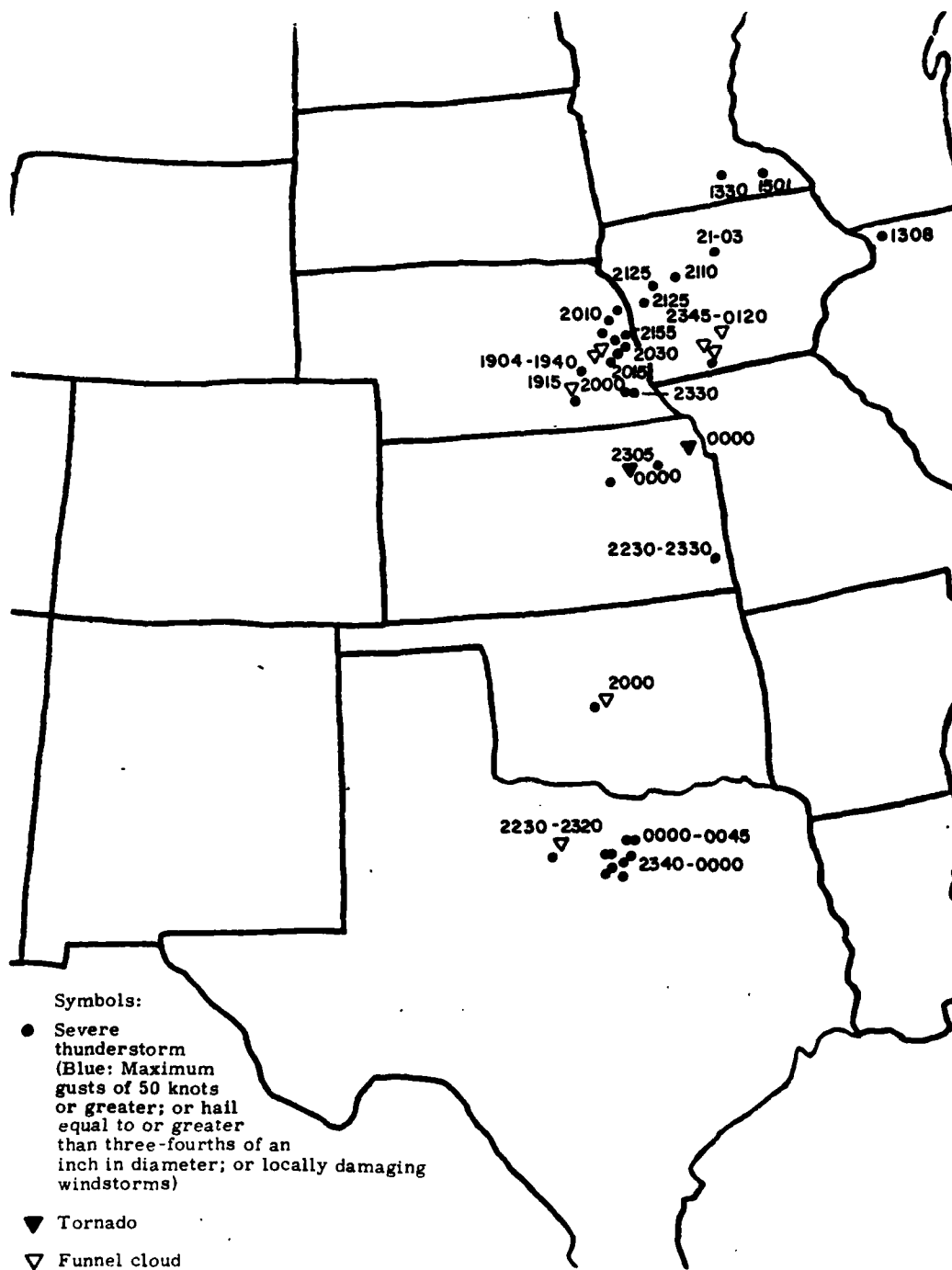


Figure 21a. Severe Weather Reports for 1200 GMT 3 April-0000 GMT 4 April 1981. Approximate time of occurrence (in GMT) is shown next to event

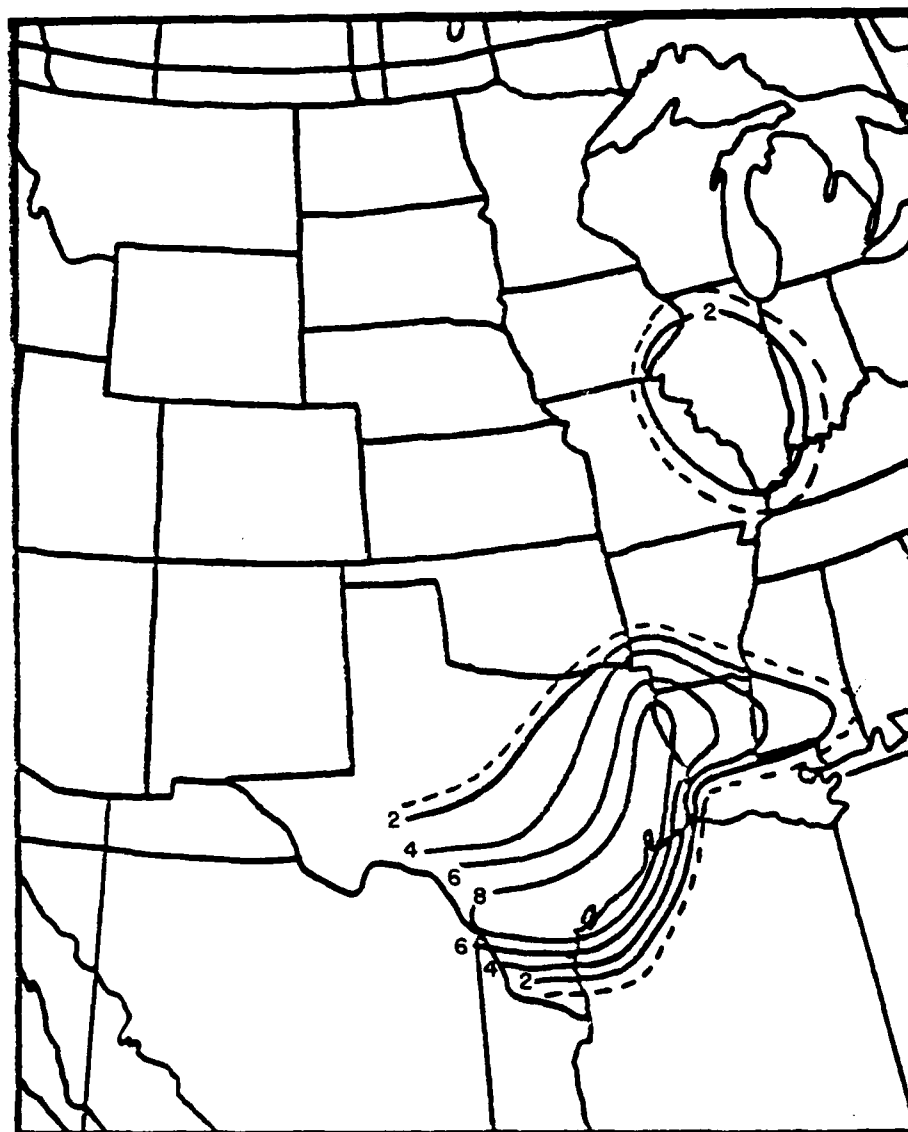


Figure 21b. Lid-Strength Analysis (in °C) for 0000 GMT 4 April 1981. Dashed contour (1° C lid strength) denotes lid edge

rain and rainshowers over most of Montana, Wyoming, Colorado, and portions of South Dakota, Iowa, and Missouri.

5.2.2 COMPOSITE ANALYSES

The composite surface analysis for 0000 GMT on the 13th is shown in Figure 22. Strong low-level convergence is taking place over eastern Colorado and

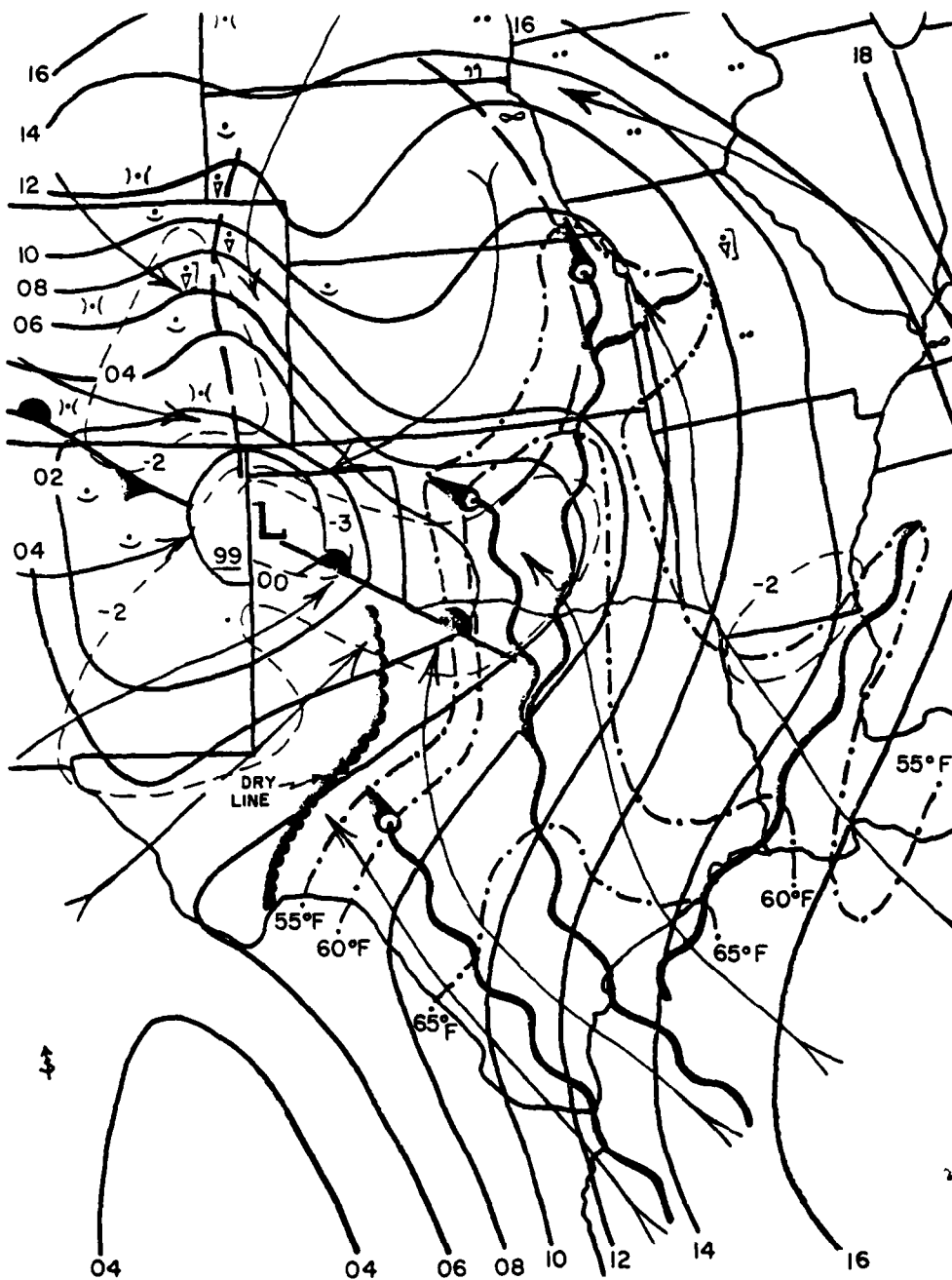


Figure 22. Surface Composite Chart for 0000 GMT 13 May 1981. Streamlines are denoted by thin arrows, while moisture axes are shown by thick curvy lines. Isallobars are dashed lines, and isodrosotherms are dot-dashed lines. Other symbols are conventional

the Texas and Oklahoma Panhandles. Moisture advection axes exist over the Rio Grande valley of Texas, central and northern Texas into western Oklahoma, and the eastern portions of Oklahoma and Kansas. Also, strong surface-pressure falls ($\geq 3 \text{ mb } 3\text{h}^{-1}$) are occurring over the Texas Panhandle in advance of the surface low. A well defined dryline appears at this time over west Texas.

The upper-air composite analyses for 0000 GMT on 13 May are shown in Figures 23a, 23b, and 23c. At 850 mb (Figure 23a), convergence, a moisture advection axis, a dryline, and a favorable thermal ridge-moist axis pattern appear over southern Kansas and northern Oklahoma. To the north of the Kansas-Oklahoma border, the 700-mb temperature no-change line exists with a good crossing angle to the flow (see Figure 23b). At 500 mb (Figure 23c), a 50-knot jet streak appears over the Texas Panhandle, and the jet continues across northern Oklahoma. A cold trough appears over Colorado and New Mexico at this time. Total totals for this case (Figure 23d) indicate values greater than 52 from central Texas northward to central Nebraska. Over northern Arkansas, a low-level jet, low-level moisture advection, 700-mb temperature no-change line to the north, diffluence at 500 mb, and strong directional wind shear between the lower and middle levels suggest that this region may also be favorable for severe thunderstorms. Total totals and surface features at this time are not as supportive, indicating that this region may not experience severe thunderstorms until further destabilization can occur.

Overall, the southern Kansas-northern Oklahoma region is most favorable for severe thunderstorms within the next 12 hours, while northern Arkansas may get severe thunderstorms towards the end of the 12-hour period. As in the 3-4 April 1981 case, a 700-mb dry front is noticeably absent from the upper-air composite analyses over the southern plains because of the presence of the lid.

5.2.3 REVIEW OF LID PARAMETERS

A lid originating over the desert southwest and northern Mexico existed over the southern plains during the night of 13 May. Figure 24 shows a 700-mb lid-parameter chart. A thermal ridge is shown to extend east-west from New Mexico to Oklahoma, while 12-hour warming has taken place across eastern Texas, northern Louisiana, and the southern half of Arkansas. Smaller pockets of 700-mb warming appear over west Texas, New Mexico, and eastern Kansas. The jet at 700 mb indicates that the overall advection of the warm air is to the east-northeast. Notice that the lid features at 700 mb are not as well defined in this case as they are in the 3-4 April case.

At 850 mb (Figure 25), the two lid source-regions (northern Mexico and central New Mexico) are clearly defined. Notice the confluence between the SP and M

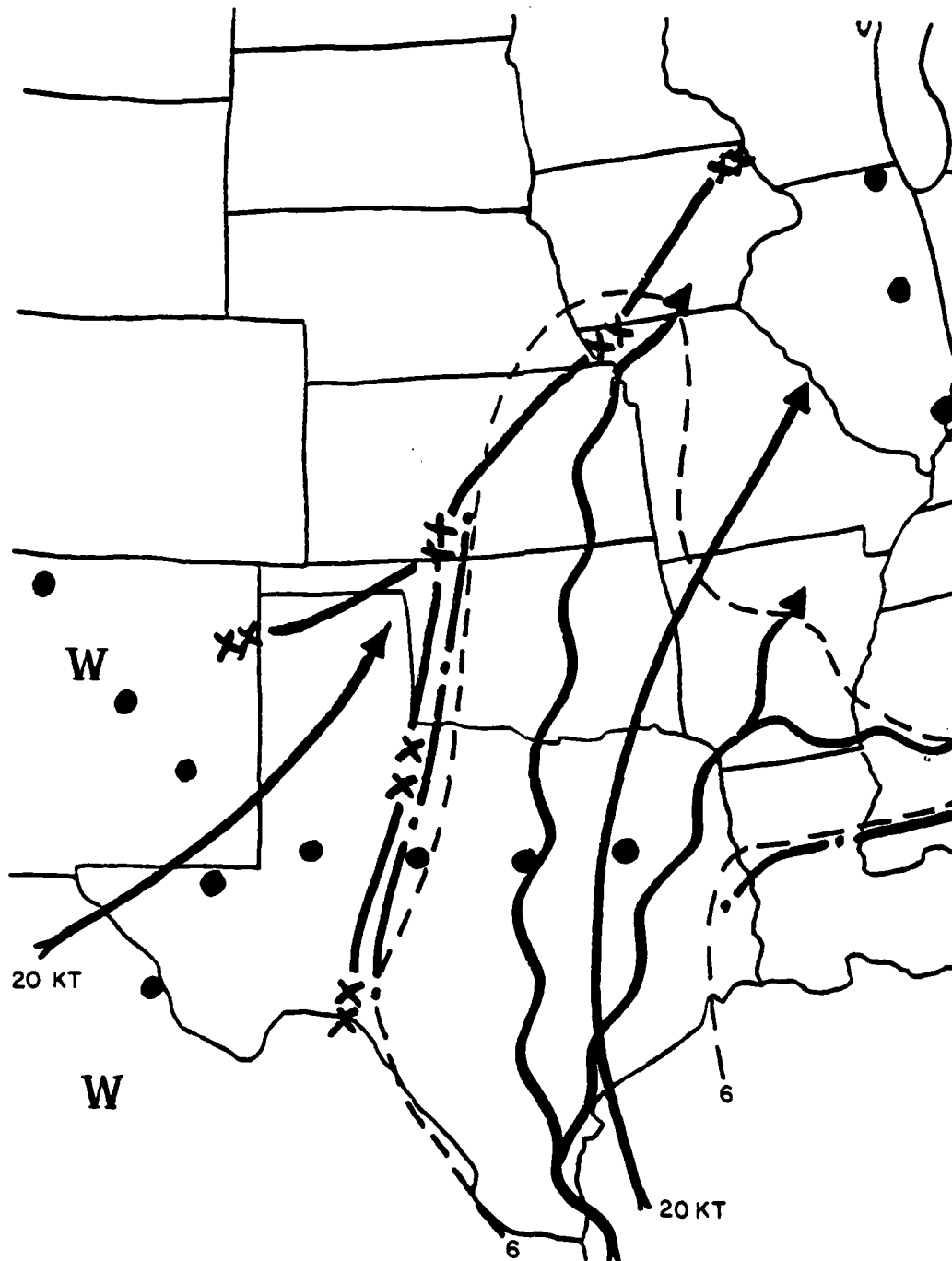


Figure 23a. Upper-Air Composite Analysis for 0000 GMT 13 May 1981. Chart shown is 850 mb. Symbols are same as in Figure A1

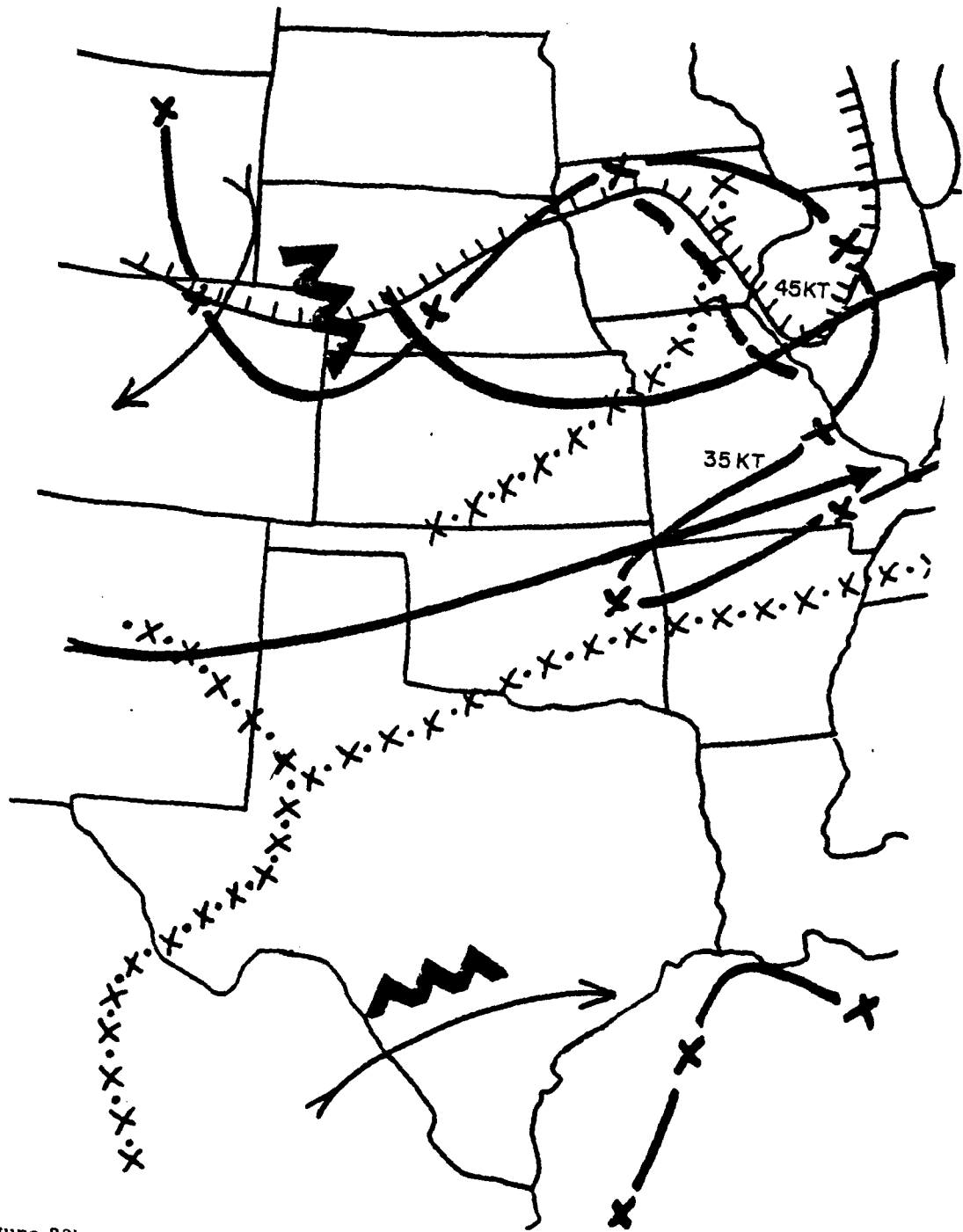


Figure 23b. Upper-Air Composite Analysis for 0000 GMT 13 May 1981. Chart shown is 700 mb. Symbols are same as in Figure A1

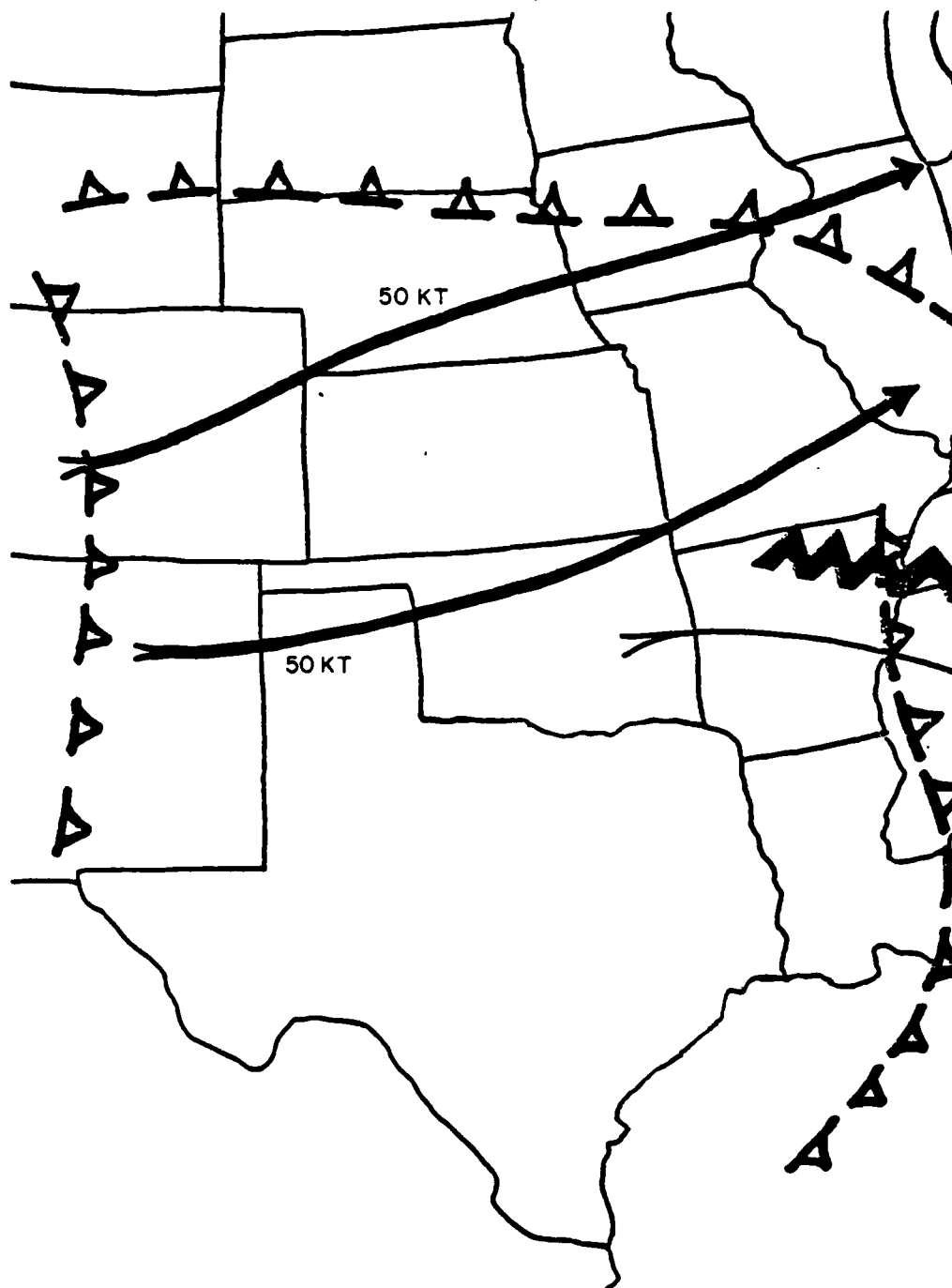


Figure 23c. Upper-Air Composite Analysis for 0000 GMT 13 May 1981. Chart shown is 500 mb. Symbols are same as in Figure A1

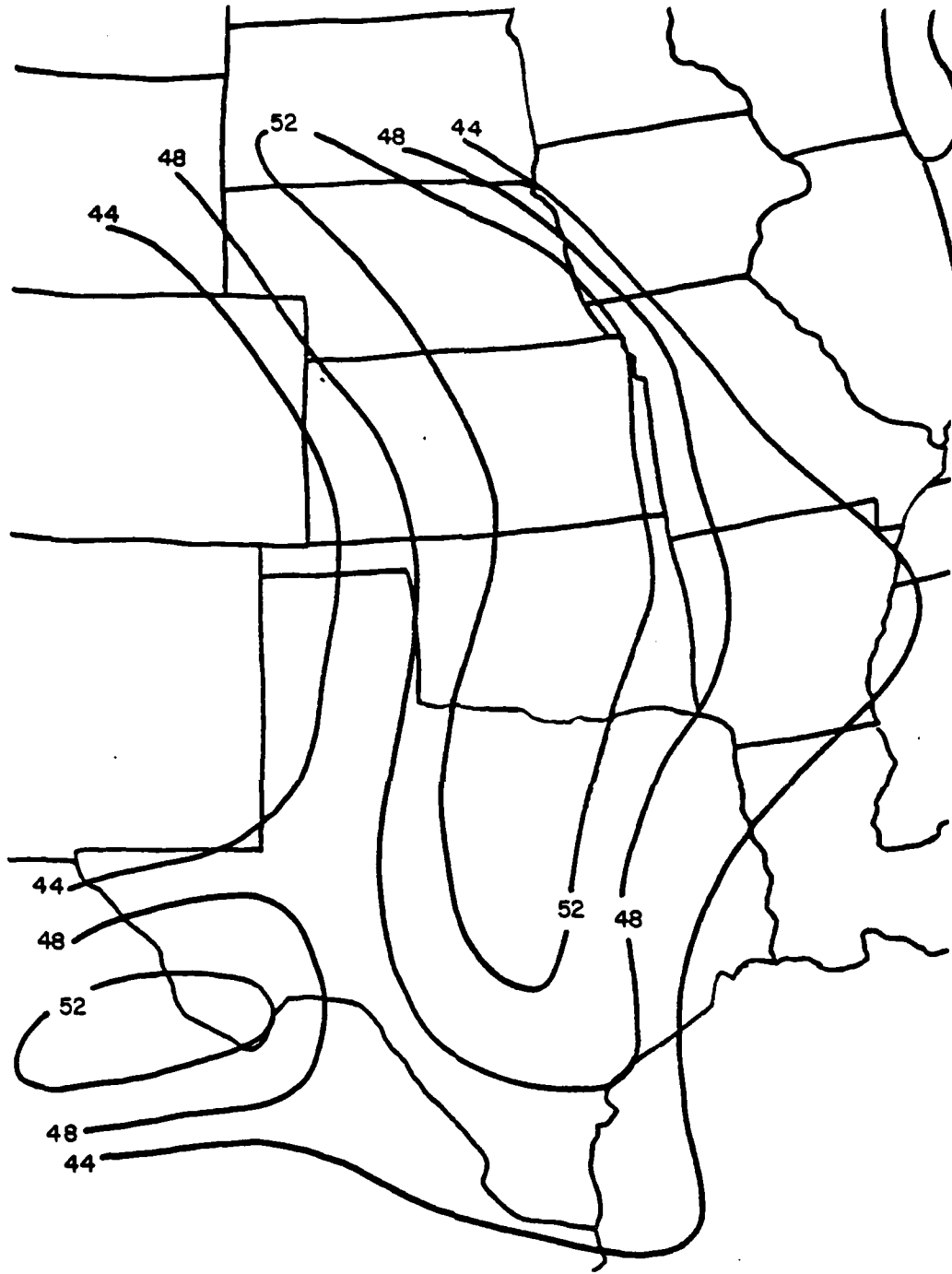


Figure 23d. Total Totals Analysis for 0000 GMT 13 May 1981

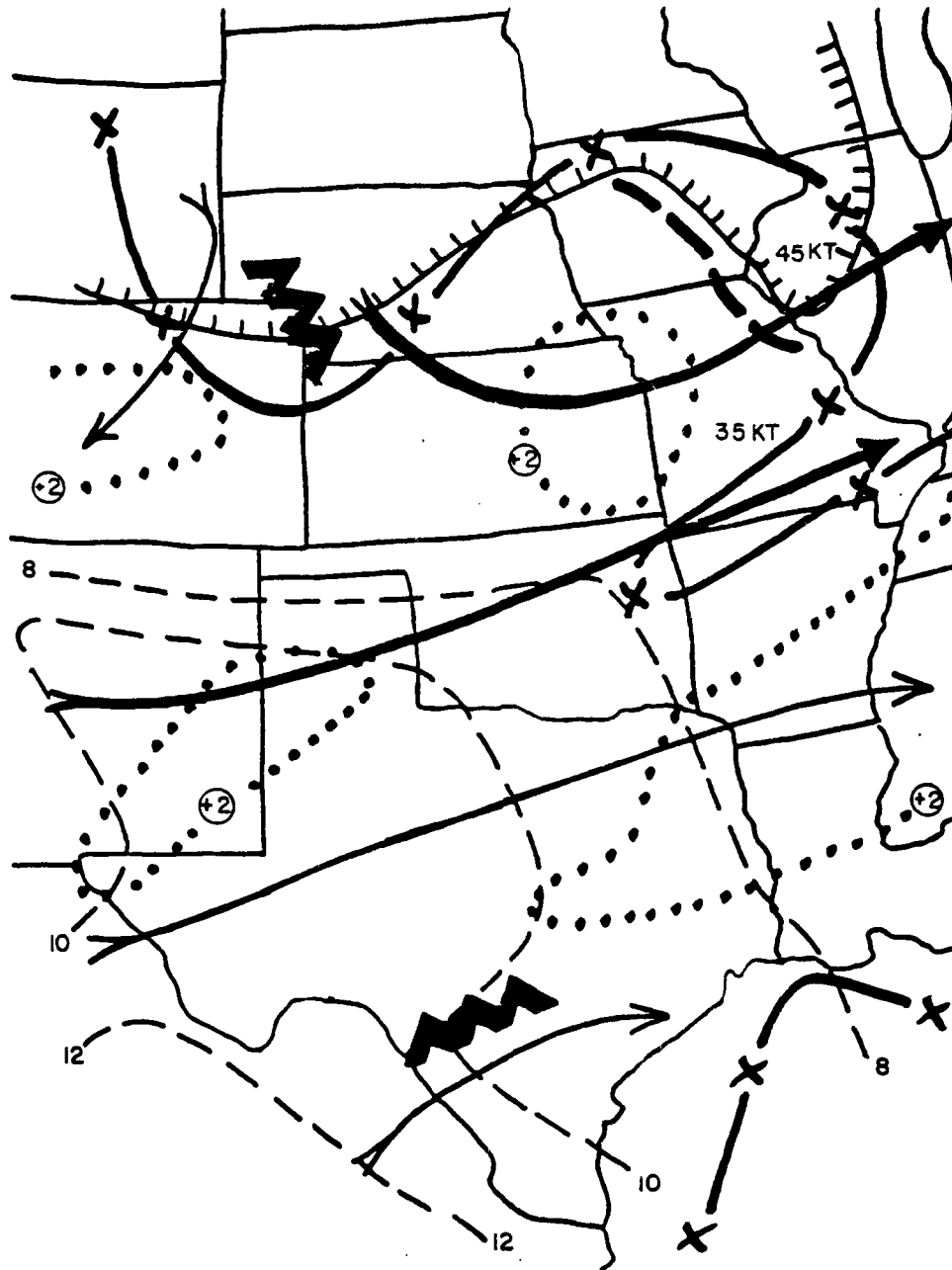


Figure 24. 700 mb Lid Parameter Chart for 0000 GMT 13 May 1981. The ribbed border denotes dewpoint depressions of 6° C or less. The dotted lines represent 12-hour temperature changes of 2° C and 4° C. The middle troposphere has become more stable during the last 12 hours over the areas enclosed by the dotted lines. The locations of temperature-change lines (including the no-change line) and the cross-isotherm flow angles help determine the movement of the lid by advection. Other symbols are defined in Figure A1

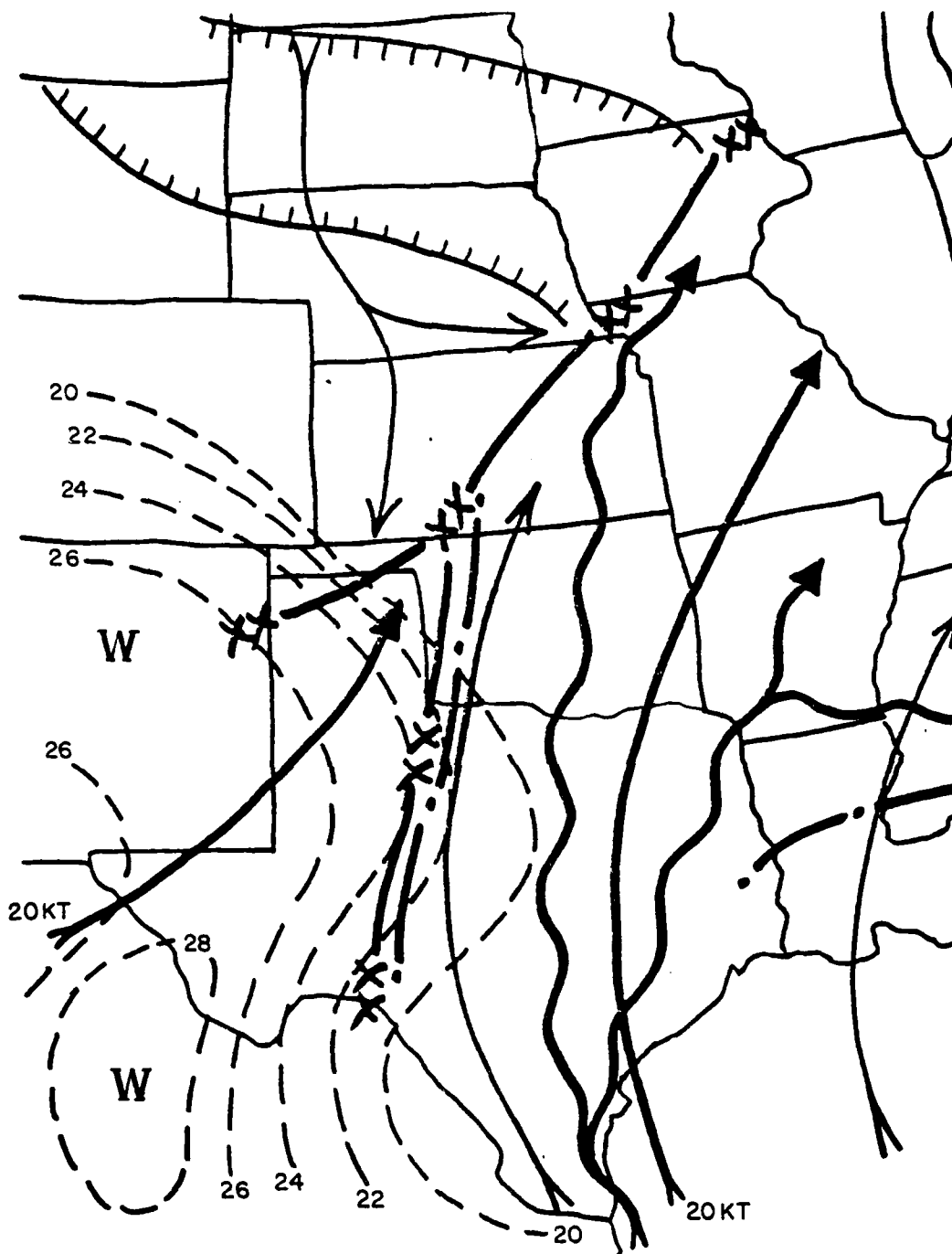


Figure 25. 850 mb Lid Parameter Chart for 0000 GMT 13 May 1981. Symbols are defined in Figure A1.

airstreams over western Texas and Oklahoma. This is a good example of the dry-line confluence zone described in section 1.

The lid strength for 0000 GMT 13 May appears in Figure 26a, and the buoyancy analysis appears in Figure 26b. Notice from the lid strength chart that the region effectively capped by the lid extends from west Texas and Oklahoma eastward to the borders of Arkansas and Louisiana. The remnants of a previous lid appear over the Omaha, Nebraska, area. Recall from the 700-mb lid chart (Figure 24) that the thermal ridge extends westward into New Mexico. The reason why no lid exists west of the Texas panhandle is that this region is west of the dryline; thus, the adiabatic layer there extends down to the surface. Quite often, the western edge of the lid closely parallels the dryline zone, and severe convection will be confined to the region east of the dryline and west of the lid edge. Notice that the "nose" of the lid strength contours in Figure 26a is in the region favorable for the outbreak of severe storms (northern Oklahoma and southern Kansas). The buoyancy chart (Figure 26b) indicates that the most unstable air is from southern and central Texas to southern Oklahoma. A typical lid sounding for this case is presented for Oklahoma City (Figure 26c). Notice the similarity between this sounding and the Miller Type I sounding shown in Figure 2.

A composite lid-parameter chart is shown in Figure 27. The anticyclonic curvature zone extends north-south across the central portion of Kansas. A secondary zone appears over central Texas. The proximity of the curvature zone to the lid edge and low-level convergence zone over the Kansas-Oklahoma border reinforces the idea that this region will experience severe thunderstorms during the forecast period through a combination of lid removal and underrunning. Another favorable parameter is the low-level moisture present over this region. While the advection of the lid appears to be towards Arkansas, if enough lifting occurs to further weaken it, severe thunderstorms could occur over northern Arkansas in the moist air.

5.2.4 FORECAST AND VERIFICATION

Figure 28 shows the analysis and Figure 29, the 12-hour forecast panels of the LFM model for this case. Figure 28 shows that weak PVA exists over western Oklahoma and western Kansas. This should assist in the lid removal over western Oklahoma. The 12-hour forecast shown in Figure 29 indicates strong PVA occurring over most of Oklahoma and Kansas, while weak PVA is over the eastern half of Texas. The surface low is predicted to move southeast into the Texas-Oklahoma border region by 1200 GMT on 13 May, while the warm front moves slightly northward into southern Oklahoma. Upward motion ($w \geq 2 \text{ cm s}^{-1}$) is shown over eastern Oklahoma, northern Arkansas, and southern Missouri. The model is predict-

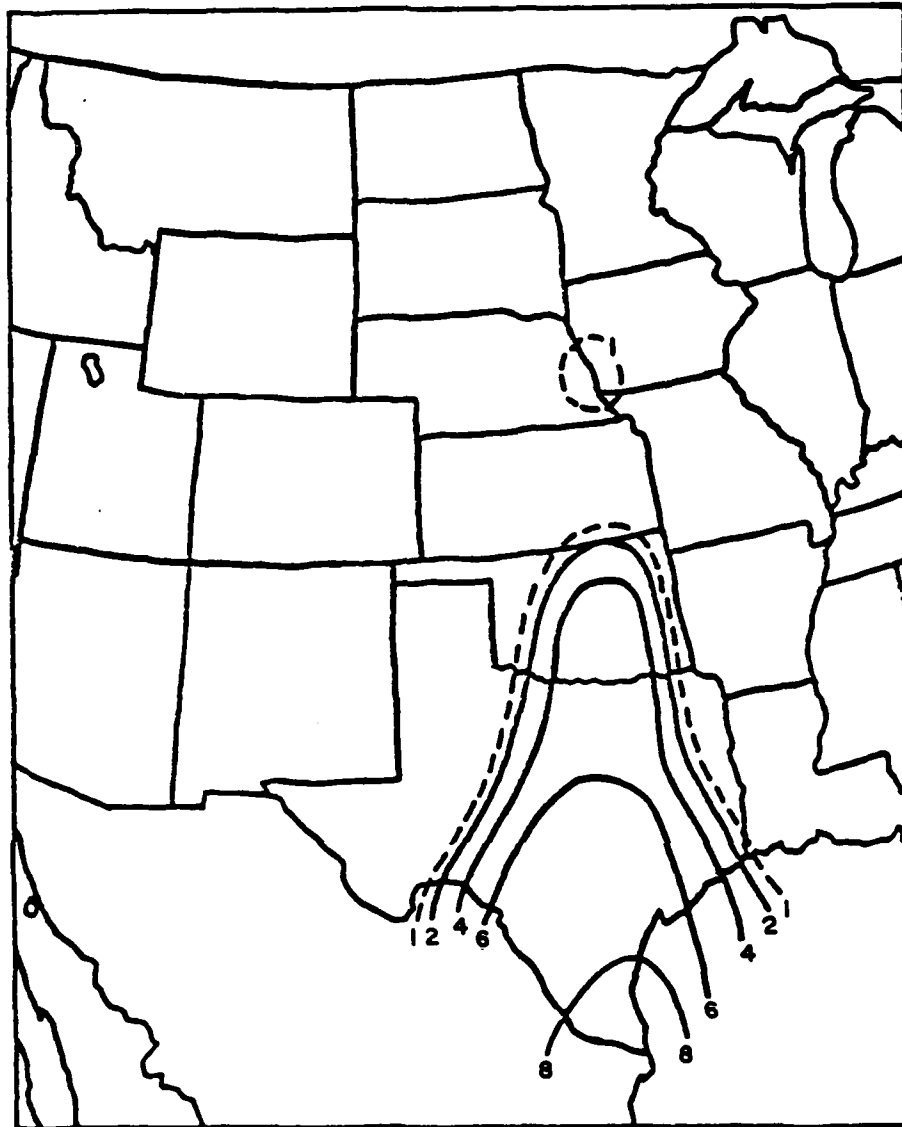


Figure 26a. Lid Strength Analysis (in °C) for 0000 GMT 13 May 1981

ing precipitation over northeastern Oklahoma, southeastern Kansas, northern Arkansas, and most of Missouri by 1200 GMT.

A complete severe-weather forecast based on information presented in the composite and LFM analyses, lid parameter charts, and 12-hour LFM forecast output can now be presented for the period 0000-1200 GMT 13 May 1981. Severe thunderstorms are forecast to develop along the central portion of the Oklahoma-Kansas border associated with a removal of the lid over northern Oklahoma and

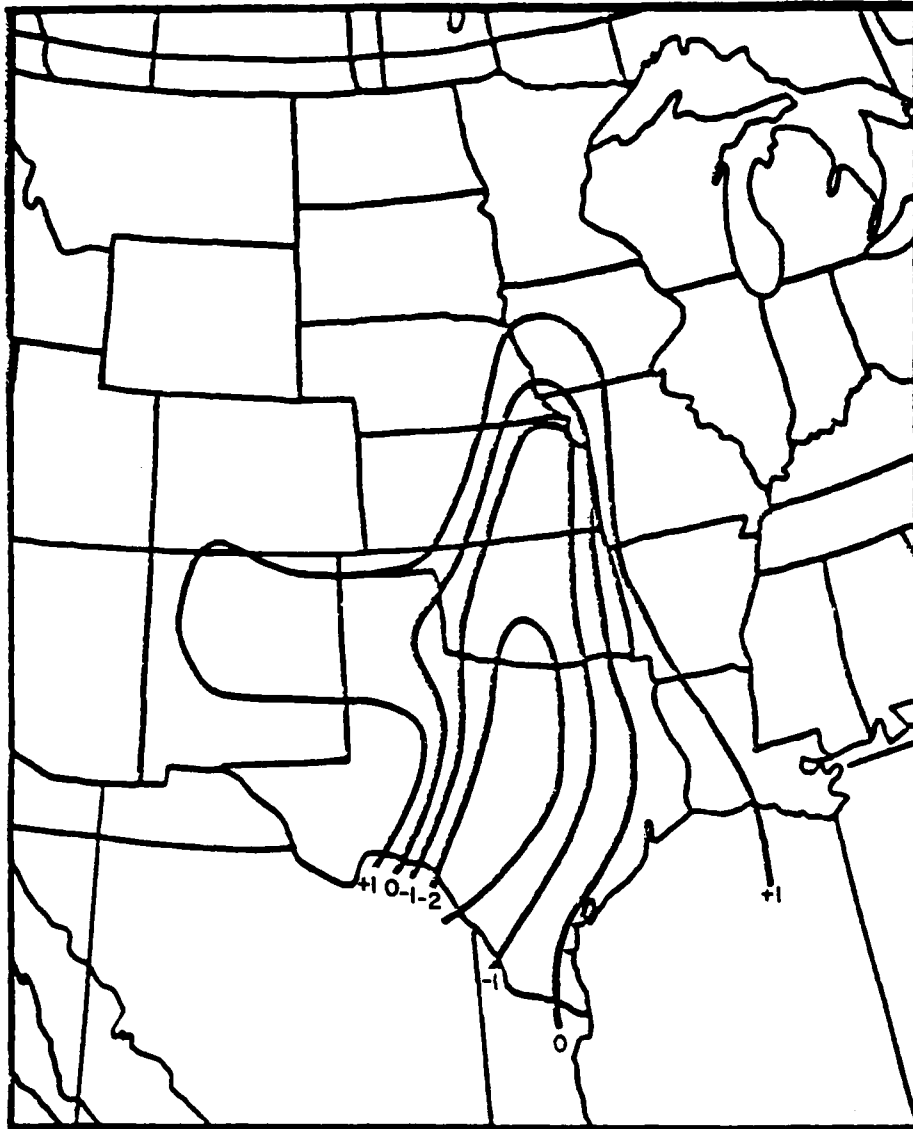


Figure 26b. Buoyancy Term Analysis (in °C) for 0000 GMT 13 May 1981

underrunning beneath the lid edge over southern Kansas. This activity should begin within six hours. Towards the latter part of the period, isolated severe thunderstorms should develop over northwestern Arkansas associated with the approaching short-wave trough. Although the lid is being advected towards this area, the advective speed is slow because of the weak flow at 700 mb, and the upward motion indicated in the LFM forecast will likely weaken the lid as it moves into the region.

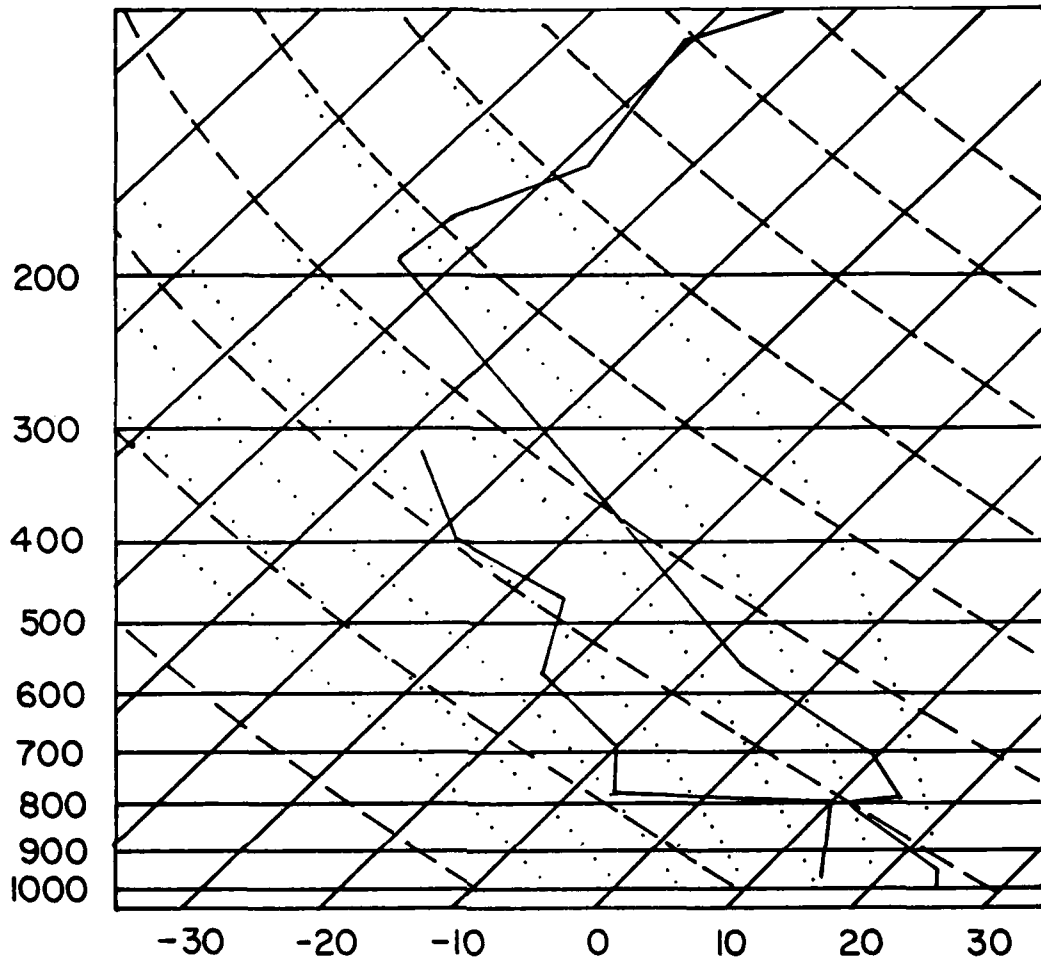


Figure 26c. Skew T-Log P Sounding for Oklahoma City, Oklahoma, at 0000 GMT 13 May 1981

Once the storms develop, the diffidence indicated at 500 mb on the analysis should maintain them.

The verification for this case is presented in Figure 30a. Around 0700 GMT on 13 April, severe storms developed over northern Oklahoma and spread into southern Kansas. These storms contained high winds and large hail, producing extensive crop damage over this area. Several hours later, thunderstorms developed over northwestern Arkansas and spread eastward, producing baseball-size hail and several funnel clouds, causing several million dollars worth of damage to small towns and farms in the area. It should be noted that, on the afternoon of

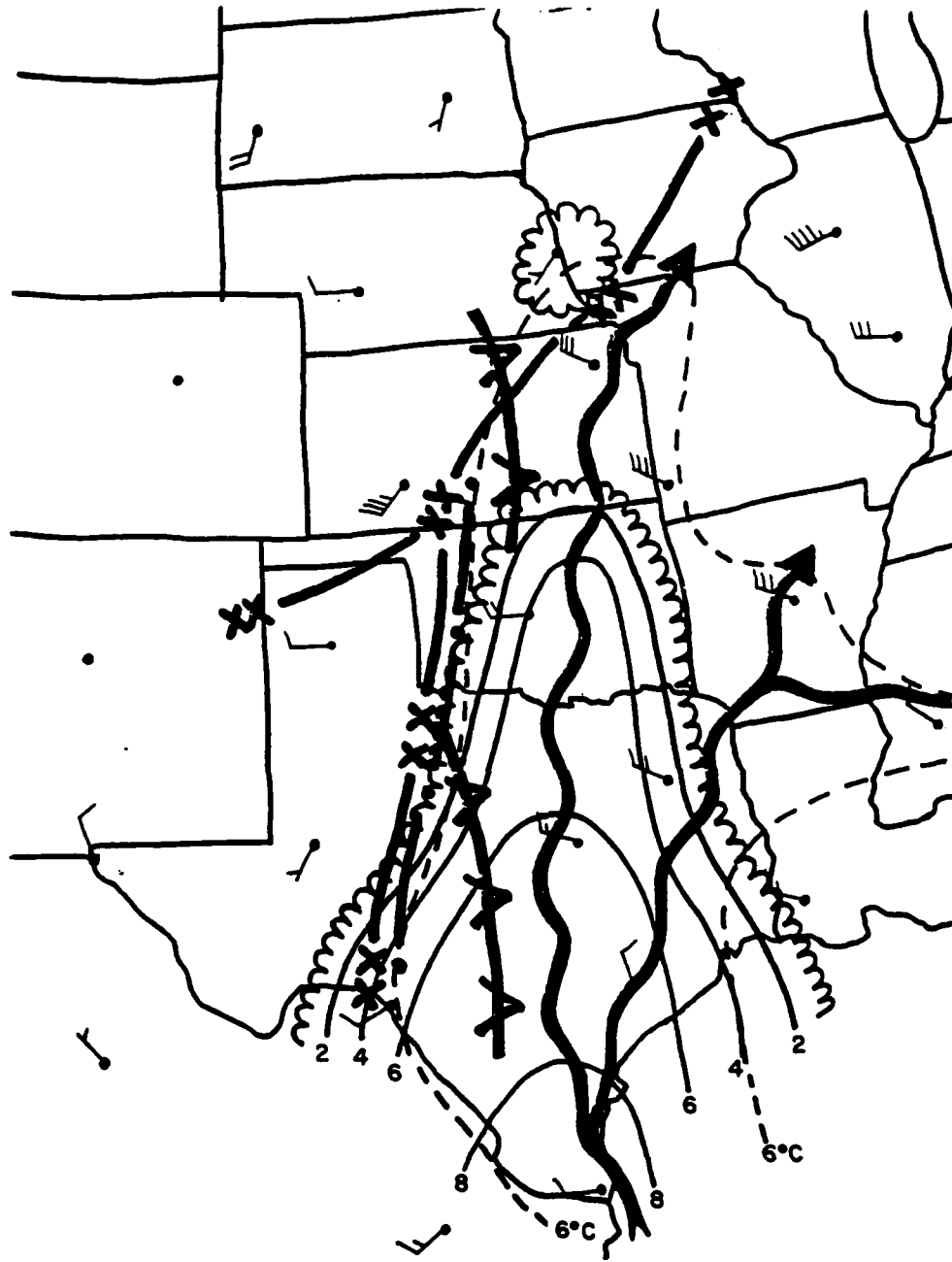


Figure 27. Composite Lid Chart Using Lid Strength Analysis, 850 mb Features, and 850-700 mb Shear Vectors for 0000 GMT 13 May 1981. The thin solid lines denote lid strength (in °C) with the scalloped border outlining the lid edge. The dashed line is the 6°C dewpoint isopleth at 850 mb. The plotted vectors denote 850-700 mb wind shear, and the thick solid line with V's denotes the axis of maximum anticyclonic curvature. Other symbols are as in Figure A1

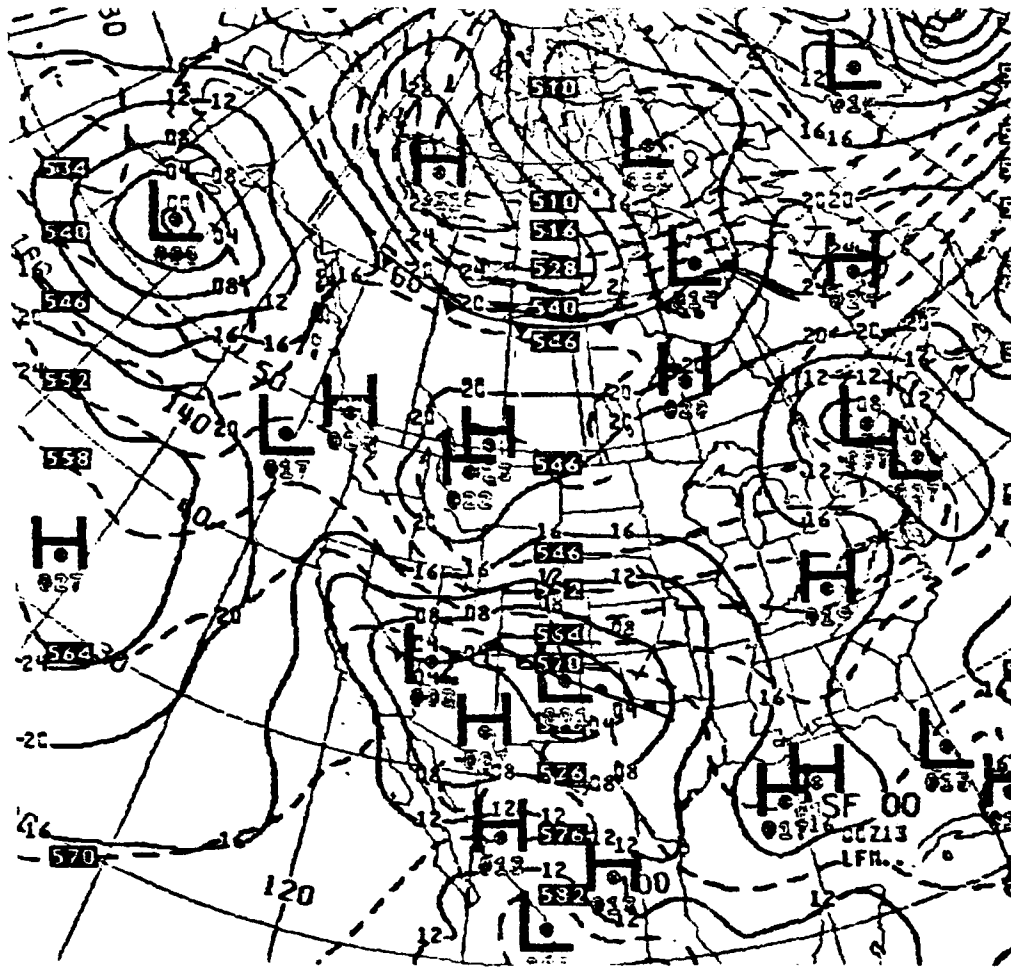


Figure 28. LFM Analyses for 0000 GMT 13 May 1981. Panel shown is sea level pressure and 1000-500 mb thickness with surface fronts

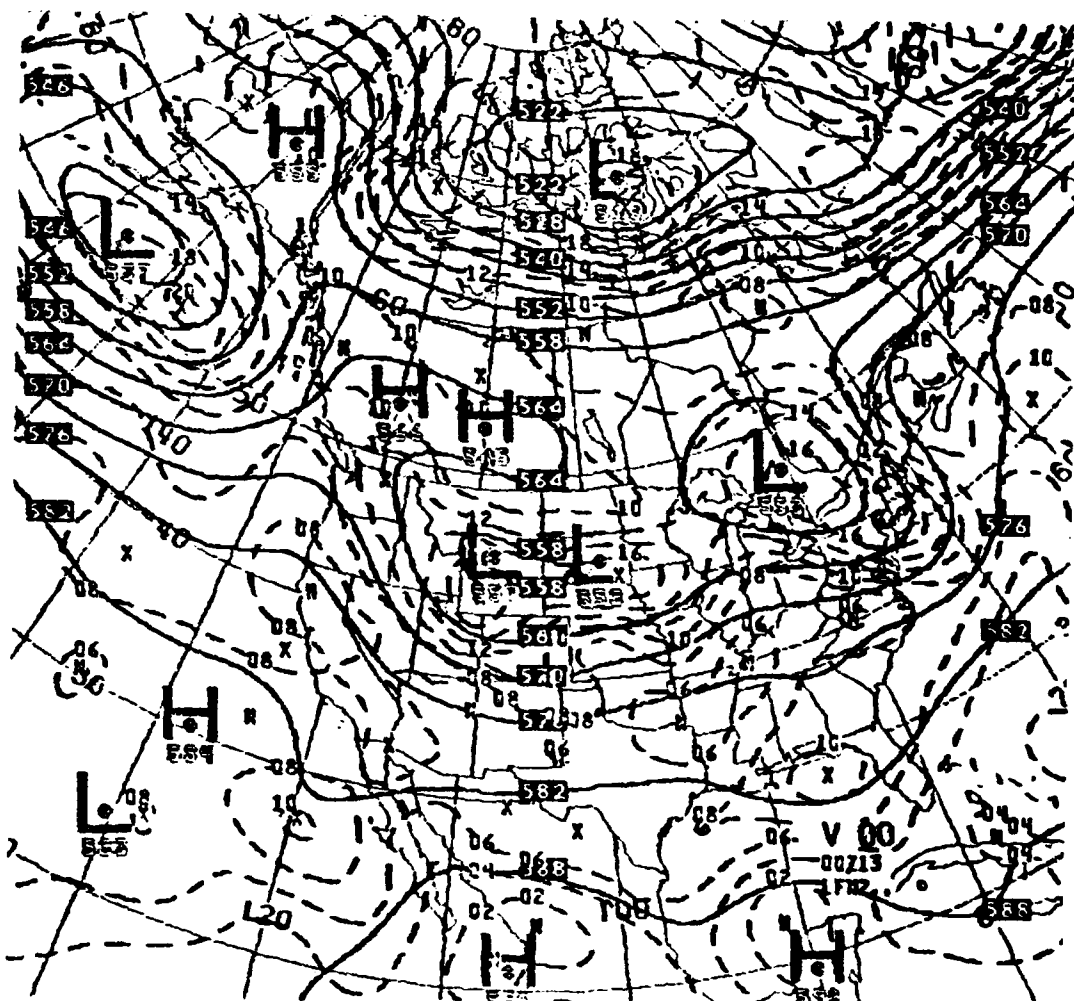


Figure 28 (Contd). LFM Analyses for 0000 GMT 13 May 1981. Panel shown is sea level pressure and 500 mb heights and absolute vorticity

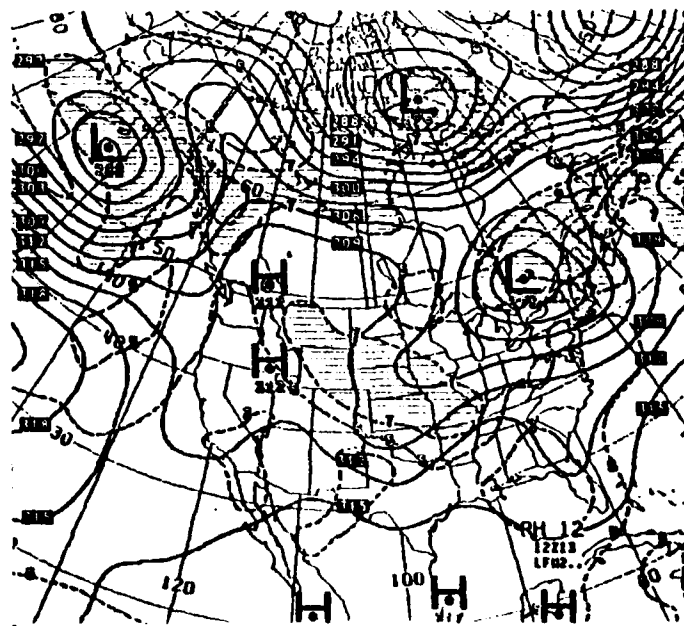
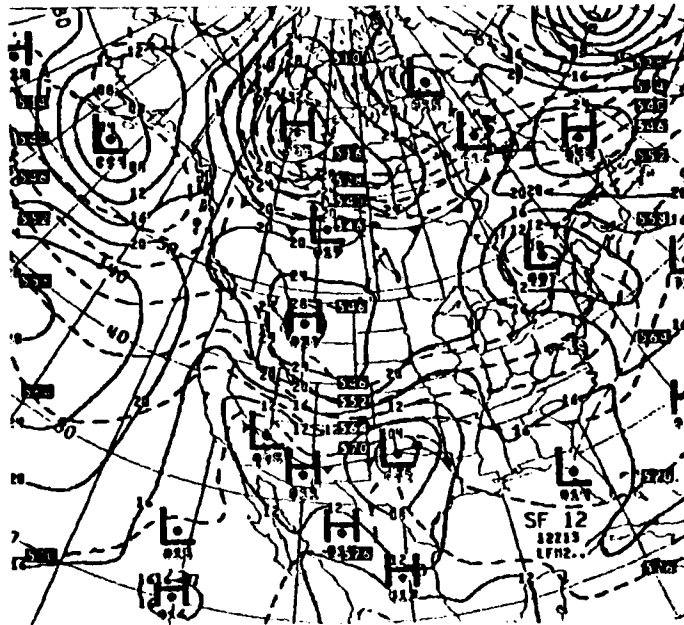


Figure 29. 12-Hour LFM Forecast for 1200 GMT 13 May 1981. Top panel is sea level pressure and 1000-500 mb thickness (with frontal positions superimposed). Bottom panel is 700 mb height and mean relative humidity between 1000 mb and 500 mb

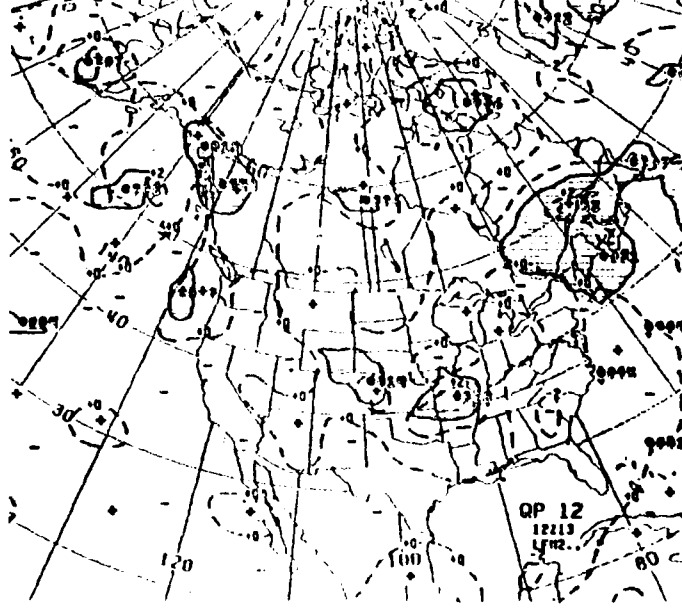
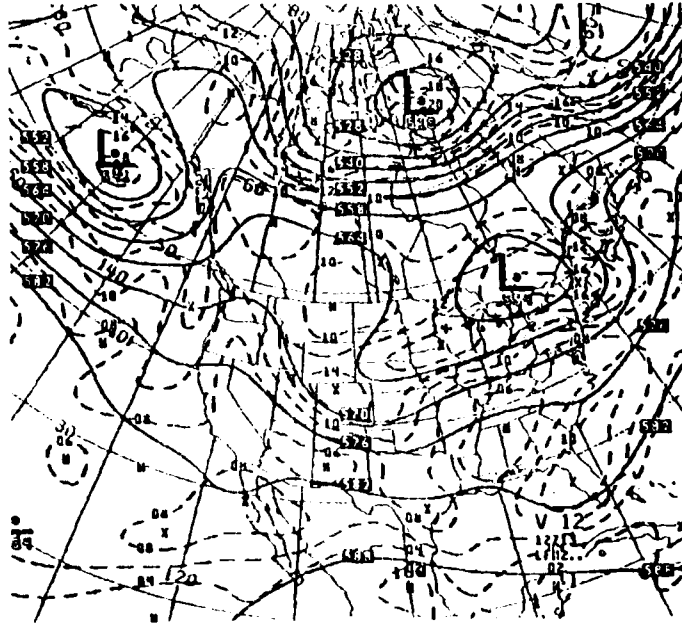


Figure 29 (Contd). 12 hour LFM forecast for 1200 GMT 13 May 1981. Top panel is 500 mb height and absolute vorticity. Bottom panel is 6 hour precipitation (in inches) and 700 mb vertical velocities (in cm s^{-1})



Figure 30a. Severe Weather Reports for 0000-1200 GMT 13 May 1981. Approximate time of occurrence (in GMT) is shown next to event

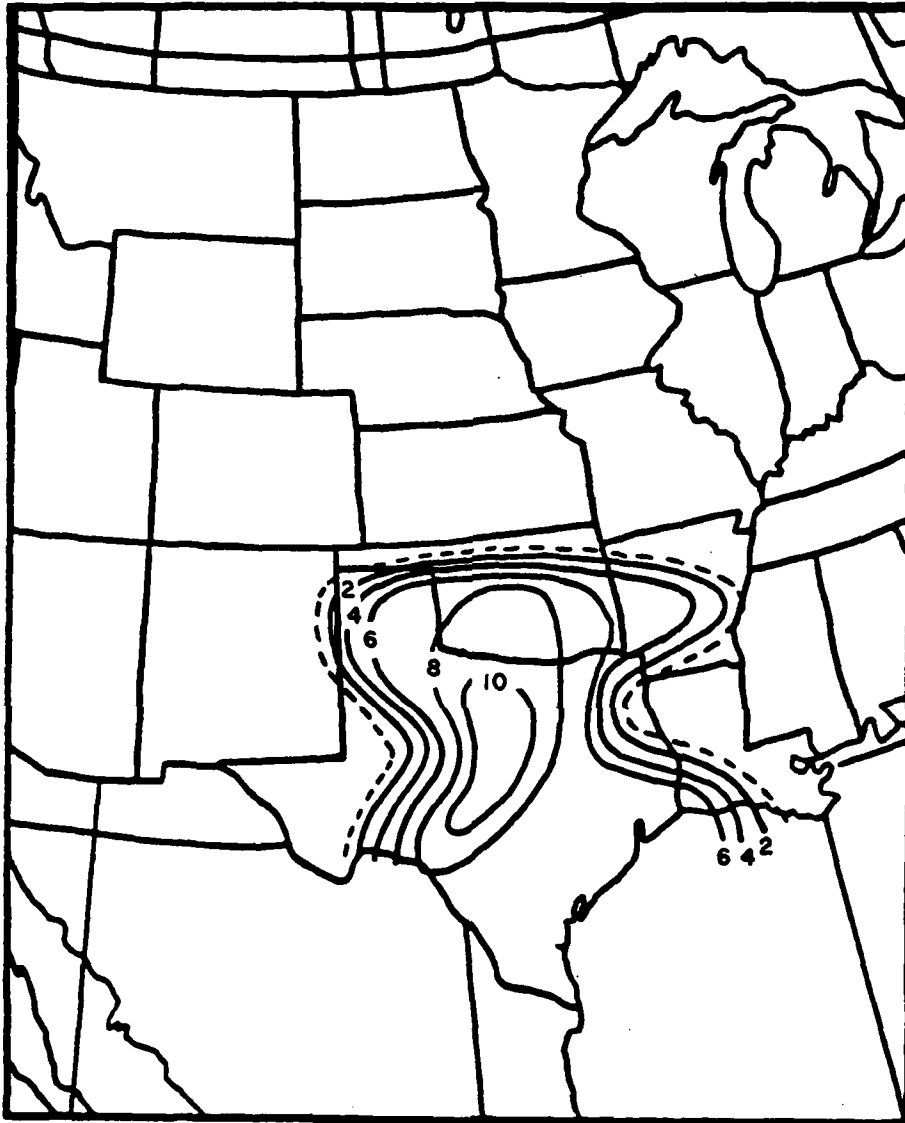


Figure 30b. Lid-Strength Analysis (in °C) for 1200 GMT 13 May 1981.
Dashed contour (1° C lid strength) denotes lid edge

13 May, a tornadic thunderstorm outbreak occurred over southeastern Oklahoma and northeastern Texas and spread into Arkansas and northern Louisiana during the evening hours.

6. CONCLUSIONS

A conceptual model of the severe-storm environment has been described, and a method has been outlined for its incorporation into the severe-weather analysis and forecast techniques used by AWS forecasters. It should be noted that the method can be tailored for use at individual detachments based on time constraints, availability of data, etc.

Although the two case studies presented here fall into one of the classical Miller synoptic categories for the Great Plains type of outbreak, it has been shown that areas of severe weather occurrence are easier to determine once the lid region has been identified. This is especially true in the 13 May 1981 case, where severe thunderstorms actually occurred along the northern and eastern edges of the lid zone as defined by the 0000 GMT and 1200 GMT lid-strength analyses (compare Figure 30a with Figures 27a and 30b).

The lid concept has previously been investigated in research studies only. This report is the first attempt to incorporate the theory into an operational scheme. We hope that the methods outlined in this report can be adapted for use by AWS personnel both in the field and at AFGWC, not only over the United States during the spring and summer, but in the European theatre as well.

References

1. Miller, R. C. (1972) Notes on Analysis and Severe-Storm Forecasting Procedures of the Air Force Global Weather Central, AWSTR-200 (Rev.), Air Weather Service (MAC), Scott AFB, Ill.
2. Ferrel, W. (1885) Recent Advances in Meteorology, Report of the Chief Signal Officer for 1885, Appendix 71, 324-325, 327.
3. Finley, J. P. (1890) Tornadoes, Am. Meteorol. J. 7:165-179.
4. Varney, B. M. (1926) Aerological evidence as to the causes of tornadoes, Mon. Wea. Rev. 54:163-165.
5. Humphreys, W. J. (1926) The tornado, Mon. Wea. Rev. 54:501-503.
6. Humphreys, W. J. (1940) Physics of the Air, 3rd ed., McGraw-Hill, New York.
7. Lloyd, J. R. (1942) The development and trajectories of tornadoes, Mon. Wea. Rev. 70:65-75.
8. Harrison, H. T., and Orendorf, W. K. (1941) Pre-Coldfrontal Squall Lines, United Air Lines Meteorology Department Circular No. 16.
9. Fawbush, E. J., Miller, R. C., and Starrett, L. G. (1951) An empirical method of forecasting tornado development, Bull. Am. Meteorol. Soc. 32:1-9.
10. Fawbush, E. J., and Miller, R. C. (1952) A mean sounding representative of the tornado air mass, Bull. Am. Meteorol. Soc. 33:303-307.
11. Showalter, A. K., and Fulks, J. R. (1943) A Preliminary Report on Tornadoes, U. S. Weather Bureau, Washington, D. C.
12. Fawbush, E. J., and Miller, R. C. (1953) A method of forecasting hailstone size at the earth's surface, Bull. Am. Meteorol. Soc. 34:235-244.
13. Fawbush, E. J., and Miller, R. C. (1954) The types of airmasses in which American tornadoes form, Bull. Am. Meteorol. Soc. 35:154-165.
14. Miller, R. C. (1959) Tornado producing synoptic patterns, Bull. Am. Meteorol. Soc. 40:465-472.

15. Air Weather Service (1956) Severe Weather Forecasting, AWSM 105-37, 2nd ed., Air Weather Service (MATS), Scott AFB, Ill.
16. Miller, R. C. (1967) Notes on Analysis and Severe-Storm Forecasting Procedures of the Military Weather Warning Center, Air Weather Service (MAC), Scott AFB, Ill.
17. Means, L. L. (1952) On thunderstorm forecasting in the central United States, Mon. Wea. Rev. 80:165-189.
18. Showalter, A. K. (1953) A stability index for thunderstorm forecasting, Bull. Am. Meteorol. Soc. 34:250-252.
19. Galway, J. G. (1956) The lifted index as a prediction of latent instability, Bull. Am. Meteorol. Soc. 37:528-529.
20. Sugg, A. L., and Foster, D. S. (1954) Oklahoma tornadoes, May 1, 1954, Mon. Wea. Rev. 82:131-140.
21. Beebe, R. G., and Bates, F. C. (1955) A mechanism for assisting in the release of convective instability, Mon. Wea. Rev. 83:1-10.
22. Whitney, L. F., and Miller, J. E. (1956) Destabilization by differential advection in the tornado situation of 8 June 1953, Bull. Am. Meteorol. Soc. 37:224-229.
23. Fuks, J. R. (1951) The instability line, in Compendium of Meteorology, T. P. Malone, Ed., Am. Meteorol. Soc., pp. 647-652.
24. Beebe, R. G. (1958) An instability line development as observed by the tornado research airplane, J. Meteorol. 15:278-282.
25. House, D. C. (1959) The mechanics of instability line formation, J. Meteorol. 16:108-120.
26. Fujita, T. T. (1958) Structure and movement of a dry front, Bull. Am. Meteorol. Soc. 39:574-582.
27. McGuire, E. L. (1962) The Vertical Structure of Three Drylines as Revealed by Aircraft Traverses, National Severe Storms Project Report No. 7, U.S. Weather Bureau, Washington, D. C.
28. National Severe Storms Project Staff (1963) Environmental and thunderstorm structures as shown by National Severe Storms Project observations in spring 1960-61, Mon. Wea. Rev. 91:271-292.
29. Rhea, J. O. (1966) A study of thunderstorm formation along drylines, J. Appl. Meteorol. 5:58-63.
30. Blackadar, A. K. (1957) Boundary-layer wind maxima and their significance for the growth of nocturnal inversions, Bull. Am. Meteorol. Soc. 38:283-290.
31. Pitchford, K. L., and London, J. (1962) The low-level jet as related to nocturnal thunderstorms over the midwest United States, J. Appl. Meteorol. 1:43-47.
32. Bonner, W. D. (1963) An Experiment in the Determination of Geostrophic and Isalobaric Winds from NSSP Pressure Data, Research Paper 26, Mesometeorology Project, U. of Chicago.
33. Bonner, W. D. (1966) Case study of thunderstorm activity in relation to the low-level jet, Mon. Wea. Rev. 94:167-178.
34. Bonner, W. D. (1968) Climatology of the low-level jet, Mon. Wea. Rev. 96:833-850.
35. Fujita, T. T. (1955) Results of detailed synoptic studies of squall lines, Tellus 7:405-436.

36. Fujita, T.T. (1958) Mesoanalysis of the Illinois tornadoes of 9 April 1953, J. Meteorol. 15:288-296.
37. Fujita, T.T., Newstein, H., and Tepper, M. (1956) Mesoanalysis, An Important Scale in the Analysis of Weather Data, Research Paper No. 39, U.S. Weather Bureau, Washington, D.C.
38. Magor, B.W. (1959) Mesoanalysis: Some operational analysis techniques utilized in tornado forecasting, Bull. Am. Meteorol. Soc. 40:499-511.
39. Miller, R.C., Bidner, A., and Maddox, R.A. (1971) The use of computer products in severe weather forecasting, Preprints of the Seventh Conference on Severe Local Storms, Am. Meteorol. Soc., Boston, Mass., 1-6.
40. Miller, R.C., and McGinley, J.A. (1978) Using Satellite Imagery to Detect and Track Comma Clouds and the Application of the Zone Technique in Forecasting Severe Storms, Environmental Sciences Group, GE/Management and Technical Services Company, Beltsville, Md.
41. Carlson, T.N., and Ludlam, F.H. (1968) Conditions for the occurrence of severe local storms, Tellus 20:203-226.
42. Carlson, T.N., Benjamin, S.G., Forbes, G.S., and Li, Y.-F. (1983) Elevated mixed layers in the regional severe storm environment - Conceptual model and case studies, Mon. Wea. Rev. 111:1453-1473.
43. Palmen, E., and Newton, C.W. (1969) Atmospheric Circulation Systems, Academic Press, New York.
44. Ramaswamy, C. (1956) On the sub-tropical jet stream and its role in the development of large-scale convection, Tellus 8:26-60.
45. Crisp, C.A. (1979) Training Guide for Severe Weather Forecasters, AFGWC Technical Note 79/002, Air Force Global Weather Central, Offutt AFB, Neb.
46. Goldman, J.D. (1981) A Conceptual Model and Its Application in the Analysis of Severe Convective Storm Situations, M.S. thesis, The Pennsylvania State U., University Park, Pa.
47. Lanicci, J.M. (1984) The Influence of Soil Moisture Distribution on Severe-Storm Environment of the Southern Great Plains: A Numerical Study of the SESAME IV Case, M.S. thesis, The Pennsylvania State U., University Park, Pa.
48. Carlson, T.N., and Farrell, R.J. (1983) The lid strength index as an aid in predicting severe local storms, Nat. Wea. Digest 8:27-39.
49. Benjamin, S.G. (1983) Some Effects of Heating and Topography on the Regional Severe Storm Environment, Ph.D. thesis, The Pennsylvania State U., University Park, Pa.
50. Air Weather Service (1969) Use of the Skew T, Log P Diagram in Analysis and Forecasting, AWSM 105-124, Air Weather Service (MAC), Scott AFB, Ill.
51. Graziano, T. (1984) M.S. thesis, research in progress, The Pennsylvania State U., University Park, Pa.

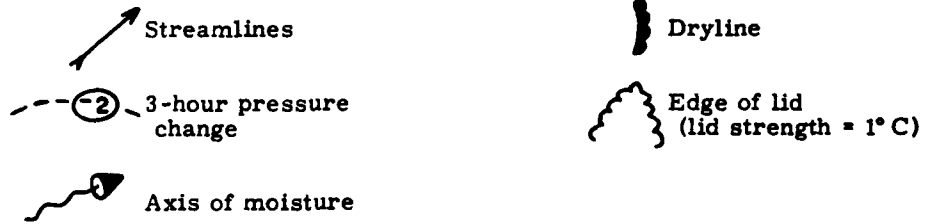
Appendix A

Chart Symbology

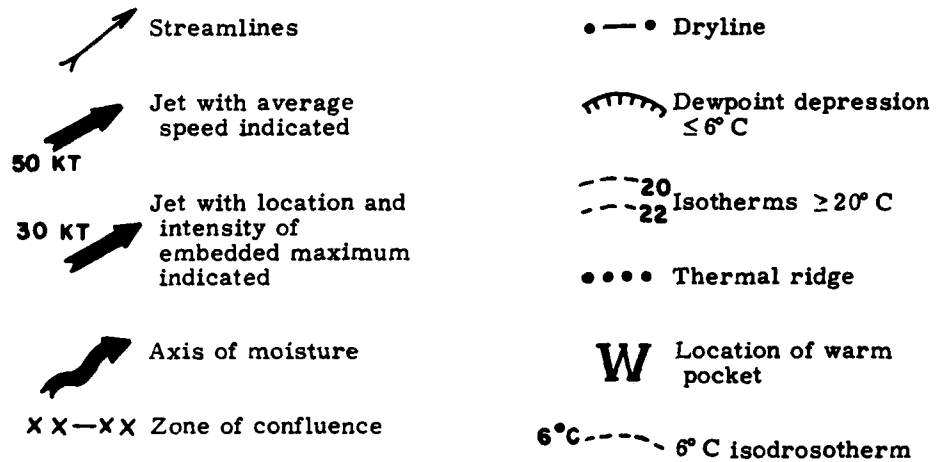
A complete legend for the symbols used in the various charts in this report appears in Figure A1. Conventional symbols have been used where possible for features such as highs, lows, fronts, and isobars. Most of the conventional severe-weather symbols used in AWSTR-200 have been used here. The reader is referred to AWSTR-200¹ and AFGWC TN 79/002⁴⁵ for further explanation of severe-weather analyses and the symbology used.



Surface chart:



850-mb chart:



700-mb chart:

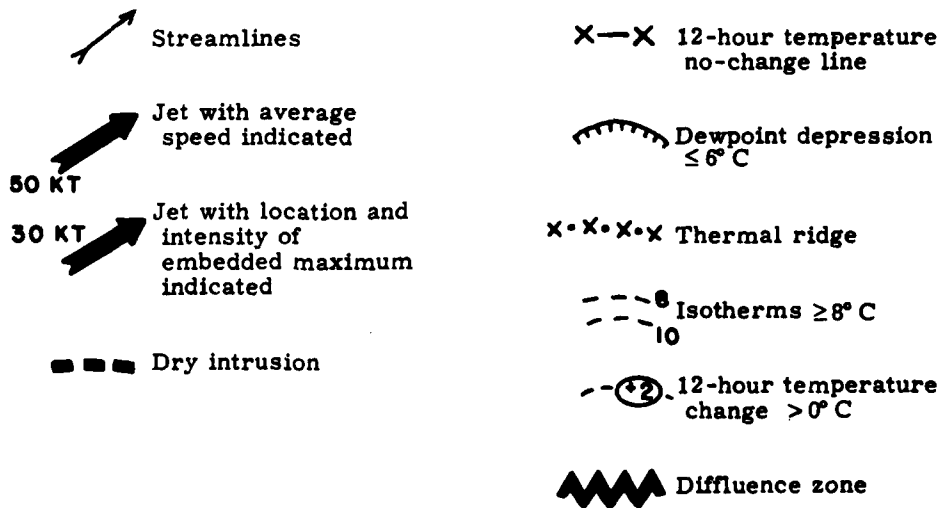
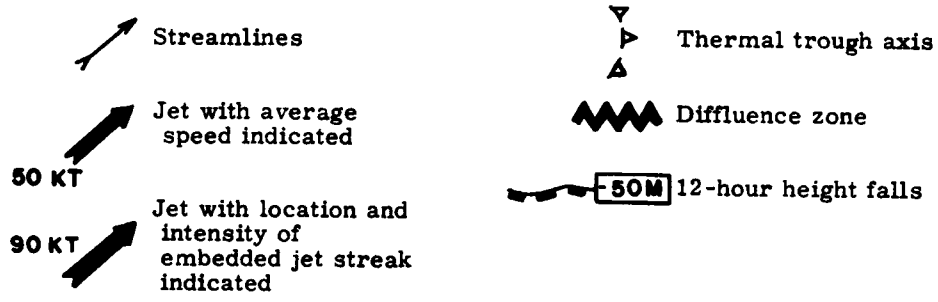


Figure A1. Chart Symbology

500-mb chart:



Lid Composite chart:

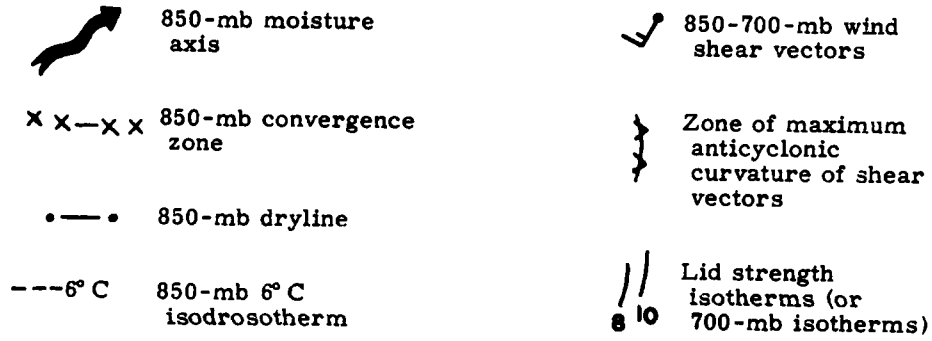


Figure A1 (Contd). Chart Symbology

Appendix B

Alternate Method of Constructing the Lid Composite Chart

In this appendix, we present a method for constructing the lid composite chart (see section 4.3 for a definition) using 700-mb temperatures instead of lid strength isotherms. This alternative method is intended for stations where an automated lid strength index (LSI) program is not available. The 700-mb temperature field has been shown to indicate the presence of a lid (see section 4.1), although caution must be exercised when using 700-mb temperatures alone because they indicate only what is occurring at one level in the atmosphere. Once this chart has been created, examination of both 700-mb temperatures and 850-mb moisture is necessary to delineate areas covered by a lid.

The construction of this chart is simple. The 850-mb parameters to be included are the 6° C dewpoint isopleth, moisture axes, convergence zones, and dry-lines. The 700-mb isotherms greater than or equal to 8° C should be included, as well as the 850-700-mb wind shear vectors. The wind shear vectors can be computed numerically with a hand calculator, or graphically with a hodograph. The zone of maximum anticyclonic curvature of the shear vectors should be analyzed. This feature will indicate destabilization through differential advection in areas where low-level moisture and convergence exist. This zone may be coincident with the 8-10° C isotherms at 700 mb, but remember that a necessary condition for lid existence is that these lid isotherms overlap significant moisture at 850 mb. An example of this analysis for the 3 April 1981 case appears in Figure B1. Notice

how the anticyclonic curvature zone is nearly coincident with the 8-10° C isotherms at 700 mb over southern Kansas and Oklahoma.

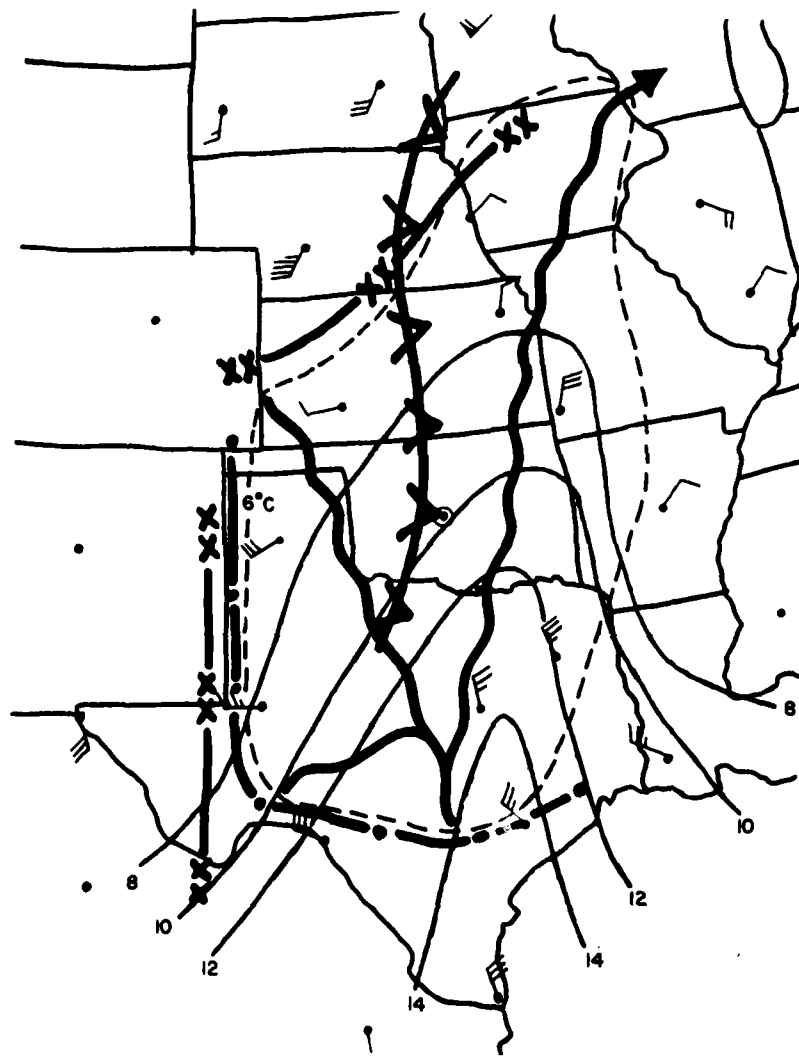


Figure B1. Composite Chart of Lid Parameters. The thin solid lines denote 700 mb isotherms (in °C), with the scalloped border outlining the lid edge. The dashed line is the 6° C dewpoint isopleth at 850 mb. The plotted vectors denote 850-700 mb wind shear, and the thick solid line with V's denotes the axis of maximum anticyclonic curvature. Other symbols are as in Figure A1

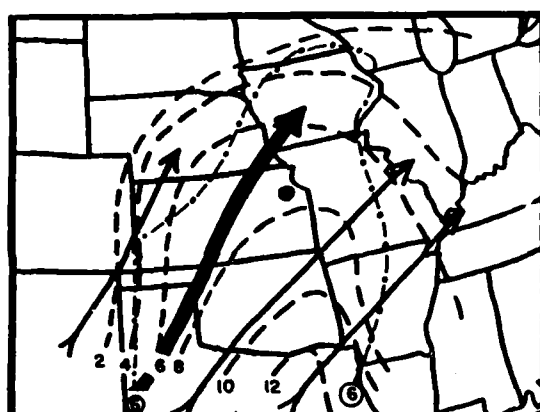
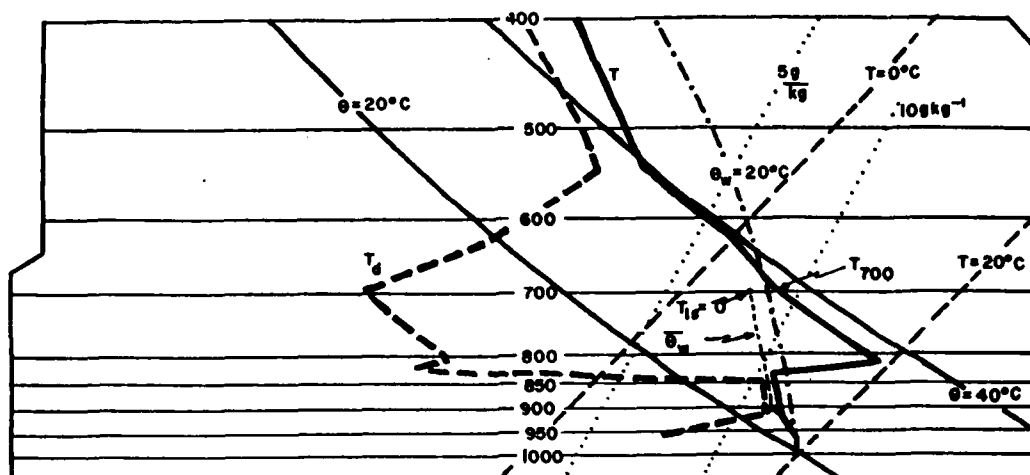
Appendix C

Single Station Lid Forecast Techniques

After the lid strength has been determined from the sounding, and after a lid composite chart (with either lid strength isotherms or 700-mb temperatures) has been created, some single-station forecasting techniques can determine whether lid removal and/or underrunning is likely to occur over the local area.

The first technique involves diagnosing the 700-mb temperature corresponding to a lid strength of zero over the local area ($T_{LS=0}$). Recall from section 4.1 that the lid usually appears with 700-mb temperatures greater than or equal to 8° C, but that this isotherm does not necessarily correspond to the lid edge. The method for diagnosing the 700-mb zero lid strength isotherm is as follows (see Figure C1):

Using a temperature-dewpoint sounding, determine the maximum wet-bulb potential temperature $\bar{\theta}_w$ over the lowest 50 mb (see AWSM 105-124,⁵⁰ section 4.10, for definition and description of $\bar{\theta}_w$). Follow this moist adiabat until it intersects the 700-mb level. The temperature at the intersection of the moist adiabat and 700-mb level is the zero lid-strength isotherm. Compare this value with the actual 700-mb temperature from the sounding and note the difference. Locate the value of the zero lid-strength isotherm on the 700-mb analysis and its proximity to the station. Now, using the forecast methods presented in sections 4 and 5, determine whether the 700-mb zero lid-strength isotherm could be advected over the station during the forecast period. If it can, this method can help the forecaster decide on the timing for the onset of convection, provided that the other severe-storm parameters also remain favorable during this time.

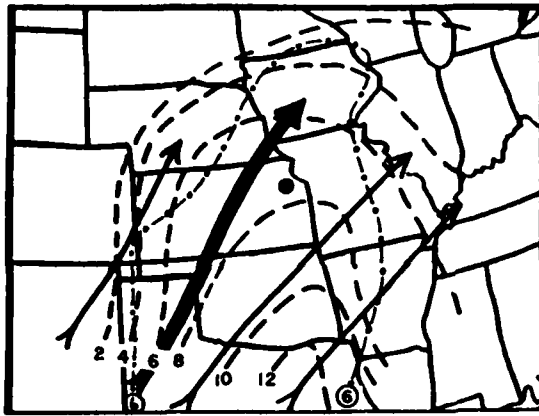
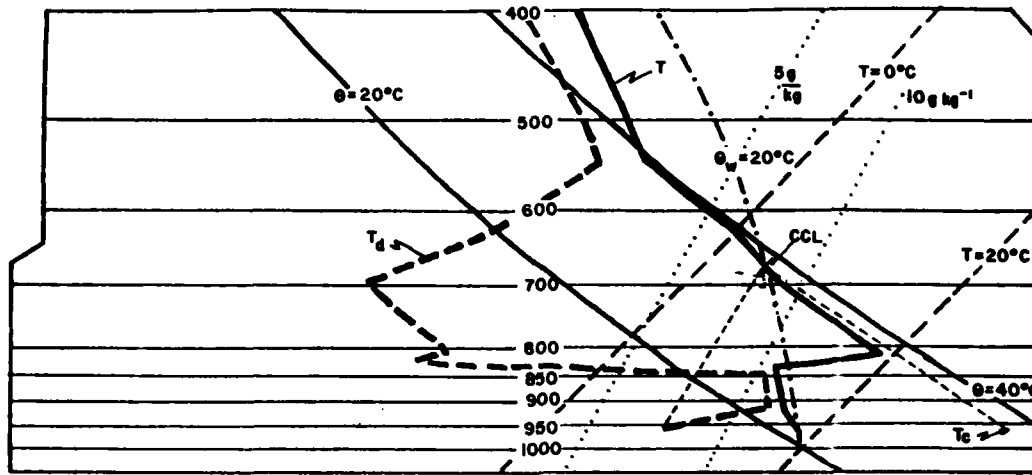


$\bar{\theta}_w = 18.6^\circ\text{C}$
 $T_{LS} = 0 = 4^\circ\text{C}$
 $T_{700} = 7^\circ\text{C}$
 $T_{700} - T_{LS} = 0 = 3^\circ\text{C}$

Figure C1. Skew T-log P Sounding for Topeka, Kansas, at 1200 GMT 3 April 1981. Calculation of $\bar{\theta}_w$ and $T_{LS=0}$ at 700 mb is shown. Lower portion of figure shows 700-mb isotherms (dashed lines), streamlines, and 6°C dewpoint isopleth at 850 mb (dot-dashed line). Location of Topeka is indicated by solid black dot. In this case, advection alone will not bring 4°C isotherm over Topeka

The second technique is designed to allow the forecaster to determine whether strong surface heating and vertical mixing can erode the lid. This method makes use of the convective condensation level (CCL) and the convective temperature (T_c) on a sounding (see AWSM 105-124,⁵⁰ sections 4.18 and 4.19). The method is presented in Figure C2. Once the CCL and T_c have been determined, the forecaster must consider the following questions: (1) Is the T_c attainable at the station during the forecast period? and (2) If it is, what time will this occur, and when will the first thunderstorm cells appear?

The values of the CCL and T_c yield important information about lid erosion caused by daytime heating and vertical mixing over the station. It is possible,



CCL = 670 mb
Tc = 35°C (95°F)

Figure C2. Skew T-Log P Sounding for Topeka, Kansas, at 1200 GMT 3 April 1981. CCL and Tc analyses are shown on sounding. From lower portion of figure, note that $T_{LS=0}$ of 6°C is closer to Topeka than $T_{LS=0} = 4^\circ\text{C}$. It is possible that the 6°C isotherm can approach Topeka later in the day. Thus, destabilization of sounding is possible through a combination of surface heating and cold advection aloft

using the forecast tools presented in sections 4 and 5, to determine whether Tc can be attained and whether a combination of strong surface heating and cold advection at 700 mb can remove the lid over the station during the forecast period. This method can also assist the forecaster in determining the timing for the onset of thunderstorms at the station.

In summary, the first technique considers the 700-mb advection as the primary process in destabilization or stabilization over the station. The second technique considers a combination of surface heating and vertical mixing over the station to determine the change in stability. Ideally, both methods should be tried by

the forecaster before he decides whether conditions for lid removal and underrunning are favorable. However, these techniques should always be used in conjunction with other severe-storm forecast techniques.

END

FILMED

10-85

DTIC